2022/1

Prof. Dr. Gömze Antal László
(1950-2022)

Mély megrendüléssel adjuk hírül, hogy 2022. január 18.-án Prof. Dr. Gömze Antal László, a Miskolci Egyetem, Kerámia és Polimermérnöki Intézetének professzor emeritusa, a Szilikátipari Tudományos Egyesület által kiadott Építőanyag c. online folyóirat (Journal of Silicate Based and Composite Materials) szerkesztőbizottságának elnöke életének 72. évében nem vár hirtelenséggel elhunyt. A Miskolci Egyetem elismert oktatóját, szakterületének kiváló ismerőjét az egyetem saját halottjának tekinti, és emlékét kegyelettel megőrzi.

Gömze Antal László 1973-ban szerzett kitüntetéses gépészmérnöki oklevelet a moszkvai V.V. Kujbisev Építőmérnöki Egyetemen. Ezután Budapesten, az Épületkerámia-ipari vállalatnál kezdte meg pályafutását tervező, szerkesztő munkakörben. 1975-től a KEVITERV vállalatnál osztályvezetőként, majd 1977-től 1986-ig már a miskolci Nehézipari Műszaki Egyetemen dolgozott, mint egyetemi tanársegéd, majd adjunktus. Ezen időszak alatt egyetemi munkáját megszakítva, a moszkvai Mengyelejev Kémiai-technológiák Egyetemen okleveles szilikátvegyészként végzett 1979-ben, majd szintén Moszkvában 1981-1984 között aspiráns, majd 1985-ben megszerezte doktori fokozatát. 1986-ban felkérték a Hollóházi Porcelángyár vezetésére, ahol vezérigazgatóként dolgozott 1990-ig.

1990-1993 között saját cégét vezette, majd 1993-tól ismét a Miskolci Egyetem, Gépészmérnöki Kar Anyagmozgatási és Logisztikai Tanszékén dolgozott, mint egyetemi docens, szakcsoportvezető, szakirány vezető. Feladata a szilikátipari gépészeti főszakirány, a kerámiák és kompozitok kiegészítő szakirány működtetése, valamint ipari kutatások szervezése, irányítása volt. Ekkoriban több nemzetközi pályázatot is nyert, és jó kapcsolatot alakított ki több európai egyetemmel, ahová hallgatóit tanulmányútra küldte.

1999-ben felkérték, hogy vegyen részt a Miskolci Egyetem Anyag- és Kohómérnöki Karán az anyagmérnök oktatásban. A karon megalapította a Kerámia- és Szilikátmérnöki Tanszéket, melynek vezetője volt egészen 2014-ig. Kidolgozta a szilikáttechnológiai BSc, valamint a Kerámia- és Szilikátmérnöki MSc szakirány struktúráját és tantervi programját. Egyetemi oktatóként aktívan részt vett a doktori képzésben is, ahol 4 fő végzett irányítása alatt.

Több szabadalom, 5 könyv és több mint 250 tudományos cikk szerzője vagy társszerzője volt, a legtöbb cikke 2008 előtt magyar vagy orosz nyelven készült.

2012 óta a Tomsk State University, Russian Federation, vendégprofesszora is volt, ahol a mérnökfizikus MSc és PhD képzésben vett részt.

2020-ban egyetemi tanárként vonult nyugdíjba, de hirtelen bekövetkezett haláláig továbbra is közreműködött az egyetemi oktatásban és a doktoranduszképzésben is.

Az oktatási tevékenység mellett számos kutatás-fejlesztési munkában vett részt effektíven vagy irányítóként egyetemi munkatársaival vagy céges szakemberekkel, hiszen rendkívül szerteágazó, és jó szakmai kapcsolatot ápolt szinte minden kerámia- és szilikátipari vállalattal.

Egyetemi életútja mellett Gömze A. László tudományos és szakmai közéleti tevékenysége is rendkívül sokrétű és szerteágazó volt.

Több mint 20 európai és nemzetközi konferencián tartott plenáris előadást, illetve több mint 50 rangos nemzetközi konferencián szóbeli előadást.

2012-től kezdve óriási lelkesedéssel és kitartással hívott életre több magyarországi nemzetközi konferenciát. Főszervezője és mindenkori elnöke volt a kétévente Miskolc-Lillafüreden megrendezésre kerülő, nagy sikerű International Conference on Competitive Materials and Technology Processes, az International Conference on Rheology and Modeling of Materials, valamint az European Conference on Silicon and Silica Based Materials nemzetközi tudományos konferenciáknak, melyeken szinte minden nemzet képviseltette magát.

Ezen rangos nemzetközi konferenciák sok magyar fiatal számára nyújtottak nemzetközi bemutatkozási lehetőséget.

Tudományszervezési munkája mellett elnöke volt a Magyar Tudományos Akadémia Miskolci Akadémiai Bizottság, Kerámiák és Szilikátok Munkabizottságának.

1973-tól volt a Szilikátipari Tudományos Egyesület tagja. A Magyar Kerámia Szövetség egyik alapítója és annak elnöke volt 2002-2004 között. Ezek mellett tagja volt az Európai Kerámia szövetségnek is.

Pályafutása során több egyetemi, szakmai és országos kitüntetést is kapott, többek között a 1998-ban a „Szilikátiparért Emlékérem", majd 2006-ban a „Kitüntetés a magyar iparért és gazdaságért végzett tevékenységért" kitüntetés birtokosa lett.

Gömze A. László 2005-től egészen haláláig a SZTE lapja, az Építőanyag folyóirat szerkesztőbizottságának elnöke volt. Első cikkét ebben az újságban 1974-ben publikálta „A képlékeny agyag aprításának matematikai elemzése" címmel, mely után még több mint 60 cikket jelentetett meg itt társszerzőivel. Szervezőmunkájának eredményeképpen a lapban számos külföldi szerző is publikált és szerkesztése alatt vált újságunk nemzetközi szinten is referált tudományos folyóirattá.

Kevesen tudják, de 1983-ban Ő és családja honosította meg Magyarországon az orosz feketeterrier kutyákat, és részben innen indulva terjedt el a fajta Nyugat-Európában is.

Halálával egy rendkívül sokoldalú, jólelkű, emberséges kollégát vesztettünk el, aki mindig nagy hangsúlyt fektetett az utánpótlás nevelésre.

2022. február 11-én délután 14:00 órakor a miskolci Mindszenti temetőben vettek Tőle végső búcsút családtagjai, barátai, kollégái.

Tisztelettel búcsúzunk Gömze A. Lászlótól, nyugodjék békében!

It is with great sadness that we have to inform you that Prof. Dr. Antal László Gömze, Professor Emeritus of the University of Miskolc – Faculty of Ceramic and Polymer Engineering, President of the Editorial Board of Építőanyag – Journal of Silicate Based and Composite Materials online magazine published by the Scientific Society of the Silicate Industry, unexpectedly and suddenly passed away at the age of 72, on 18th January 2022. The respected teacher of the University of Miskolc and an outstanding expert of his field is mourned by the University of Miskolc where his memory will be honoured and preserved.

Prof. Dr. Antal László Gömze
(1950-2022)

Antal László Gömze acquired a mechanical engineer diploma with honours in 1973 in the V.V. Kuibyshev State University in Moscow. After this, he started his career in Budapest, at the Épületkerámia-ipari vállalat (Building Ceramics Industrial Company) as a designer and editor. From 1975, he worked at KEVITERV as Head of Department, then from 1977 until 1986 he worked at the Nehézipari Műszaki Egyetem (Heavy Industry University) in Miskolc as an Academic Assistant, later Assistant Professor. During this period – pausing his work at the University – he graduated as a silicate chemist in 1979 at the Dmitry Mendeleev University of Chemical Technology in Moscow, then still in Moscow he was a candidate between 1981 and 1984, acquiring his doctoral degree in 1985. In 1986, he was asked to manage the Hollóháza Porcelain Factory, where he worked as Chief Executive Officer until 1990.

Between 1990 and 1993 he managed his own company, then from 1993 he worked again at the University of Miskolc – Department of Material Handling and Logistics Systems as an Associate Professor, Head of Specialty Group, and Head of Specialty. His responsibility was to operate the main silicate machinery

specialty, the supplementary ceramics and composites specialty and organize and manage industrial research. He won several international tenders during these years, and established good connections with many other European universities, where he sent his students for study trips.

In 1999, he was asked to participate in materials engineering education conducted at the University of Miskolc, Faculty of Material and Metallurgical Engineering. He established the Faculty of Ceramic and Silicate Engineering, of which he was the head until 2014. He developed the structure and curriculum program of the Silicate Technology BSc and the Ceramic and Silicate Engineering MSc Specialty. As a university teacher he participated actively in the doctoral training, where 4 people graduated under his supervision.

He was an author or co-author of several patents, 5 books and more than 250 scientific articles; most of his articles were written in Hungarian or Russian before 2008.

Since 2012, he was also a guest professor at the Tomsk State University, Russian Federation, where he participated in the Physicist Engineering MSc and PhD education.

He retired in 2020 as a university teacher, but he continued to actively participate in university education and doctoral training until his sudden death.

Besides teaching, he participated in several research & development projects effectively or as a supervisor with his university or business colleagues, as he maintained very wide-ranged and good connections with almost every company in the ceramics and silicate industry.

Besides his university career, the scientific and professional public activities of A. László Gömze's were also very diverse and wide-ranged.

He presented plenary talks at more than 20 European and international conferences, and oral presentations at more then 50 acknowledged international conferences.

From 2012, he worked on organizing several international conferences in Hungary with great enthusiasm and persistence. He was the main organizer and all-time chairman of the International Conference on Competitive Materials and Technology Processes, the International Conference on Rheology and Modeling of Materials, and the European Conference on Silicon and Silica Based Materials international conferences held biannually in Miskolc-Lillafüred, where almost all nations represented themselves. These prestigious international conferences provided opportunity for an international debut for many young Hungarians.

Besides his scientific organizational work, he was head of the Hungarian Academy of Sciences, Miskolc Academic Committee, Ceramics and Silicates Work Committee.

He was a member of the Scientific Society of the Silicate Industry from 1973. He was a founder of Magyar Kerámia Szövetség (Hungarian Ceramics Association), and was its president between 2002 and 2004. Besides these, he was also a member of the European Ceramic Society.

During his career, he received several university, professional and national awards, including the "Szilikátiparért Emlékérem" (Medal for the Silicate Industry) in 1998, then in 2006 the "Kitüntetés a magyar iparért és gazdaságért végzett tevékenységért" (Medal for the Work Performed for the Hungarian Industry and Economy).

A. László Gömze was the President of the Editorial Board of Építőanyag – Journal of Silicate Based and Composite Materials published by SZTE from 2005 until his death. He published his first article in the magazine in 1974, titled "A képlékeny agyag aprításának matematikai elemzése" (The Mathematical Analysis of Chopping Moldable Clay), which was followed by over 60 articles published by him together with his co-authors. As a result of his organizational work, several foreign authors also published articles in the magazine, and our magazine became an internationally referenced scientific magazine while he was editor.

Few people know, but in 1983 He and his family introduced the Black Russian Terrier dog breed to Hungary, and the breed became widespread in Western-Europe partly from here.

With his death we have lost an exceptionally versatile, good-hearted, humane colleague in him, who have always placed great emphasis on the development of the younger generation.

His family, friends and colleagues said their final goodbyes to Him on February 11, 2022 at 2:00 p.m. in the Mindszenti cemetery in Miskolc.

We respectfully say our farewell to A. László Gömze. May he rest in peace!

építőanyag

Journal of Silicate Based and Composite Materials

TARTALOM

CONTENT

Flame retardants, their beginning, types, and environmental impact: a review

Ali I. AL-MOSAWI
PhD in polymers Engineering at Institute of Ceramic and Polymer Engineering, Faculty of Materials Science and Engineering, University of Miskolc, Hungary. Research Interests: Polymers, Composite Materials, Rubber Technology, Flame Retardants, Materials Testing, Materials Processing.

Ali I. AL-MOSAWI ▪ Institute of Ceramic and Polymer Engineering, University of Miskolc, Hungary
▪ aliibrahim76@yahoo.com, alialmosawi76@gmai.com

Abstract

Flame retardants have made the world safer by significantly reducing fire risks and reducing human and material losses. At the same time, however, environmental problems have been created and their impact on health, as the compounds that make up the flame retardant are heavy metals. Therefore, in order to make these materials safer, efforts must be focused on using environmentally friendly ones. Furthermore, this green approach must be in line with the laws and legislation developed by many countries due to the recommendations of environmental institutions that warned of the dangers of continuing to use flame retardants containing heavy metals. Not only that but all government and private institutions and civil facilities must be obliged to use flame retardants as a primary building material. This review will focus on the most critical developments that flame retardants have experienced and their impact on the environment and health through their types and mechanism of action.

Keywords: flame retardants, historical review, environmental considerations
Kulcsszavak: égésgátlók, történeti áttekintés, környezetvédelmi megfontolások

1. Historical overview of flame retardants

Flame retardants are defined as chemical agents that can withstand direct flame by stopping flame entry into the material, controlling its spread, and even extinguishing utterly. These materials can be added during or after the products' fabrication for burning protection. The development of flame retardants allowed the safe usage of fabrics that cause flammable behaviour by reducing flammability and reduce the rate of burning. The compounds of phosphorus, nitrogen, chlorine, bromine, boron, and antimony are ones of the most widely used for flame retarding [1-9]. Many materials with flame retardant properties have been known for many centuries. The earliest use of flame retardants was by the eastern civilizations, specifically by the Egyptians and Chinese. Where about 3000 years ago, the ancient Egyptians were soaking grass and reed in seawater before they used it for roofing, so when these grass and reed dry, the mineral salts will crystallize and act as a fire retardant. The Egyptians and Chinese also used alum and vinegar to paint timbers in temples to protect them from the fire [10-13]. The first attempts to use flame retardants by Western civilizations were by the army of the Roman Empire when they besieged the city of Piraeus about 87-86 B.C. The Roman army painted siege towers made of wood with a mixture of alum, vinegar, and clay to protect it from burning by the fire of city defenders. The Roman flame retardant mixture was developed from what the ancient Egyptians used.

Although the ancient civilizations did not have the necessary equipment to analyze these materials' components, they pay attention to the nature of these substances acting as retardants. The discovery of the flame retardancy properties of these materials was through coincidence. Still, they inevitably conducted some practical experiments, even if primitive, to prove these materials' effectiveness in fire protection,

in addition to searching for other materials with the same properties. Indeed, this led to the development of testing devices to detect these materials [14].

Material	Used by	Date
Potassium Aluminium Sulphate (Alum)	The Egyptians have used Alum and Vinegar to reduce wood flammability	450 B.C.
Vinegar	The Egyptians and Chinese used painted timbers by vinegar to increase their resistance to burning	360 B.C.
Alum, Vinegar, and clay	The Roman army painted the wooden siege towers with alum, vinegar, and clay to protect them from burning when they besieged Piraeus	87-86 B.C.
Clay-Gypsum Mixture	Had been used by Nicola Sabbatini in France for reducing painted canvas inflammation at Parisian theatres	1638
Alum- Ferrous Sulfate-Borax Mixture	It was discovered by Obadiah Wyld and used in Britain for preventing paper, linen, canvas, & c., from flaming or retaining fire, & c. Wyld received the first patent for fire retardants No.551	1735
Potassium Aluminium Sulphate (Alum)	Used by the French brothers Montgolfier to reduce flammability of hot air balloons	1783
$(NH_4)_3PO_4$ - NH_4Cl - Borax Mixture	Used by the French chemist Gay-Lussac for linen and hemp fabrics	1821

Table 1 A historical overview for early use of flame retardants [11-20]
1. táblázat Történeti áttekintés az égésgátlók korai használatáról [11-20]

With the development of human lifestyle, the needs to discover new materials that reduce the risk of fires have increased. This calls for relying on a scientific and practical basis and not to depend on chance only. So the first practical experiments to reduce fire risk began to appear. As a scientific

procedure recorded, the first fire testing experiments can be traced to London's 1790s done by the Associated Architects. There was Quantitative work in Germany beginning in the 1880s, and in the U.S. and England in the 1890s. A summary of the timeline for the use of flame retardants is included in *Table 1*. The growing interest in these tests led to establishing unified test standards in the early twentieth century. Where the first standard about fire testing methods was ASTM C19 (later called E 199) [14-18].

2. Categorization of flame retardants

Flame retardants are typically categorized into four major categories: Inorganic FRs; Phosphorus-containing FRs; Nitrogen-containing FRs; and Halogenated organic.

2.1 Inorganic flame retardants

The most significant types of this category are antimony trioxide containing halogen, magnesium hydroxide, zinc borate, aluminium hydroxide, and zinc sulfide. If this category of flame retardant is exposed to heat, it does not evaporate. Instead, it decomposes and released non-flammable gases, such as water vapour, carbon dioxide, sulfur dioxide, hydrogen chloride, and other gases. Most of these compounds produce endothermic reactions. These flame retardants' mechanism of action depends on its disintegration at high temperatures and causing the release of non-flammable gases, which minimize the mixture of flammable gases. Then, it separates the plastic's surface by forming a glassy protective layer on the surface of the plastic that prevents oxygen and heat access [21-27].

2.2 Phosphorus containing flame retardants

This category typically includes phosphate esters, red phosphorus, ammonium polyphosphates, and ammonium orthophosphates. Its principle of action is based on its oxidation during combustion to phosphorus oxide, which converted into phosphoric acid when interacting with water. This acid induces the release of water and removes it from the substrate layer of the thermal decomposing material, which contributes to its decomposition and thereby increases the formation of carbonaceous waste and decreases the emission of combustible gases [28-31].

2.3 Nitrogen containing flame retardants

Nitrogen-containing flame retardants: Often referred to as organic flame retardants. Melamine and its derivatives are the essential compounds in this category. These retardants' principle of action depends on the formation of an insulating surface layer by gases released from these retardants during combustion cause the material to swell [32-37].

2.4 Halogenated organic flame retardants

This category contains primary bromine and chlorine in particular. Its principle working action depends on chemical interference with the root chain mechanism, which occurs in the gaseous phase during combustion. Halogen flame retardants eliminate the high-energy hydrogen and hydroxide

generated during the combustion process by combining them, so the flame is poisoned by the halogen radicals released during combustion [21,38-41].

3. Classification of flame retardants

Flame retardants can be classified into three primary groups, depending on how they are applied to the polymer, and these two groups are: Additive FRs; Reactive FRs.; and Additive-Reactive FRs

3.1 Additive flame retardants

This type is used for thermoplastics in particular. Additive flame retardants can be added to plastics in three ways: (1) before polymerization, (2) during the process, or (3) after polymerization, and it is the most common way to add them. In addition to its direct action as flame retardants, it can be a plasticizer if they are compatible with the plastic or as fillers if they aren't compatible with it. The main disadvantage of these retardants, is their instability, where they sometimes can be volatile or even bled from the plastic, especially from the layers near the surface, causing plastic to lose its ability to resist burning, which is very dangerous because this state can only be realized when combustion occurs [42-44].

3.2 Reactive flame retardants

This type of flame retardant is binding to the polymer molecule with the other components. This chemical bonding prevents it from evaporating and bleeding from the polymer over time. It happens with additive flame retardants, enabling the polymer to maintain flame retardant properties as long as possible. Although they are chemically binding to the polymer molecules, they have no plasticizing effect and are non-affecting the polymer's thermal stability. The practical and widespread use of reactive flame retardants is with thermosets [41-44].

3.3 Additive- Reactive flame retardants

This type of flame retardants is referred to also as synergism. Several materials are not classified as stand-alone flame retardants, which will often work as fillers if used alone. Still, they have a special synergistic effect if they are added to other retardants, where the effectiveness and efficiency of these retardants increase to resist fire. An example of such materials is antimony compounds, especially antimony trioxide. The main purpose of this combination is to reduce the cost and, as mentioned, increase the effectiveness of the primary flame retardant [21, 42, 43, 42, 45, 46].

4. Working mechanism of flame retardants

The method of slowing or even stopping the flame depends on the nature of the flame retardant, as the flame retardant can act chemically or physically in the solid, liquid, and gas state, where the flame retardant is interpenetrating with the combustion process during the various stages of this process, i.e., heating, decomposition, ignition, or flame propagation [21,47,48]. In general, there are two standard methods of flame retardation. The first method is based on preventing oxygen

from accessing the flame area by generating non-combustible gases, where these gases can poison and extinguish the flame with free radicals. The second method is based on the thermal flame theory, which states that flame retardants require thermal energy for decomposition, leading to a decrease in the material's surface temperature to a temperature lower than its burning point, and the combustion breaks down [49].

4.1. Physical mode

This working mode can be achieved in three ways [47,50,51]:

4.1.1 Cooling

Additives cause endothermic processes that cool the substrate of the material to a temperature lower than the level of combustion. An example of flame retardants behaving like this is aluminum hydroxide. The cooling mechanism is shown in *Fig 1*.
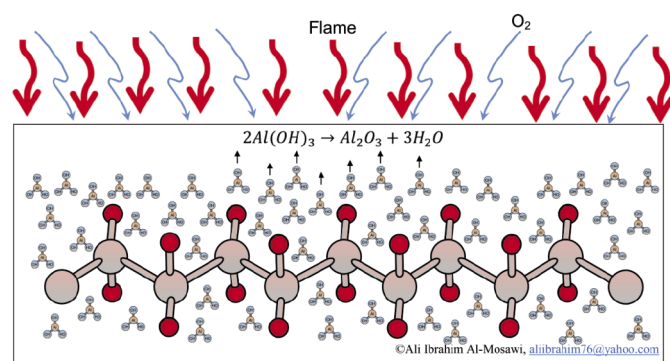
Fig. 1   Cooling mechanism
1. ábra   Hűtési mechanizmus

4.1.2 Formation of insulation layer

The insulating semi-glass layer is created by a flame retardant that expels the oxygen needed to begin the combustion process, preventing heat transfer. Inorganic phosphorous compounds and boron are behaving like this mode.

4.1.3 Dilution

The incorporation of inert materials (fillers) and additives that release inert gases after their thermal decomposition dilute the fuel in both the solid and gaseous states in such a way that the minimum ignition limits for the gas mixture are not exceeded. Phosphorous and boron compounds work this way.

4.2 Chemical mode

Can be achieved in two ways:

4.2.1 Gaseous phase reaction

The free radical mechanism is stopped by the flame-retardant materials, causing eliminating the exothermic processes and, so the system will cool down. The percentage of flammable gases is reduced and even wholly prohibited as shown in *Fig 2*. The flame retardant which exhibits this behavior is halogen compounds [21,51].
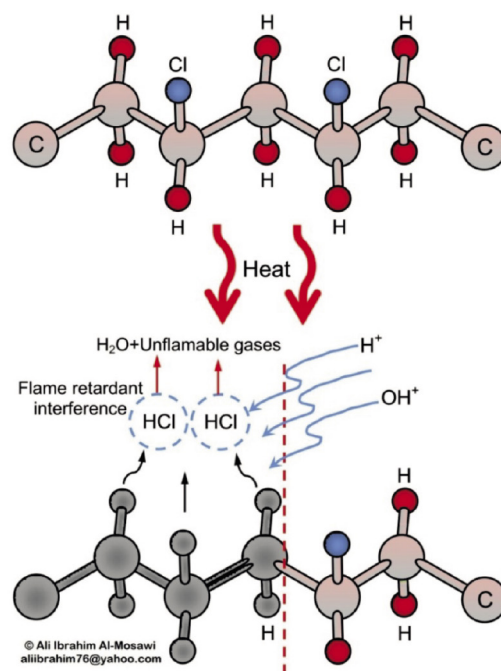
Fig. 2   Gaseous phase reaction
2. ábra   Gáz-halmazállapotú fázisreakció

4.2.2 Solid Phase Reaction

A carbon film is formed on the surface of the polymer by the dehydrating action of flame retardant, forming double bonds in the polymer (see *Fig 3*). These double bonds will create a carbon film by cross-linking. An example of these retardants is phosphorous compounds. In the case of phosphorous compounds addition, their mode of action depends on substituting the hydroxyl and hydrogen radicals in the combustion cycle by low-potency radicals, eliminating their damage as shown in the equations below, which represents the combustion reaction (Chain reaction equations), and the hinderation reaction (Chain hinderation equations). This mechanism is similar to that of the halogen compounds. The change in the combustion cycle's radical composition in the gaseous phase leads to flame suppression and reduced heat production, which cools the combustion zone. The combustion process activated several sequential reactions, which include: chemical chain-branching, chain-propagating, and chain-breaking reactions. These chemical processes help preserve the flame by changing the quantity, form, and mole ratio of the radicals present in the gas phase. Therefore, in order to change this state, Lower energy radicals are required to remove the unstable radicals of OH and H. Replacing the unstable OH and H radicals with less reactive and more stable radicals works to inhibit the combustion chain reaction and lead to cut this reaction. Thus the self-extinguishing process of the system will occur [21,52-54].
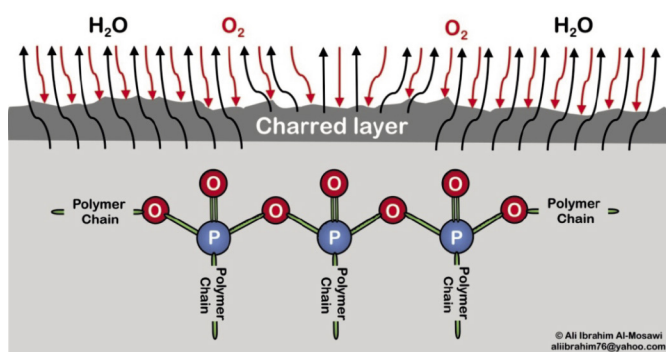
Fig. 3   Solid phase reaction
3. ábra   Szilárd fázis reakció

Chain reaction equations [54]:

$$OH^{.}+CO \rightarrow CO_2+H^{.} \tag{1}$$
$$CH_4+O_2 \rightarrow CH_3^{.}+H^{.}+O_2 \tag{2}$$
$$H^{.}+O_2 \rightarrow OH^{.}+0.5O_2 \tag{3}$$
$$OH^{.}+CH_4 \rightarrow H_2O+CH_3^{.} \tag{4}$$
$$CH_3^{.}+O_2 \rightarrow CH_2O+HO^{.} \tag{5}$$
$$CH_2O+HO^{.} \rightarrow CHO^{.}+H_2O \tag{6}$$
$$CHO^{.}+O_2 \rightarrow CO+H^{.}+O_2 \tag{7}$$

Chain hinderation equations [54]:

$$PO^{.}+H^{.} \rightarrow HPO \tag{8}$$
$$PO^{.}+OH^{.} \rightarrow HPO_2 \tag{9}$$
$$HPO+H^{.} \rightarrow H_2+PO^{.} \tag{10}$$
$$HPO+CH_3^{.} \rightarrow H_2+PO^{.} \tag{11}$$
$$HPO_2^{.}+H^{.} \rightarrow H_2O+PO \tag{12}$$
$$HPO_2^{.}+H^{.} \rightarrow H_2+PO_2 \tag{13}$$
$$HPO_2^{.}+OH^{.} \rightarrow H_2O+PO_2 \tag{14}$$

Polymer	Flash-ignition Temperature, °C	Self-ignition temperature, °C
Poly(methyl methacrylate)	300	430
Polypropylene	320	350
Polyethylene	340	350
Polystyrene	350	490
Rigid Poly(vinyl chloride)	390	450
Plasticized Poly(vinyl chloride) (Insulation)	330	385
Plasticized Poly(vinyl chloride) (Fire resistant, low acid emission)	400	410
Poly(acrylonitrile)	480	560
Polyamide 6'6	490	530
Poly(tetrafluoroethylene)	560	580

Table 2   Flash and self ignition temperatures for various polymers [58,59]
2. táblázat   Vaku- és öngyulladási hőmérséklet különböző polimerekhez [58,59]

5. Flammability and combustibility

Many people think that flammability or ignitability and combustibility is similar in denoting the same characteristic. Still, the truth is that they are different, so I will explain what these two terms refer to in this paragraph. The flammability or ignitability is defined as a material's ability to catch fire (ignite), causing a fire, combustion, or even an explosion if the material is unstable. Whereas combustibility is defined as how easily a material burns to cause a fire or combustion [55]. The main criterion by which materials are classified as flammable or combustible is the flash point, where flammable materials have a lower flash point than combustible materials. The flash point of flammable materials is less than 37.8 °C, while in the case of combustible materials; its value is higher than 37.8 °C and less than 93.3 °C [55-58]. *Table 2* represents the flash-ignition and self-ignition temperatures for various polymers.

6. Flame retardants and the environment
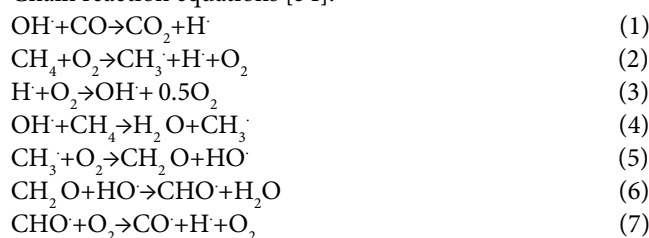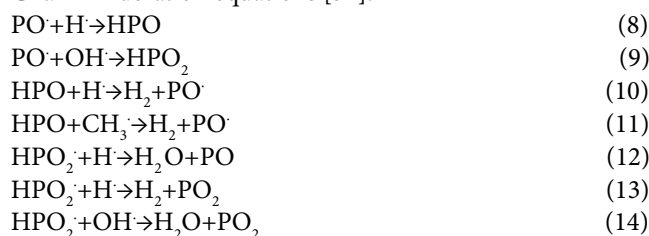
Most of conventional flame retardants and stabilizers for plastics contain heavy metals or other ingredients e.g., bromine being potentially harmful to the environment or health. For example, in European countries, concentrations of flame retardants have been found in human milk and the bodies of birth cohorts (but their concentrations were lower than in the United States) and household dust. Concentrations of flame retardants were also found in the bodies of birds and their eggs [60-69]. Therefore, in light of these environmental challenges and responsibilities, most of these flame retardants must be reconsidered in terms of use and finding an environmentally friendly and sustainable alternative. Especially since countries have already started issuing laws prohibiting the use of certain types of flame retardants due to their severe damage to the environment after research has proven this [70-72]. Many of flame retardants currently in use are included in European Union regulation (EC) No. 1272/2008 and its amendments for materials classification, which have been classified as dangerous materials. So it has become imperative to search for safe alternatives to these materials [73]. There are heavy metal-free flame retardants (earth metal hydroxides), but it must be used in high concentrations (40- 60 phr), which in turn will reduce the mechanical properties and wear resistance of the plastic [60].

Therefore, there must be a precise harmony between environmentally friendly flame retardants and preserving the materials' properties. This matter requires more time and research for a complete shift from traditional flame retardants to those environmentally friendly [7, 60, 73-75]. Certain recent flame retardants are now available to comply with the successful flammability tests regulations. Also, the interference of retardants with flame reaction chains will restrict the oxidation of the hydrocarbon. This interference will prevent the process of converting carbon monoxide to carbon dioxide, which causes highly volatile, very smoky fire effluents and rich in incomplete combustion products [76]. With the tendency to replace traditional flame retardants with environmentally friendly ones, the environmental conditions surrounding the product containing this type of retardants must be taken into account and the applications for which it is used. One study revealed that environmentally friendly retardants could be harmful when breaking down by heat and ultraviolet rays [77]. Therefore, it is necessary to use these retardants carefully. Obtaining the ideal flame retardant requires great research efforts that may not take as long as research in the past due

to scientific research development. Whereas the chemical stability of environmentally friendly flame retardants in different conditions is of critical importance to increase safety level when using these retardants.

7. Conclusions

Every year, flame retardants save thousands of lives around the world. Still, unfortunately, many also lose their lives because many of these retardants are made from harmful components to both health and the environment. Many legislations and laws have restricted the use of flame retardants containing heavy metals, which will make the heavy metals-free ones (green flame retardants) commonly used. To obtain the maximum effectiveness of flame retardants, each type must be used with the appropriate material intended to improve its flame resistance.

References

[1] Al-Mosawi, A.I. and Marossy, K. (2018): Heat Effected Zone in Unburned, Antimony Trioxide Containing Plasticized Poly(vinyl chloride). Építőanyag-Journal of Silicate Based and Composite Materials, Vol.70, No.3, pp.86-89.
https://doi.org/10.14382/epitoanyag-jsbcm.2018.16

[2] Winberg, D. (2016): International Fire Death Rate Trends, SP Technical Research Institute of Sweden. Report No.32. ISBN: 978-91-88349-36-1

[3] Al-Mosawi, A.I. (2011): Hybrid Fire Retardants to Increasing Composting Resistance for Fibres-Reinforced Composites. Iraqi National Journal Of Chemistry, Vol. 41, pp 48-54.
https://doi.org/10.6084/m9.figshare.13550177

[4] Velasquez, K. and Viani, T. (2006): Flame Retardants Families. Capstone Design Project, University of Oklahoma, Chemical Engineering.

[5] Al-Mosawi, A.I. (2021): Flame Retarding-Stabilizing Behavior of Plasticized Poly(vinyl chloride) Containing Novel Heavy Metal Free Modifier. PhD dissertation, Faculty of Material Science and Engineering, University of Miskolc, Hungary.

[6] Levchik, S.V. (2006) Introduction to Flame Retardancy and Polymer Flammability. Chapter 1, In: Morgan, A. and Wilkie Ch.(eds.), Flame Retardant Polymer Nanocomposites. John Wiley & Sons, Inc., pp. 1-29.
https://doi.org/10.1002/9780470109038.ch1

[7] Babrauskas V. et al. (2020): Fire Hazard Comparison of Fire Retarded and Non-Fire-Retarded Products. Kindle Edition, NBS Special Publications No.749. ASIN: B084TZMN2N

[8] Hilado, C.J. (1998): Flammability Handbook for Plastics. 5th Edition, CRC Press: Boca Raton. https://doi.org/10.1201/9780585248684

[9] Liu, Q. et al. (2020): Recent Developments in the Flame-Retardant System of Epoxy Resin, Materials. Vol.13, Issue. 9, pp.2145.
https://doi.org/10.3390/ma13092145

[10] Al-Mosawi, A.I., Amash, H.K. Al-Maamori, M.H., and Hashim, A.A. (2014): Enhancement of thermal resistance of aircraft tires by using magnesium hydroxide. Central Organization for Standardization and Quality Control (COSQC), No.3877, International Classification (B608C13/00) , Iraqi Classification (34).

[11] Hindersinn, R.R. (1990): Historical Aspects of Polymer Fire Retardance. Chapter 7, In: Gordon L. Nelson, G. (ed.) Fire and Polymers: Hazards Identification and Prevention, ACS Symposium Series, Vol. 425, American Chemical Society, pp 87-96.
https://doi.org/10.1021/bk-1990-0425.ch007

[12] Watson, D.A.V. and Schiraldi, D.A. (2020): Biomolecules as Flame Retardant Additives for Polymers: A Review. Polymers, Vol.12, Issue.4, 2020, pp.849 (31 pages). https://doi.org/10.3390/polym12040849

[13] Kozlowski, R. and Wladyka-Przybylak, M. (2001): Natural Polymers, Wood and Lignocellulosic Materials. Chapter 9, In: Horrocks, A., Price, D. (eds.) Fire Retardant Materials, Woodhead Publishing Limited, UK, pp.305-317.

[14] Brown, F. L. (1958): Theories of the combustion of wood and its control: A Survey of the Literature. Forest Service Report No.2136, Forest Products Laboratory, Madison Wis., in cooperation with the University of Wisconsin.

[15] Gay-Lussac, J.L (1821): Note sur la propriete qu'ont les matieres salines de rendre les tissus incombustibles (Note on the property that saline materials have to make tissues incombustible). Annales de chimie et de physique, Vol.18, pp.211-261.

[16] Babrauskas, V. and Williamson, R.B. (1978): The historical basis of fire resistance testing - Part I. Fire Technology vol.14, Issue.3, pp.184–194. https://doi.org/10.1007/BF01983053

[17] Babrauskas, V. and Williamson, R.B., (1978): The historical basis of fire resistance testing - Part II. Fire Technology vol.14, Issue.4, pp. 304–316. https://doi.org/10.1007/BF01998390

[18] Hall, J.R. (2004): A Century of Fire Standards: The History of Committee E05, 1904-2004. ASTM Standardization News, ASTM International.

[19] Lawson, J.R. (2009): A History of Fire Testing, NIST Technical Note 1628. National Institute of Standards and Technology, U.S. Department of Commerce.

[20] Wyld, O. (1735): Making or Preparing of Paper, Linen, Canvass and Such Like Substances, Which Will Neither Flame nor Retain Fire, and Which Hath Also a Property in it of Resisting Moisture and Damps. British Patent No.551, London.

[21] Al-Mosawi, A.I. (2003): Using Study of Antimony Trioxide Material as a Flame Retardant Material. M. Sc. Thesis, Engineering College, Babylon University, Iraq. https://doi.org/10.13140/RG.2.1.4718.1529

[22] Lawson, J.R. (2009): A History of Fire Testing: Past, Present, and Future. Journal of ASTM International, Vol. 6, No.4, pp. 1-19.
https://doi.org/10.1520/JAI102265

[23] Ai, L., Chen, S., Yang, L. and Liu, P. (2021): Synergistic Flame Retardant Effect of Organic Boron Flame Retardant and Aluminum Hydroxide on Polyethylene. Fibers and Polymers, Vol.22, Issue.2, pp.354-365.
https://doi.org/10.1007/s12221-021-9385-6

[24] Walter, M.D. and Wajer, M.T. (2015): Overview of Flame Retardants Including Magnesium Hydroxide. Martin Marietta Magnesia Specialties LLC, Maryland, USA.

[25] Al-Mosawi, A.I. et al. (2010): Performance Evaluation of Zinc Borate to improvement thermal properties of Antimony Trioxide at Elevated Temperatures. The Iraqi Journal for Mechanical and Material Engineering, Special Issue for 2nd scientific conference, engineering College, University of Babylon , Iraq, 24-25 March.
https://doi.org/10.6084/m9.figshare.16548054

[26] Luo, H. et al. (2020): An Efficient Organic/Inorganic Phosphorus-Nitrogen-Silicon Flame Retardant Towards Low-Flammability Epoxy Resin. Polymer Degradation and Stability, Vol.178, pp. 1-9 .
https://doi.org/10.1016/j.polymdegradstab.2020.109195

[27] Al-Mosawi, A.I., Ammash, H.K., Al-Maamori, M.H., and Hashim, A.A (2012): Increasing flammability resistance for aircrafts tires by using magnesium hydroxide. Academic Research International, Vol.3, No.2, pp. 11–14. https://doi.org/10.6084/m9.figshare.16547274

[28] Al-Mosawi, A.I. (2012): Formation Hybrid Flame Retardant and its Effect on Thermal Resistance of Araldite resin Composite. Academic Research International, Vol.3, Issue.2, pp. 66-69.
https://doi.org/10.6084/m9.figshare.13633481

[29] Huo, S. et al. (2020): A Liquid Phosphorus-Containing Imidazole Derivative as Flame-Retardant Curing Agent for Epoxy Resin with Enhanced Thermal Latency, Mechanical, and Flame-Retardant Performances. Journal of Hazardous Materials, Vol.386, pp.121984.
https://doi.org/10.1016/j.jhazmat.2019.121984

[30] Al-Mosawi, A.I. (2012): Flame Retardancy of Polymers. 1st Edition, LAP LAMBERT Academic Publishing, Germany. ISBN: 25531 -659 -3-978

[31] Zhang, W. et al. (2014): The Influence of the Phosphorus-Based Flame Retardant on the Flame Retardancy of the Epoxy Resins. Polymer Degradation and Stability, Vol.109, pp.209-217.
https://doi.org/10.1016/j.polymdegradstab.2014.07.023

[32] Levchik, S. (2014): Phosphorus-Based FRs. Chapter 2, In: Morgan, A. and Wilkie Ch.(eds.), Non-Halogenated Flame Retardant Handbook, John Wiley and Sons, Inc., pp. 17-74. https://doi.org/10.1002/9781118939239.ch2

[33] Horacek, H. and Pieh, S. (2000): The Importance of Intumescent Systems for Fire Protection of Plastic Materials. Polymer International, Vol.49, Issue.10, pp. 1114-1106. https://doi.org/10.1002/1097-0126(200010)49:10<1106::AID-PI539>3.0.CO;2-I

[34] Çetin, A. et al. (2019): Various Combinations of Flame Retardants for Poly (vinyl chloride). Open Chemistry, Vol.17, Issue.1, pp.980-987. https://doi.org/10.1515/chem-2019-0105

[35] Ray, S.S.and Kuruma, M. (2019): Types of Flame Retardants Used for the Synthesis of Flame-Retardant Polymers. Chapter 4 In: Ray, S., Kuruma, M. (auth.) Halogen-Free Flame-Retardant Polymers Springer Series in Materials Science, Springer, Cham., Vol 294, pp.15-45. https://doi.org/10.1007/978-3-030-35491-6_4

[36] Duquesne, S. and Futterer, T. (2014): Intumescent Systems, Chapter 8, In: Morgan, A. and Wilkie Ch.(eds.), Non-Halogenated Flame Retardant Handbook. Co-published by CoJohn Wiley and Sons, Inc. And Scrivener Publishing LLC., USA, pp. 293-346. https://doi.org/10.1002/9781118939239.ch8

[37] Wang, J. et al. (2020): A Novel Intumescent Flame Retardant Imparts High Flame Retardancy to Epoxy Resin. Polymers for Advanced Technologies, Vol.31, Issue.5, pp.932-940. https://doi.org/10.1002/pat.4827

[38] Al-Mosawi, A.I. (2016): Flammability of Composites. Chapter 14, In: Njuguna, J. (ed.) Lightweight Composite Structures in Transport: Design, Manufacturing, Analysis and Performance, Woodhead Publishing, UK, pp. 361-369. https://doi.org/10.1016/B978-1-78242-325-6.00014-1

[39] Klatt, M. (2014): Nitrogen-Based Flame Retardants. Chapter 4, In: Morgan, A. and Wilkie Ch.(eds.), Non-Halogenated Flame Retardant Handbook, John Wiley and Sons, Inc., pp. 143-168. https://doi.org/10.1002/9781118939239.ch4

[40] Guerra, P. et al. (2011): Introduction to Brominated Flame Retardants: Commercially Products, Applications, and Physicochemical Properties. chapter 1, In Eljarrat, E., Barceló, D., Brominated Flame Retardants The Handbook Of Environmental Chemistry, 1st Edition, Springer Berlin Heidelberg, Germany, pp.1-17. https://doi.org/10.1007/698_2010_93

[41] Vahabi, H. et al. (2021): Flame Retardancy of Reactive and Functional Polymers. Chapter 8, In: Gutiérrez, T. (ed.) Reactive and Functional Polymers, Vol.3, Springer Nature Switzerland AG, pp. 165-195. https://doi.org/10.1007/978-3-030-50457-1_8

[42] Lens, J., Sun, X. and Kagumba, L. (2019): Polymeric Flame Retardants for Reinforced Thermoplastic and Thermoset Resins. Reinforced Plastics, Vol.63, Issue.1, pp.36-39. https://doi.org/10.1016/j.repl.2017.11.016

[42] Lassen, C. et al. (1999): Brominated Flame Retardants: Substance Flow Analysis and Assessment of Alternatives, Environmental Project, Danish Environmental Protection Agency. ISBN: 87-7909-416-3

[44] Baby, A. et al. (2020): Reactive and Additive Modifications of Styrenic Polymers with Phosphorus-Containing Compounds and Their Effects on Fire Retardance. Molecules, Vol.25, Issue.17, pp.3779. https://doi.org/10.3390/molecules25173779

[45] Adewale, K.P. (2016): Thermoplastic Additives Flame Retardants. Chapter 26, In: Olabisi, O., Adewale, K. (eds.) Handbook of Thermoplastics, 2nd Edition, CRC Press, pp. 877-917. https://doi.org/10.1201/b19190-27

[46] Al-Mosawi, A.I. et al. (2010): Effect of Compilation Between Two Types of Inorganic Flame Retardants on Thermal Resistance for Advanced Composite Material at Elevated Temperatures. Proceedings of 5th Scientific Conference (CSASC 2010), College of Science, University of Babylon , Iraq, 19-20 May, pp.448-455. https://doi.org/10.6084/m9.figshare.13633760

[47] Zirnstein, B. et al. (2019): Combination of Phosphorous Flame Retardants and Aluminum Trihydrate in Multicomponent EPDM Composites. Polymer Engineering and Science, Vol.60, Issue.2, pp.267-280. https://doi.org/10.1002/pen.25280

[48] Troitzsch, J.H. (1998): Overview of Flame Retardants . Chimica Oggi/Chemistry Today , Vol.16, No.1, pp.18-24.

[49] Hu, Y. and Wang, X. (2019): Flame Retardant Polymeric Materials: A Handbook. 1st Edition, CRC Press, USA. https://doi.org/10.1201/b22345

[50] Mohammed, A.A. (1993): Plastics Chemistry. 1st Edition, House of Books for Printing and Publishing - Mosul, Iraq.

[51] Tawfik, S.Y. (2017): Flame Retardants: Additives in Plastic Technology. Chapter 15, In: Palsule S. (eds.) Polymers and Polymeric Composites: A Reference Series. Springer, Berlin, Heidelberg, pp.1-27. https://doi.org/10.1007/978-3-642-37179-0_76-2

[52] Salmeia, K.A. et al. (2015): An Overview of Mode of Action and Analytical Methods for Evaluation of Gas Phase Activities of Flame Retardants. Polymers, Vol.7, Issue.3, pp.504-526. https://doi.org/10.3390/polym7030504

[53] Schartel, B. (2010): Phosphorus-based Flame Retardancy Mechanisms-Old Hat or a Starting Point for Future Development?. Materials, Vol.3, Issue.10, pp. 4710-4745. https://doi.org/10.3390/ma3104710

[54] Lazar, S.T. et al. (2020): Flame-Retardant Surface Treatments. Nature Reviews Materials, Vol.5, Issue.4, pp.259-275. https://doi.org/10.1038/s41578-019-0164-6

[55] Goodger, E.M. (1979): Flammability and Ignitability. Applied Energy, Vol.5, Issue.1, pp.81-84. https://doi.org/10.1016/0306-2619(79)90007-2

[56] Burton, L. (2019): What Are the Key Differences Between Flammable and Combustible Materials?. High Speed Training Ltd., UK.

[57] Dickens, E.D. (1983): The Fire Performance of PVC. Journal of Vinyl Technology, Vol.5, Issue.3, pp.150-157. https://doi.org/10.1002/vnl.730050315

[58] Pawelec, W. (2014): New Families of Highly Efficient, Halogen-Free Flame Retardants for Polypropylene (PP). Doctoral Thesis, Åbo Akademi University, Finland.

[59] PVC and Fire (2011): Poly Marketing Pty Limited T/A Envorinex company, Australia.

[60] Al-Mosawi, A.I. and Marossy, K. (2020): Heavy Metal Free Thermal Stabilizing-flame Retarding Modifier for Plasticized Poly(vinyl chloride). Materials Research Express, Vol.7, Issue.1, pp. 015320. https://doi.org/10.1088/2053-1591/ab6249

[61] Čechová, E. et al. (2017): Legacy and Alternative Halogenated Flame Retardants in Human Milk in Europe: Implications for Children's Health. Environment International, Vol.108, pp.137-145. https://doi.org/10.1016/j.envint.2017.08.008

[62] Casas, M. et al. (2013): Exposure to Brominated Flame Retardants, Perfluorinated Compounds, Phthalates and Phenols in European Birth Cohorts: ENRIECO Evaluation, First Human Biomonitoring Results, and Recommendations. International Journal of Hygiene and Environmental Health, Vol. 216, Issue.3, pp.230-242. https://doi.org/10.1016/j.ijheh.2012.05.009

[63] de la Torre, A. et al. (2020): Organophosphate Compounds, Polybrominated Diphenyl Ethers and Novel Brominated Flame Retardants in European Indoor House Dust: Use, Evidence for Replacements and Assessment of Human Exposure. Journal of Hazardous Materials, Vol.382, pp.121009. https://doi.org/10.1016/j.jhazmat.2019.121009

[64] Lee, H. et al. (2020): Legacy and Novel Flame Retardants in Water and Sediment from Highly Industrialized Bays of Korea: Occurrence, Source Tracking, Decadal Time Trend, and Ecological Risks. Marine Pollution Bulletin, Vol.160, pp.111639. https://doi.org/10.1016/j.marpolbul.2020.111639

[65] Venier, M. et al. (2014): Flame retardants and legacy chemicals in Great Lakes' water. Environmental Science and Technology, Vol.48, Issue.16, pp.9563-72. https://doi.org/10.1021/es501509r

[66] Liu, J. et al. (2021): Legacy and Alternative Flame Retardants in Typical Freshwater Cultured Fish Ponds of South China: Implications for Evolving Industry and Pollution Control. Science of The Total Environment, Vol.763, pp.143016. https://doi.org/10.1016/j.scitotenv.2020.143016

[67] Zhang, J. et al. (2021): Pollution of Plastic Debris and Halogenated Flame Retardants (HFRs) in Soil from an Abandoned E-Waste Recycling Site: Do Plastics Contribute to (HFRs) in Soil?. Journal of Hazardous Materials, Vol. 410, pp.124649. https://doi.org/10.1016/j.jhazmat.2020.124649

[68] Wang, Y. et al. (2021): Ornamental Houseplants as Potential Biosamplers for Indoor Pollution of Organophosphorus Flame Retardants. Science of The Total Environment, Vol. 767, pp.144433. https://doi.org/10.1016/j.scitotenv.2020.144433

[69] Barhoumi, B. et al. (2020): Halogenated Flame Retardants in Atmospheric Particles from a North African Coastal City (Bizerte, Tunisia): Pollution Characteristics and Human Exposure. Atmospheric Pollution Research, Vol.11, Issue. 4, pp.831-840. https://doi.org/10.1016/j.apr.2020.01.011

[70] Jarosinski, A. et al. (2020): New Production Route of Magnesium Hydroxide and Related Environmental Impact. Sustainability, Vol.12, Issue. 21, pp.8822. https://doi.org/10.3390/su12218822

[71] Gebke, S. et al. (2020): Suitability and Modification of Different Renewable Materials as Feedstock for Sustainable Flame Retardants. Molecules, Vol.25, Issue.21, pp.5122. https://doi.org/10.3390/molecules25215122

[72] González-Rubio, S. et al. (2021): A Review on Contaminants of Emerging Concern in European Raptors (2002–2020). Science of The Total Environment, Vol.760, pp.143337. https://doi.org/10.1016/j.scitotenv.2020.143337

[73] European Parliament and Council of the European Union (2008): Regulation (EC) No 1272/2008 of the European Parliament and of the Council of 16 December 2008 on Classification, Labelling and Packaging of Substances and Mixtures, Amending And Repealing Directives 67/548/EEC and 1999/45/EC, and Amending Regulation (EC) No 1907/2006, Official Journal of the European Union, Vol.51.

[74] Zhang, A. et al. (2021): Construction Of Durable Eco-Friendly Biomass-Based Flame-Retardant Coating For Cotton Fabrics. Chemical Engineering Journal, Vol.410, pp.128361. https://doi.org/10.1016/j.cej.2020.128361

[75] Li, N. et al. (2020): Novel Eco-Friendly Flame Retardants Based on Nitrogen-Silicone Schiff Base and Application in Cellulose. ACS Sustainable Chemistry and Engineering, Vol.8, Issue.1, pp.290-301. https://doi.org/10.1021/acssuschemeng.9b05338

[76] Kausar, A. (2019): Fire Protection: Flame-Retardant Polymers in. Chapter 61, In: Mishra, M. (ed.) Encyclopedia of Polymer Applications, First Edition, CRC Press, Taylor & Francis Group, USA, pp.1258-1272. https://doi.org/10.1201/9781351019422-140000019

[77] Koch, C. et al. (2019): Degradation of the Polymeric Brominated Flame Retardant "Polymeric FR" by Heat and UV Exposure, Environmental Science and Technology, 2019, Vol.53, Issue.3, pp.1453–1462. https://doi.org/10.1021/acs.est.8b03872

ICCM 2022
XVI. International Conference on Composite Materials
August 08-09, 2022 in Amsterdam, Netherlands

XVI. International Composite Materials is the premier interdisciplinary forum for the presentation of new advances and research results in the fields of Materials and Metallurgical Engineering.

Today more than ever before it is extremely important to stay abreast of the changing landscapes of the Materials and Metallurgical Engineering world. The multidisciplinary focus of this event aims to bring together presenters and attendees from different fields with expertise in various areas of Materials and Metallurgical Engineering, providing an excellent opportunity to participate in the international exchange of ideas, current strategies, concepts and best practices, collaborations, and cooperation, offering a broader perspective and more enriching experience.
The program includes time allocated for networking, peer-to-peer discussions, and exploring the host city.

We invite the participation of leading academic scientists, researchers and scholars in the domain of interest from around the world to submit original research contributions relating to all aspects of:

- Additive manufacturing
- Applications
- Bio-based composites
- Biomimetic composites
- Ceramic matrix composites
- Concrete and cementitious composites
- Damage and fracture
- Durability and ageing
- Experimental techniques
- Fibers and matrices
- FRP reinforced concrete
- Health monitoring
- Hybrid composites

- Infrastructure
- Interfaces and interphases
- Interlaminar reinforcements
- Joint and bearing behaviour
- Life cycle analysis and sustainability
- Low cost technologies
- Mechanical and physical properties
- Metal matrix composites
- Multifunctional composites
- Multiscale modelling
- Nanocomposites
- Nanotechnologies
- NDE technologies

- Polymer matrix composites
- Probabilistic approaches and design
- Processing and manufacturing technologies
- Recycling
- Repair technologies
- Sandwich technologies
- Standardisation
- Structural design
- Testing and characterization
- Textile composites

waset.org/composite-materials-conference-in-august-2022-in-amsterdam

Viscoelastic behavior of clay and slip used in ceramic

Souad Hassene Daouadji ▪ Modeling and Computational Methods Laboratory, University of Dr. Moulay Tahar of Saida, Algeria

Larbi Hammadi ▪ Laboratory of Rheology, Transport and Treatment of the Complex Fluids, University of Science and Technology, Mohamed Boudiaf, Algeria ▪ hammadi7280@yahoo.fr, larbi.hammadi@univ-usto.dz

Abdelkrim Hazzab ▪ Modeling and Computational Methods Laboratory, University of Dr. Moulay Tahar of Saida, Algeria

Abstract

In this article we studied the effect of time and mass concentration on the viscoelastic behavior of a clay and slip used in the manufacture of ceramics from CERAMIR Algeria. The generalized model of Kelvin-Voigt is successfully applied to fit the creep and recovery data and to analyse the viscoelastic properties of clay and slip. The increase of time of creep-recovery shows a slow increase in Newtonian viscosity corresponding to the steady-state and instantaneous and delayed elastic compliance. On the other hand, the increase in the mass concentration of clay causes a rapid increase in the Newtonian viscosity corresponding to the steady-state and a decrease in instantaneous and delayed elastic compliance.

Keywords: clay, slip, ceramic, viscoelastic behavior

Kulcsszavak: agyag, agyagmassza kerámia, viszkoelasztikus viselkedés

Souad HASSENE DAOUADJI
He is master in hydraulic, preparing the PHD thesis on Rheological and mechanical characteristics of ceramic slips containing additives, at University Moulay Tahar of Saida under the direction of Professor Larbi HAMMADI and Professor Abdelkrim HAZZAB

Larbi HAMMADI
Larbi Hammadi is professor in Hydraulics (University of Science and Technology of Oran) and Engineer in Mechanical Engineering. Since 2002, he is Researcher Professor at the University of Science and Technology of Oran (USTOMB) where he exercised many teaching activities. He is actually the director of Laboratory of Rheology, Transport and Complex Fluids Treatment (LRTTFC) Oran Algeria. Significant results have been obtained in recent years, for example, in emulsions for pharmaceutical use, drilling muds, vases of dams, sewage treatment plant sludge's, ceramic , polymers and cavitation. See https://scholar.google.com/citations?user=LLbBaNAAAAAJ&hl=fr&oi=ao

Abdelkrim HAZZAB
Abdelkrim Hazzab, Professor and currently works in the Department of Civil and Hydraulic Engineering, University Moulay Tahar of Saida, Algeria.He heads a research group in the Modeling and Computational Methods Laboratory, Saida University, Algeria. His research focuses on subjects in hydraulics, in particular the study and modeling of floods, solid transport, and in materials science through rheology.

1. Introduction

Clays are used in different branches of industry, such as in drilling fluids in order to control the viscosity and the yield stress of drilling muds [1-3], in ceramic industry [4], in the treatment of polluted water, for example in the adsorption of toxic organic compounds [5-6] and pharmaceutical application [7-9]. The clays are also employed as a thickener in stabilizing the oil-water emulsions [10-12]. Knowledge of rheological properties of clays plays a fundamental role in industrial application such as in a ceramic construction plant in order to determine good operating conditions of the pumps during ceramic manufacturing operations. Numerous researches have been devoted to the study of the rheological properties of suspensions of clays used in ceramics [13-14].The effect of a number of additives on rheological properties of slip of ceramic has been widely studied and it was the subject of many previous works [15] for example the sodium tripolyphosphate and sodium hexameto-phosphate [16], polyelectrolyt [17] and the non-traditional biopolymeric [18].

The main objective of this study is to achieve a fine characterization of the rheological properties of clay and slip used by the New Company of ceramic tiles of Remchi, Algeria in order to define a good condition of use of these clays for the operation of the pumps during the ceramic manufacturing operation in this factory.

2. Materials and methods

2.1 Materials and sample preparation

The Nedroma clay and slip were, recovered from the New Company of Ceramic tiles of Remchi, Algeria in powder form. The Nedroma clay as a powder was brought to the oven for 24 hours at 40 °C for dehydration then crushed and passed away a sieve of 80 μm to perform a size sorting compatible with cone and plate geometry used for rheological measurements. Then the clay powder was dispersed in the required amount of distilled water by continuous magnetic stirring at room temperature during 24 hours in order to ensure their homogenization. Note that the slip is mixed in distilled water without sieving. The *Table 1* shows the composition of slip used in this study.

Nedroma Clay	Yellow Clay	Blue Clay	Feld-spars	Sand	Lime-stone	Fire-clay
20%	20%	21%	21%	6%	7%	5%

Table 1 The composition of slip
1. táblázat Az agyagmassza összetétele

2.2 Experimental set up

The rheological measurements was performed by using a torque controlled rheometer (RS600 from Thermo-Fischer) connected to a temperature controlled water bath and equipped with a plate-cone geometry (diameter: 60 mm; angle: 2 degree; gap: 105 μm). A solvent trap was placed around the measuring device in order to minimize solvent evaporation.

3. Results and discussion

3.1 Effect of time on creep and recovery

The study was carried out on a mass concentration of 50% in slip and 55% in Nedroma clay with the following protocol: after a pre-shear at 100 s^{-1} for 60 s following a rest of 120 s after rest time we applied a constant stress of 10 Pa, in the field of linear viscoelasticity, for different durations (50 s, 150 s, 300 s and 700 s) while recording the evolution over time of the elastic

complacency during the creep phase during each duration. At the end of each phase of the creep, the stress is instantly brought back to zero and the elastic compliance is measured during the recovery phase for different durations. *Fig. 1* and *2* show the evolution of the elastic compliance of the slip and Nedroma clay as a function of time.
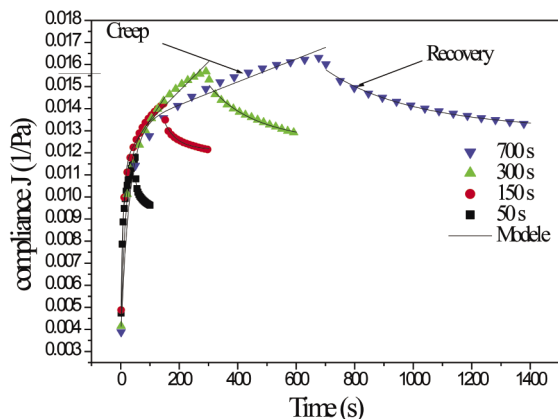

Fig. 1 Evolution of the elastic compliance of the slip as a function of time for different time applied

1. ábra Az agyagmassza rugalmassági tulajdonságának alakulása az idő függvényében

The viscoelastic behaviour were defined by correlating the results with the well-known viscoelastic models of Burger model or Generalized Kelvin–Voigt model, comprising the association in series of the Maxwell model and the Kelvin–Voigt
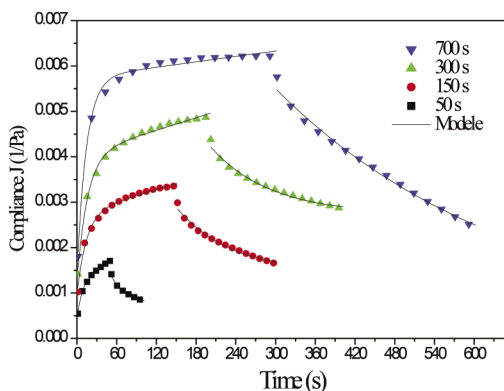

Fig. 2 Evolution of the elastic compliance of the Nedroma clay as a function of time for different time applied

2. ábra Nedroma agyag rugalmassági tulajdonságának alakulása az idő függvényében

The function of creep of this model is than written:

$$J_F = J_0 + \frac{t}{\mu_0} + \sum_{i=1}^{N} J_i \left[- \exp\left(-\frac{t}{\theta_i}\right) \right] \tag{1}$$

$$\theta_i = \frac{J_i}{\eta_i} \tag{2}$$

Whereas the recovery strain is given by:

$$J_R = \frac{t_1}{\mu_0} + \sum_{i=1}^{N} J_i \left[\exp\left(\frac{t_1}{\theta_i}\right) - \right] \exp\left(-\frac{t}{\theta_i}\right) \tag{3}$$

where J_0 is the purely elastic contribution (or the instantaneous elastic compliance), η_0 is the purely viscous contribution,

represented by the dashpot of the Maxwell model, i.e., the uncoupled or residual steady-state viscosity obtained from the creep curve at long times when the compliance curve is linear, J_i is the contribution to retarded elastic compliance, θ_i is the retarded time, η_i is the retarded viscosity and t_1 is the time where the stress is applied for $t \leq t_1$ and removed at $t = t_1$.

Fig. 3 and *4* show the evolution of the creep and recovery parameters as a function of applied time. The figures show an increase in instantaneous and delayed elastic compliance as well as Newtonian viscosity with increasing time [19]. The increase in instantaneous delayed elastic compliance and the Newtonian viscosity of the slip and the Nedroma clay with time indicating the transition from a viscoelastic regime to a viscous regime.
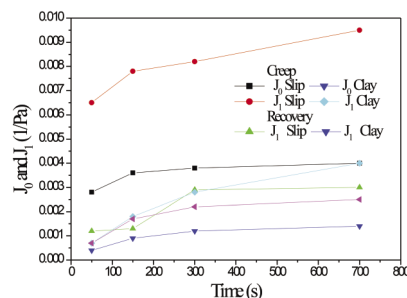
Fig. 3 Variation of the instantaneous elastic compliance J_0 and delayed J_1 of the Nedroma clay and slip of ceramic as a function of applied time

3. ábra A Nedroma agyag és agyagmassza J_0 és késleltetett J_1 pillanatnyi rugalmassági tulajdonságának változása az idő függvényében
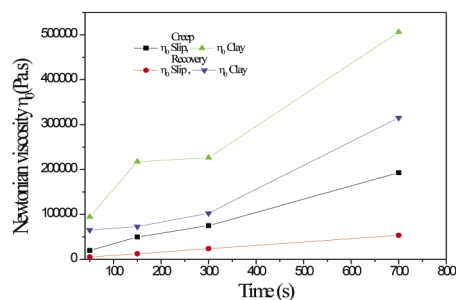
Fig. 4 Variation of Newtonian viscosity of the slip and the Nedroma clay as a function of applied time

4. ábra A Nedroma agyag és agyagmassza newtoni viszkozitásának változása az idő függvényében

3.2 Effect of mass concentration on creep and recovery of clay

The effect of mass concentration was performed only Nedroma clay for different concentration (40%, 45%, 50%, 55% and 60%). After a pre-shear at 100 s, for 60 s following a rest time of 120 s, we applied a constant stress of 2 Pa during 180 s and recording the evolution of elastic compliance during the creep phase. After 180 s the stress is instantly reduced to zero and the elastic compliance is measured during the recovery phase for a time of 180s. *Fig. 5* and *6* show the evolution of elastic compliance as a function of time for different concentration of clay.
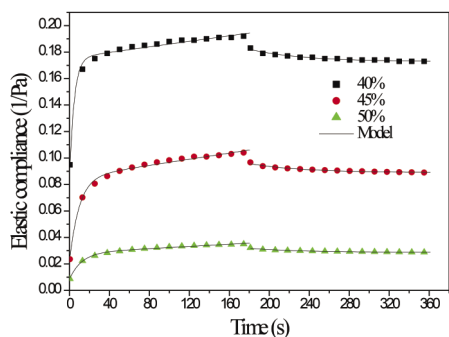
Fig. 5 Variation of elastic compliance of clay as a function of time (concentration: 40%, 45% and 50%)

5. ábra Agyag rugalmassági tulajdonságában változása az idő függvényében (40%, 45% és 50%-os kocentráció esetén)

Fig. 7 Variation of instantaneous elastic compliance J_0 and retarded elastic compliance J_1 of Nedroma clay as a function of mass concentration

7. ábra Nedroma agyag J_0 pillanatnyi rugalmas összeférhetőségének és J_1 késleltetett rugalmassági tulajdonságának változása az agyagtartalom függvényében

We observed in *Fig. 5* and *6* for weak concentrations of clay the deformation the clay during the creep phase is much greater and the system quickly relaxes during the recovery phase, we can explain this phenomena by weak liaisons of the internal structure of the clay on the other hand for high mass concentrations of clay the deformation during the creep phase becomes weak and the system slowly relaxes in this case the liaisons of the internal structure of the clay becomes rigid.

Fig. 8 Variation of Newtonian viscosity as a function of mass concentrations of clay

8. ábra A newtoni viszkozitás változása az agyagtartalom függvényében

4. Conclusions

The viscoelastic properties of clay and slip used in the manufacture of ceramic by New Company of Ceramic tiles of Remchi, Algeria at different times and mass concentration were studied. The generalized Kelvin-Voigt model was chosen to adjust the dependence of elastic compliance as a function of time for creep and recovery times range between 50 s and 700 s and mass concentrations range between 40% and 60% in solid particles. The increase in the creep-recovery applied time shows a slow increase in the Newtonian viscosity 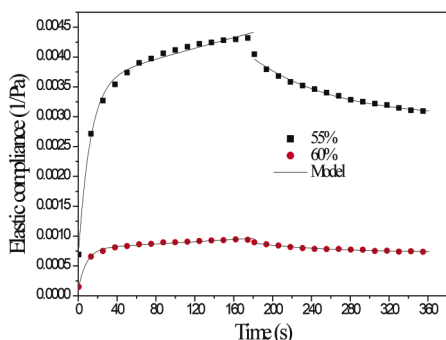of the clay and of the slip corresponding to the steady state and of the instantaneous and delayed elastic compliance. For a creep-recovery time, the study shows that the concentration of 40% to 60% causes a rapid increase in the Newtonian viscosity of Nedroma clay. The study also shows a decrease in instantaneous elastic compliance J_0 and delayed J_1 of clay with mass concentration.

Fig. 6 Variation of elastic compliance of clay as a function of time (concentration : 55% and 60%)

6. ábra Agyag rugalmassági tulajdonságában változása az idő függvényében (55% és 60%-os kocentráció esetén)

The evolution of elastic compliance as a function of time for different mass concentrations of clay was correlated using the generalized Kelvin-Voigt model (*Eqs. 1* and *3*). *Fig. 7* shows a decrease in instantaneous elastic compliance J_0 and retarded elastic compliance J_1 of Nedroma clay with mass concentration. On the other hand, *Fig. 8* shows an increase in Newtonian viscosity with the mass concentration of clay. Although these suspensions are initially formed from viscoelastic networks, they quickly disintegrate with concentration. A strong increase in Newtonian viscosity is observed for strong concentrations. In this case, the shear stress of 2 Pa is not sufficient to break weak particle-to-particle bonds of the clay and the suspension does not flow.

References

[1] BS., Bageri – AR., Adebayo- JAL., Jaberi – S., Patil (2020): Effect of perlite particles on the filtration properties of high-density barite weighted water-based drilling fluid. Powder Technology. Vol.360 pp1157–1166, https://doi.org/10.1016/j.powtec.2019.11.030.

[2] L., Hammadi - N., Boudjenane - M., Belhadri (2014): Effect of polyethylene oxide (PEO) and shear rate on rheological properties of bentonite clay. Applied Clay Science. Vol. 99, pp. 306-311, https://doi.org/10.1016/j.clay.2014.07.016.

[3] R., Jain - V., Mahto (2015): Evaluation of polyacrylamide/clay composite as a potential drilling fluid additive in inhibitive water based drilling fluid

system. Journal of Petroleum Science and Engineering Vol.133, pp. 612-621, https://doi.org/10.1016/j.petrol.2015.07.009.

[4] MHA., Aziz –MHD., Othman-NA., Hashim- MR., Adam-A., Mustafa (2019): Fabrication and characterization of mullite ceramic hollow fiber membrane from natural occurring ball clay. Applied Clay Science. Vol. 177, pp. 51-62, https://doi.org/10.1016/j.clay.2019.05.003

[5] H., Han – MK., Rafiq – T., Zhou – R., Xu –O.,Mašek –X., Li (2019): A critical review of clay-based composites with enhanced adsorption performance for metal and organic pollutants. Journal of hazardous materials Vol.369, pp. 780-796, https://doi.org/10.1016/j.jhazmat.2019.02.003.

[6] AM., Awad- SM., Shaikh – R., Jalab – MH., Gulied –MS., Nasser –A., Benamor –S., Adham (2019) : Adsorption of Organic Pollutants by Natural and Modified Clays: A Comprehensive Review. Separation and Purification Technology. Vol. 228, pp. 115719, https://doi.org/10.1016/j.seppur.2019.115719.

[7] H., Kohay – II., Bilkis –YG., Mishael (2019): Effect of polycation charge density on polymer conformation at the clay surface and consequently on pharmaceutical binding. Journal of colloid and interface science. Vol.552, pp.517-527, https://doi.org/10.1016/j.jcis.2019.05.079.

[8] S., Gamoudi –E.Srasra (2017): Characterization of Tunisian clay suitable for pharmaceutical and cosmetic applications. Applied clay Science. Vol.146, pp.162-166, https://doi.org/10.1016/j.clay.2017.05.03.

[9] T., Thiebault – M., Boussafir – L., Fougère –E., Destandau –L., Monnin –C., LeMilbeau (2019) : Clay minerals for the removal of pharmaceuticals: Initial investigations of their adsorption properties in real wastewater effluents. Environmental Nanotechnology, Monitoring & Management. Vol.12 , pp. 100266, https://doi.org/10.1016/j.enmm.2019.100266.

[10] M., Khalid – A. Sultan –MN. Noui-Mehidi –A. Al-Sarkhi –O. Salim (2020): Effect of Nano-Clay Cloisite 20A on water-in-oil stable emulsion flow at different temperatures. Journal of Petroleum Science and Engineering. Vol. 184, pp. 106595, https://doi.org/10.1016/j.petrol.2019.106595.

[11] H., Nciri – M., Benna-Zayani-M., Stambouli –N., Kbir-Ariguib –M., Trabelsi-Ayadi M-V., Rosilio –JL., Grossiord (2009): Influence of clay addition on the properties of olive oil in water emulsions. Applied Clay Science. Vol.43, pp.383-391, https://doi.org/10.1016/j.clay.2008.11.006.

[12] SM., Shaikh –MS., Nasser – I., Hussein –A., Benamor-SA. Onaizi –H., Qiblawey (2017): Influence of polyelectrolytes and other polymer complexes on the flocculation and rheological behaviors of clay minerals: A comprehensive review," Separation and Purification Technology. Vol.187, pp.137-161, https://doi.org/10.1016/j.seppur.2017.06.050.

[13] L., Hammadi (2018): Improving of the mechanical and rheological properties of slip of ceramic. Construction and Building Materials. Vol.173pp.118-123, https://doi.org/10.1016/j.conbuildmat.2018.04.035.

[14] YA. Klimosh- IA., Levitskii (2004): Rheological properties of slips based on polymineral clays with electrolyte additives. Glass and Ceramics. Vol. 61, pp.375-378, https://doi.org/10.1007/s10717-005-0006-4.

[15] OA., Slyusar- V. M., Uvarov (2017): Effect of complex additives on ceramic slip mobility. Glass and Ceramics. Vol.74, pp.110-111, https://doi.org/10.1007/s10717-017-9940-1.

[16] A. Slyusar –O., Slyusar –N. Zdorenko (2008): Rheological properties and critical structure-forming concentration of kaolin suspensions with complex additives. Glass & Ceramics. Vol. 65, pp.285-286, https://doi.org/10.1007/s10717-008-9060-z.

[17] P., Marco – J., Labanda-J.Llorens (2004): The effects of some polyelectrolyte chemical compositions on the rheological behaviour of kaolin suspensions. Powder Technology. Vol.148, pp. 43-47, https://doi.org/10.1016/j.powtec.2004.09.019.

[18] T., Žižlavský- M., Vyšvařil-P., Rovnaníková (2019): Rheology of natural hydraulic lime pastes modified by non-traditional biopolymeric admixtures. Epitoanyag-Journal of Silicate Based & Composite Materials. Vol.6, pp. 204-209, https://doi.org/10.14382/epitoanyag-jsbcm.2019.36

[19] MMS., Quiambao-DD.,Laplana- MID.,Abobo- AG., Jancon- SD., Salvador-HC., Siy (2019): Rheological characterization of the curing process for a water-based epoxy added with polythiol crosslinking agent. Epitoanyag-Journal of Silicate Based & Composite Materials. Vol.71,No.5,pp.162-167, https://doi.org/10.14382/epitoanyag-jsbcm.2019.28.

Reliability analysis of compaction characteristics of tropical black clay admixed with lime and iron ore-silica based dominant tailing

Paul YOHANNA ▪ Department of Civil Engineering, University of Jos, Plateau State, Nigeria
Roland K. ETIM ▪ Department of Civil Engineering, Akwa Ibom State University, Ikot Akpaden, Nigeria ▪ rolandkufre24@gmail.com
Thomas S. IJIMDIYA ▪ Department of Civil Engineering, Ahmadu Bello University, Zaria, Nigeria
Kolawole J. OSINUBI ▪ Department of Civil Engineering, Ahmadu Bello University, Zaria, Nigeria
John M. BUKI ▪ Department of Civil Engineering, Ahmadu Bello University, Zaria, Nigeria

Paul YOHANNA
is a Lecturer in the Department of Civil Engineering, University of Jos, Nigeria. He specializes in Geotechnical and Geo-Environmental Engineering. His current research effort is focused on sustainable and eco-friendly materials for Civil Engineering works

Roland K. ETIM
is a Lecturer in the Department of Civil Engineering, Akwa Ibom State University, Ikot Akpaden, Nigeria. His research interest is in the field of Geotechnical and Geo-Environmental Engineering as well as sustainable cleaner materials for Civil Engineering infrastructures. He is a member of several Professional societies.

Thomas S. IJIMDIYA
is a Professor in the Department of Civil Engineering, Ahmadu Bello University, Zaria, Nigeria. His research interests include Geotechnical and Geo-Environmental Engineering. He is a member of several professional societies.

Kolawole J. OSINUBI
is a Professor in the Department of Civil Engineering, Ahmadu Bello University, Zaria, Nigeria. His research interests include Geotechnical and Geoenvironmental Engineering. He is a member of several professional societies

John M. BUKI
is B.Eng. and M.Sc. in Civil Engineering from Ahmadu Bello University Zaria. He is currently the Manager of Engineering marketing in China Harbour Engineering Company, Abuja.

Abstract

Reliability estimates of compaction characteristics of lime-iron ore tailings (IOT) modified tropical black clay (i.e black cotton soil, BCS) for use as road construction material was carried out. A model was generated from measured laboratory test results, and then used in a FORTRAN-based first-order reliability program (FORM) to generate reliability indices (RI). Samples tested in the laboratory were subjected to index tests and British standard light (BSL) compaction test. In the midst of all the variables, specific gravity (Gs) recorded the greatest significant effect followed by sand content (Sa) and then Iron ore tailing (IOT) and Lime (Li) content on MDD. In the case of optimum moisture content (OMC), specific gravity (Gs), iron ore tailing content (IOT) and lime content (Li) has the most significant influence on OMC followed by sand content (Sa). Generally, RI values were less than 1.0 and thus fails to meet the conditions of Nordic Committee on Building Regulation (NKP) for serviceability limit state design. Stochastically, BSL compactive efforts recorded positive results but did not meet the requirement for modeling compaction characteristics of lime-IOT treated BCS as pavement sub-base material. Finally, higher compactive effort is recommended to model compaction characteristics of lime-IOT treated BCS in other to achieve more effective RI which that can be prudently examined during field compaction.
Keywords: reliability index, reliability analysis, tropical black clay, lime, iron ore tailings, compaction characteristics
Kulcsszavak: megbízhatósági index, megbízhatósági elemzés, trópusi fekete agyag, mész, vasérc zagy, tömörítési jellemzők

1. Introduction

The overall performance of a designed engineering infrastructure depends on the magnitude of induced load as well as the mechanical strength and stiffness. Köhler [1] reported that this performance is a function of the factor of safety or reliability of structural component against failure. In other words, failure due to collapse or deflection or any other mode that may result to consequential damages in cost, loss of lives and over bearing influence to the environment are of interest [1].

The design of any engineering structure should ultimately meet the safety requirement without compromising basic condition of functionality, aesthetics and cost or economy value [2]. When an engineering structure bears a load, the expected reaction is dependent on load magnitude, load type and the structural stiffness and strength. The response of an engineering structure to loading should be considered satisfactory relative to how well it meets safety requirement [3].

Recent researches in modern times have applied the technique of reliability estimation in evaluating diverse engineering functions [4-7]. The results recorded some innovative approach which has shown varieties of far reaching outcome [8]. Before the advent of optimization by reliability approach, inspection of structural members and subsequent approval for maintenance activities were exclusively centred on past engineering evaluations, experiences and judgement. Also, probability theory and functions in which random statistical variables such as coefficient of variations (COV), mean values and standard deviations were use has presented increasing success in a broad scope of engineering designs and applications [9].

It has been reported by Oriola and Moses [10] that expansive soils referred to as "black cotton soil (BCS)" in some world regions exhibit some form of undesired engineering characteristics. Most expansive soils have varying colours that could be either light to dark grey. BCS are found in tropical and temperate zones of the semi-arid regions where the rate of annual evaporation surpasses the rainfall [11, 12]. Black cotton soils cover an approximated land area of about $104 \times 10^3 \, km^2$ in Northeastern Nigeria [13]. Montmorillonite clay mineral in BCS is responsible for the unprecedented rate of swell or shrink during wet and dry seasons, respectively [14].

The probabilistic based methods of measuring uncertainties in structural engineering [15-18], pavement design [19-

22] and geotechnical engineering [23-25], has been largely successful. The First Order Reliability Method (FORM) integrated in FORTRAN program was employed to measure the suitability of BCS-Li-IOT admixtures as sub-base structure in road construction. This research is centred on developing a procedure that could be useful in estimating the structural RI for the stabilization potential of Li-IOT-BCS blend as road sub-base materials. The objectives of the study are but not limited to evaluating the influence of admixtures (lime and iron ore tailing), particle sizes (gravel, sand and fine content), specific gravity as well as COV on RI for BCS using BSL compaction energy.

2. Theoretical background of reliability index

The factor of safety i.e., reliability or safety index, β is an important parameter used in appraising the competence of engineering design. The safety index is a function of the ratio between the mean and standard deviation of the safety margin of the system expressed as;

$$\beta = \frac{\mu}{d} \qquad (1)$$

where β = the safety index or reliability index, μ = the mean value of the safety margin and d = the standard deviation. Alternatively, it is expressed as the number of standard deviation dx between the mean of the safety margin.

$$E(s) = \mu \qquad (2)$$

Also, critical value expressed as

$$S = 0 \qquad (3)$$

Also, the RI also expressed as β is the inverse of the COV of the safety margin $(COV)_s$ [26], that is

$$\beta = \frac{1}{(COV)_s} \qquad (4)$$

The principle of First Order Reliability Method (FORM) is based on the probabilistic and deterministic approaches of design which differ in principle as applied in different engineering uses. The deterministic optimization design approach is based on design which is constrained to the design limit with no room for uncertainties i.e the likelihood of failure is completely eliminated [4, 7, 27]. Probabilistic design measure of a pavement or structure is concerned with the certainty or probability of assurance that is able to realize the post-construction functions associated or assigned to it [28]. This functions are unconnected with basic engineering properties characterised for the purpose which in the case of a sub-base pavement are compaction behaviour, index properties and ultimately the CBR [27, 29]. In order to study the effect of the variables on the system performance, a limit state equation (LSE) in relations to the design variable is mandatory [28]. This LSE is stated as performance function and is defined as:

$$G(t) = G(X_1 X_2 X_3 X_n) \qquad (5)$$

Where X_i for I = 1, 2, 3,……...n, denote the basic design variables. The system limit state is thus defined as

$$G(t) = 0 \qquad (6)$$

It has been reported by Duncan [30] that reliability computations require a process of assessing the joint effects of unlikelihood and also a way of differentiating between circumstances where indecision varies. Probabilistic concept of reliability analysis is suitable for evaluating the uncertainties that is involved in the choice of value for a soil variable in geotechnical analysis [30]. If the mean, variance, standard deviation etc associated with the distribution of a probability function for K are established, then the soil reliability can be evaluated from *Eq. (7)*. The potential of *Eq. (7)* is possible only with the probability of survival as given in *Eq. (8)*:

$$P_s = 1 - P_f \qquad (7)$$

Where P_s = probability of survival and P_f = probability of failure. The probability of failure (Pf) can then be formulated as:

$$P_f = P(K_0 - K_e(Li, IOT, Sa, F \ and \ Gs) < 0) \qquad (8)$$

where: Ke and Ko are expected compaction properties (MDD and OMC) and compaction properties (MDD and OMC) of untreated soil, respectively. The probability of failure depends absolutely on the Lime (Li), IOT (iron ore tailing), Sa (sand), and Fine (F) content and specific gravity, (G_s)

3. Materials and methods

The clay sample was sourced from Dandin Kowa which is 30 km from Gombe town in Gombe State, Nigeria. Iron ore-silica based tailing waste was procured from a mining site in Itakpe, Nigeria. Lime (Li) was sourced from an open market in Kaduna State. The composition of tailing and lime used had been reported in [33]. The database results used for this analysis were extracted from analysis of laboratory experiments of an unpublished work [31] on Li-IOT modification of BCS. The statistical properties of the compositional and compaction variables for the Li-IOT treated soil are given *Table 1*. A conceptual regression models (as shown in *Eq. 9* and *10*) were developed for predicting MDD and OMC. The Mini-tab R15 statistical software tool was used to establish the basic statistics for the various compositional variables/constraints. The potentials of Li-IOT combination on the compaction parameters (MDD and OMC) of BCS was assessed using first order reliability methods' version 5.0 (FORM 5) written in FORTRAN language. The statistical properties of the various compositional variables (MDD and OMC), Li, IOT, Gr, Sa, F content and Gs) as well as their probability distribution functions forms were conventionally proven and well established. The various statistical properties (mean, standard deviations and coefficient of variations) for Li-IOT mixtures were then integrated into a FORTRAN based program for a field based predictive model. Response to sensitivity study for each of the independent variables, their impact on compaction characteristics was accomplished by varying the assumed values of COV ranging from 10-100% in step of 10% to obtain reliability/safety indices or β-values. The β-values for the dependent (MDD and OMC) and independent (Li, IOT, Gr, Sa, F content and Gs) variables were evaluated.

$$MDD = 2.475 - 0.0105Li + 0.00831IOT - 0.0086Gr + 0.00Sa - 0.0046F + 5.415Gs \qquad (9) \ R^2 = 91.4$$

$$OMC = 32.684 + 0.2498Li - 0.1722IOT - 0.146Gr + 0.00Sa - 0.0133F - 3.461Gs \qquad (10) \ R^2 = 89.8$$

S/No	Variables	Distribution type	Mean E(x)	Standard deviation S(x)	Coefficient of Variation COV (%)
1	Maximum dry density	Lognormal	15.77	0.28	56.32
2	Optimum moisture content	Lognormal	22.42	0.92	24.37
3	Lime content	Normal	2.00	1.44	1.39
4	Iron ore tailings content	Normal	5.00	3.47	1.44
5	Gravel content	Normal	1.05	0.93	1.13
6	Sand content	Normal	21.29	4.04	5.27
7	Fine Content	Normal	77.66	4.07	19.08
8	Specific gravity	Normal	2.52	0.04	63.00

Table 1   Compositional parameters from laboratory measured compaction characteristics for reliability based design for seven independent variables using FORM 5

1. táblázat   A kompozíciós paraméterek laboratóriumban mért tömörítési jellemzőkből a megbízhatóság alapú tervezéshez (hét független változó a FORM 5 szoftverhez)

4. Results and discussions

4.1 Effect of lime and iron ore tailing on compaction characteristics

It is obvious that the results from the conceptual model revealed a robust connection between soil dependent variable (MDD) and the soil independent variables (Li, IOT, Gr, Sa, F content and Gs) with correlation coefficient R= 0.914 (see *Eq. 9*). Multiple regression analysis revealed that the MDD was much more influenced by IOT content and Gs with higher values of positive coefficients. The indication from this study suggests that the higher positive coefficients could be ascribed to the higher Gs value of IOT (3.29) replacing the soil particles with lower Gs (2.47). This finding is in agreement with Sani et al., [6] which showed that Gs provide a valid parameter and was used jointly with other variables for developing a predictive model for MDD. The possible explanation to the negative coefficient of lime content in the regression model (see *Eq. 9*) may be linked to lower specific of lime (2.14) when related to that of the natural soil (2.47) thereafter causing a reduction in the MDD values. This implies that lime has little impact on the MDD and care need be taken to certify that an optimum blend is used in the course of field compaction of BCS- lime-IOT mixtures. Similarly, a strong relationship was expressed by the multiple regression model between soil OMC (dependent variable) and soil multiple independent variables (Li, IOT, Gr, Sa, F content and Gs), with correlation coefficient R= 0.898 (see *Eq. 10*). Results showed that the OMC was much more influenced by lime content and specific gravity with higher coefficients. This implies that lime has positive impact on the optimum moisture content and control of admixtures content should be adequately supervised to guarantee optimum blend of lime is used in the course of field compaction of BCS- lime-IOT mixtures.

4.2 Comparison between measured and predicted values of regression model

Results of laboratory estimates of MDD showed a strong relationship with its predicted estimates, and having coefficient of correlation R=0.963 (see *Fig. 1*). In the case of OMC, results showed a strong relationship between the measured OMC attained in the laboratory and the predicted results achieved with the model having correlation coefficient R=0.950 (see *Fig. 2*). Findings from the models suggest that the correlation coefficient values validate the combined effect of the various parameters (independent variables) in predicting MDD and OMC. This point toward the fact that specification during field compaction and control can easily be checked by a good measure of moisture that will yield an adequate dry density. This could simply be controlled using those variables in field application.
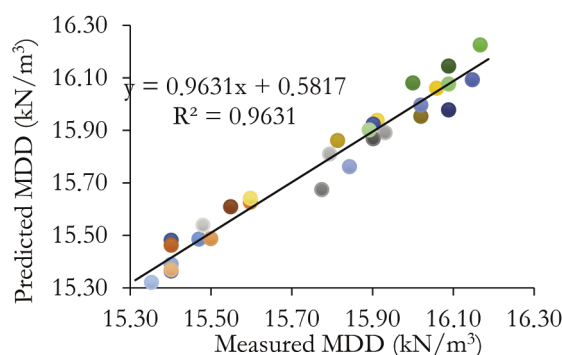
Fig. 1   Predicted MDD versus measured MDD values for the various Li-IOT-BCS mixtures

1. ábra   A becsült MDD értéke a mért MDD értékek függvényében a különböző Li-IOT-BCS keverékeknél
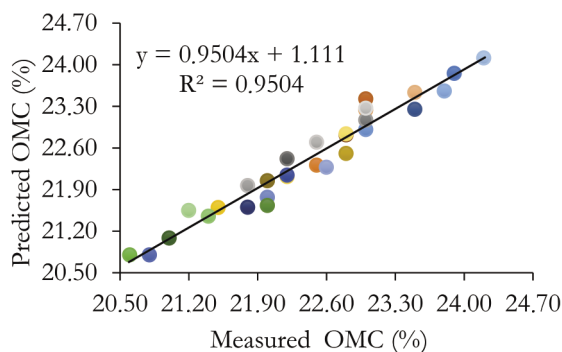
Fig. 2   Predicted OMC versus measured OMC values for the various Li-IOT-BCS mixtures

2. ábra   A becsült OMC értéke a mért OMC értékek függvényében a különböző Li-IOT-BCS keverékeknél

4.3 Reliability estimate on compaction characteristics

4.3.1 Effect of MDD and OMC on reliability index

The effect of MDD and OMC on RI as the COV is varied is shown in *Fig. 3*. MDD yielded a linear but declining trend as the COV increased in step of 10% from 10 to 100%. Consuently, as COV increased from 10 to 100%, RI reduced from -0.16 to -0.436. When MDD value of 15.47 kN/m³ for the unmodified soil was used, the RI value reduced from -0.459 to -0.401. Comparatively, the Li-IOT modified soil recorded higher RI values than the unmodified (natural soil). These observations

indicate that there is a far reaching enhancement on the MDD of the soil mixed with lime-IOT blends. Basically, the significant alteration in RI is sign that compaction properties could have a far-reaching influence on the RI for a sub-base material of road pavement. For OMC, RI decreased linearly from -0.365 to -0.456. Similarly, when RI was computed with OMC value of 23% for the unmodified BCS, the value dropped linearly from -0.121 to -0.425. Comparatively, lower RI values (-0.365 to -0.456) were documented for the Li-IOT treated BCS soil than the natural BCS (-0.121 to -0.425). These observations indicate that there is no significant improvement on the OMC of the soil with increased in Li-IOT blends.
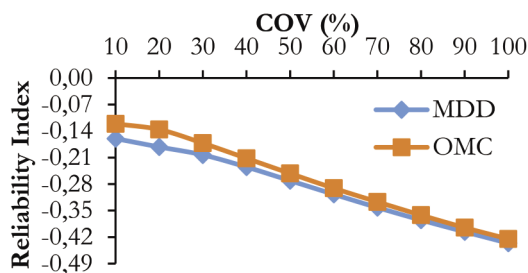
Fig. 3   Relationship between reliability index and COV for compaction characteristics
3. ábra   A megbízhatósági index és a COV közötti összefüggés a tömörítési jellemzőkhöz

4.3.2 Effect of lime content on reliability index of compaction characteristics

Changes in RI for lime content of Li-IOT treated soil with COV is displayed in *Fig. 4*. The RI marginally increased from -0.723 to -0.722 and -0.693 to -0.634 for MDD and OMC, in that order. This show that lime content is a parameter which should be cautiously controlled in soil improvement using Li-IOT. When estimated with unmodified soil of MDD and OMC value of 15.47 kN/m³ and 23%, in that order; the RI ranged from -1.53 to -1.53 and -0.175 to -0.16 for MDD and OMC, in that order. It is evident that lime has no drastic effect on MDD since no reasonable variation in RI was observed for MDD of the untreated soil.

Fig. 4   Relationship between reliability index and COV for lime content
4. ábra   A megbízhatósági index és a COV közötti összefüggés a mész tartalomhoz

4.3.3 Effect of IOT content on reliability index of compaction characteristics

The change in RI for IOT content of Li-IOT treated soil with COV (i.e 10-100%) is revealed in *Fig. 5*. The RI ranged from -0.723 to -0.722 and -0.763 to -0.587 for MDD and OMC in that order. This suggest that iron ore tailing content is a
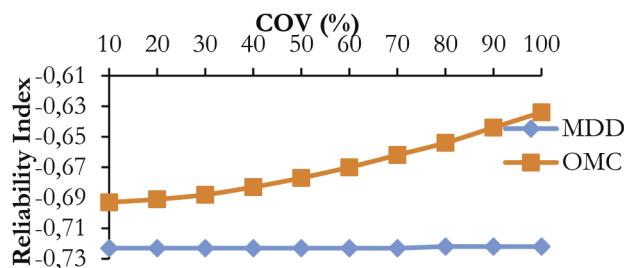
parameter which need to be prudently supervised all through field compaction for Li-IOT modified BCS. Also, a comparison of the two results (treated and untreated) for MDD reveals that a higher safety value for MDD of the treated soil (-0.723 to -0.723) is greater than the untreated soil (-1.53 to -1.52). This simply suggest that IOT has tremendous effect on the MDD safety values of Li-IOT-BCS (treated) materials for sub-base of road pavement in contrast to the MDD of the untreated (natural BCS). Also, high IOT content could well shoot up the specific gravity of the Li-IOT-BCS mixtures [32-33], which may have contributed to the increased reliability values of MDD of treated soil. This condition could also mean that adequate ground solidification would be achieved in the long run, typically after complete long term lime reaction within the entire matrix. Interestingly, the RI for OMC of treated soil (-0.763 to -0.587) is comparatively lower than the safety value of the natural soil (0.193 to −0.147). This might not be unconnected with the non-plastic attribute of IOT [32-33], which suggest that IOT could be independent of moisture content in Li-IOT-BCS matrix.

Fig. 5   Relationship between reliability index and COV for IOT content
5. ábra   A megbízhatósági index és a COV közötti összefüggés az IOT tartalomhoz

4.3.4 Effect of gravel content on reliability index of compaction characteristics

As the COV rise from 10 to 100%, the RI of MDD and OMC was slightly varied due to the effect gravel content (see *Fig. 6*). It can be noticed that gravel content has little or no effect on MDD and OMC as their safety value remained constant even as the COV increased from 10-100%. A steady safety values of -0.723 and -0.661 were estimated for MDD and OMC respectively. Also, the computed RI values of unmodified soil remain almost constant between -1.53 and -0.167 for MDD (15.47 kN/m³) and OMC (23%) value, respectively. While RI remained almost constant for both treated and untreated soil, a comparison of the two results (treated and untreated) reveals that a higher safety value for MDD of the treated soil (-0.723) is greater than the untreated soil (-1.53). This simply suggests that gravel content has tremendous effect on the MDD safety values of Li-IOT-BCS materials for sub-base of road pavement. Also, Higher MDD and as well its safety value indicates adequate ground solidification. Regardless of the reliability values, it could be said that the effect of gravel content was visible because of the considerable effect on regulating the quantity of admixtures. Interestingly, the RI for OMC of treated soil (-0.661) is relatively lower than the safety value of the natural soil (-0.167). This suggests that gravel content do not have much effect on OMC of Li-IOT stabilized BCS.

Fig. 6   Relationship between reliability index and COV for gravel content
6. ábra   A megbízhatósági index és a COV közötti összefüggés a kavics tartalomhoz

4.3.5 Effect of sand content on reliability index of compaction characteristics

Sand content produced a slightly varied RI value for MDD and OMC with COV in the range 10 to100% (see *Fig. 7*). As COV rise from 10 to100%, RI value also increased from -0.723 to -0.699 and -0.661 to -0.643 for MDD and OMC in that order. The safety values of untreated soil ranged from -1.53 to -1.48 and -0.167 to -0.162 when reliability was estimated with natural MDD (15.47 kN/m³) and OMC (23%), respectively. Comparing the two results (treated and untreated), it can be seen that the safety value for MDD of the treated soil (-0.723 to -0.699) is greater than unmodified soil (-1.53 to -1.48). This simply suggest that sand content has huge effect on the treated soil and could enhance the MDD as well as its safety values in assessing the potential of Li-IOT-BCS in sub-base structure of road pavement. In contrast, the safety index for OMC of treated soil (-0.661 to -0.643) is relatively lower than the safety value of the natural soil (-0.167 to -0.162). This results which shows a need to be explicit about the reliability of treated and untreated BCS, indicate that sand content do not have effect on OMC of Li-IOT stabilized BCS.
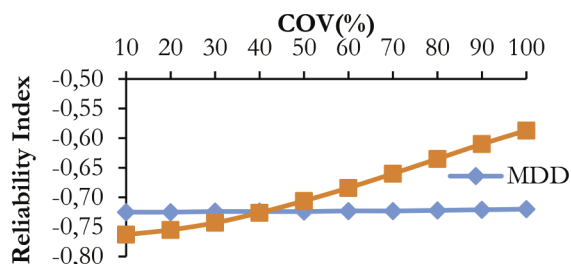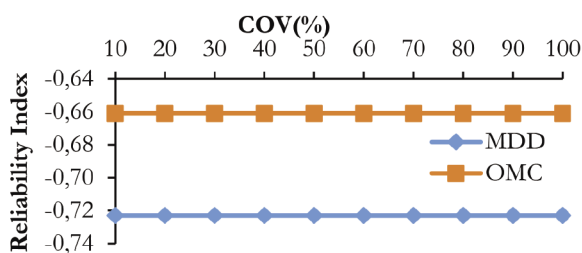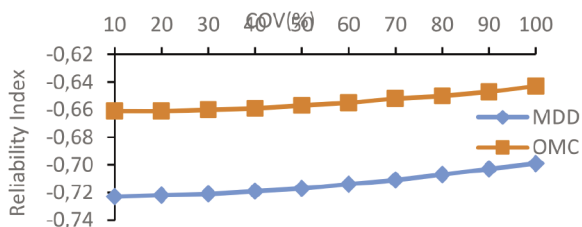

Fig. 7   Relationship between reliability index and COV for sand content
7. ábra   A megbízhatósági index és a COV közötti összefüggés a homok tartalomhoz

4.3.6 Effect of fine content on reliability index of compaction characteristics

From *Fig. 8*, it can be noticed that fine content has little or no effect on MDD and OMC as their value remained almost constant when the COV increased from 10-100%. In the case of treated soil, a continual safety index of -0.723 and -0.661 was established for MDD and OMC, in that order. When estimated with MDD and OMC value of 15.47 kN/m³ and 23% respectively for the untreated soil, β value can be seen to be constant with COV (10 to 100%) having -1.53 and -0.167 values for MDD and OMC, respectively. An assessment of the two results reveals, that the RI for MDD (-0.723) of treated soil is relatively higher than the safety value of the natural soil (-1.53). The results of this research support the idea that fine content

could have slight effect on reliability values that considerably varies from the treated soil to the untreated soil. In the case of OMC, the reverse was the case. However, the zero variation of reliability index in treated and untreated, could therefore seem that fine content may have just slight effect on MDD and OMC in contrast with other variables.
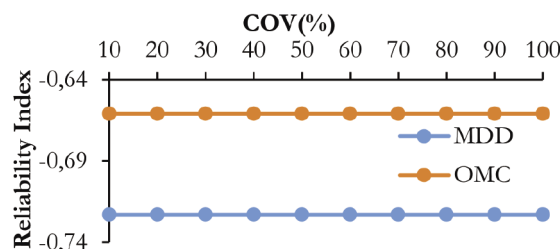

Fig. 8   Relationship between reliability index and COV for fine content
8. ábra   A megbízhatósági index és a COV közötti összefüggés a finomrész tartalomhoz

4.3.7 Effect of specific gravity on reliability index of compaction characteristics

Specific gravity impact on RI as the COV increased up to 100% is presented (see *Fig. 9*). The RI values due to the influence of specific gravity produced a semi-linear relationship with COV stretching from 10 to 100%. From the graph below, RI varied significantly. It shows that, as COV rise from 10 to 100%, reliability values correspondingly increased from -0.19 to -0.0194 and -0.534 to -0.0881 for MDD and OMC, in that order. When estimated with MDD and OMC value of 15.47 kN/m³ and 23% respectively for the unmodified soil, safety values ranged from -0.403 to -0.0411 and -0.134 to -0.0221 for MDD and OMC, respectively. Based on this analysis, it is also worth noting that safety value of MDD for treated BCS is significantly higher than the untreated soil. This simply implies that specific gravity has major effect on the MDD safety values of Li-IOT-BCS materials for construction of sub-base of road pavement. Also, higher specific gravity could translate to higher MDD as reported by [34-38]. In contrast, the RI for OMC of treated soil is relatively lower than the safety value of the natural soil. This suggests that specific gravity do not have effect on OMC of Li-IOT stabilized BCS.
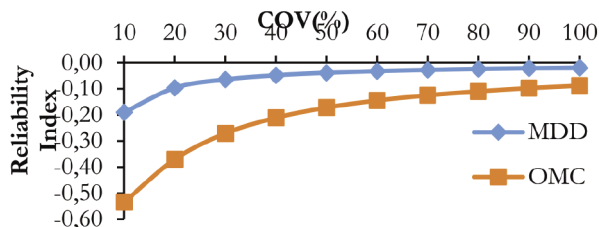
Fig. 9   Relationship between reliability index and COV for specific gravity
9. ábra   A megbízhatósági index és a COV közötti összefüggés a fajsúlyhoz

4.4 Comparison of the reliability indices of the soil compositional factors

A comparison of the reliability index (safety index or β value) for maximum dry density (MDD) showed some gradation of disparity in β - value of the variables (compositional factors) considered (*Fig. 10*). From *Fig. 10*, it can be seen that the greatest

β - value of all the compositional factors is specific gravity (Gs) which in other words generated the highest considerable influence in contrast with sand content(Sa) followed by Iron ore tailing (IOT) and Lime(Li) content. The gravel content (Gr) and percentage fines have insignificant outcome by way of their values remaining almost unchanged at all values of 10 – 100% COV input. The order of response to sensitivity analysis which can also be used to measure the influence of each of the compositional variable as they affect MDD can be represented as; Gs > Sa > IOT > Li > Gr > F. With recourse to *Fig. 11* showing the case of OMC, it can be well appreciated that the maximum range of β - value of all the compositional properties is specific gravity (Gs) which in other words brings about the most considerable influence on OMC in contrast with IOT followed by lime (Li) and then sand (Sa). The gravel content (Gr) and percentage fines have insignificant outcome by way of their values continuing unchanged at all values of 10 – 100% COV input. The order of response to sensitivity analysis that measured the influence of each of the compositional variable as they affect OMC can best be represented as; Gs > IOT > Li > Sa > Gr > F. From the results of reliability index, it could be observed that IOT and lime content has effect on both the MDD and OMC which is also a function of the molding water content available for compaction. This could depict sensitivity of compaction characteristics to the amount of IOT and lime content of the soil. The mechanism of reaction aided by the chemical compositions of materials (BCS, lime and IOT) could also be responsible for the varying changes observed from the laboratory result thereby having effect on the sensitivity analysis. These reasons explain why; exercising caution should be paramount to achieving adequate quality control of those compositional factors. This is much needed and is absolutely important during field compaction of the soil in placement for use as embankment or as road sub-base structural materials in pavement structure. Therefore, it can be understood that the satisfactory use of Li-IOT treated BCS soil to achieve good sub-base structure for a flexible pavement is a function of numerical significance of RI values based on the existing model established from the laboratory results.

Fig. 10 RI versus COV for MDD - BSL and compositional factors of BCS – Li – IOT combination

10. ábra RI a COV függvényében az MDD - BSL-re és a BCS - Li - IOT kombináció összetételi tényezőire

Fig. 11 RI versus COV for OMC -BSL and compositional factors of BCS – Li – IOT combinations
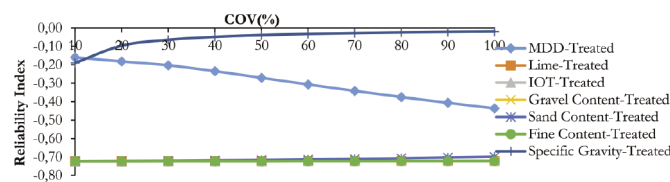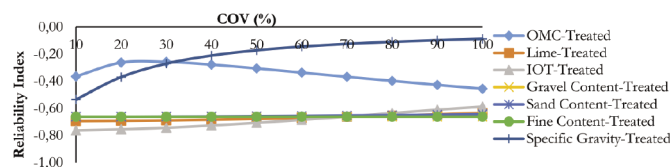
11. ábra RI a COV függvényében az OMC - BSL-re és a BCS - Li - IOT kombináció összetételi tényezőire

4.5 Statistical significance of reliability indices

The measure of statistical significance of RI on compaction parameters validate the reliability analysis that allow the study to come out with concrete decision. The decision making depends on the p-value (alpha) established. If the observed p-value is such that it is less than alpha, the outcome can be seen as statistically significant. Statistical examination of all the results acquired at 95% significant level by using the statistical F-distribution test recorded from the ANOVA test indicate that all variables have significant effect on MDD and OMC (statistical significance) (see *Table 2*). Therefore, all the variables should be carefully monitored as they bid direct effect on the compaction parameters (MDD and OMC).

4.6 Stochastic model evaluation on compaction characteristics

The evaluation of safety index was compared with the specified lowest safety index (1.0) for serviceability limit state design (*Table 3*). With variation in COV, it can be seen from *Table 3* that the beta values for all variables were less than 1.0 which of course fall shot the lowest safety index required for serviceability limit state design [39, 40].

Com-paction property	Vari-able	Source of variation	Degree of freedom	F-value calcu-lated	P- value	F-value critical	SS
MDD	MDD	COV	1	33.350	1.79E-05	4.414	SS
OMC	OMC	COV	1	33.416	1.77E-05	4.414	SS
MDD	Li	COV	1	33.873	1.63E-05	4.414	SS
OMC		COV	1	33.808	1.65E-05	4.414	SS
MDD	IOT	COV	1	33.873	1.63E-05	4.414	SS
OMC		COV	1	33.829	1.65E-05	4.414	SS
MDD	Gr	COV	1	33.873	1.63E-05	4.414	SS
OMC		COV	1	33.798	1.65E-05	4.414	SS
MDD	Sa	COV	1	33.862	1.64E-05	4.414	SS
OMC		COV	1	33.790	1.66E-05	4.414	SS
MDD	F	COV	1	33.873	1.63E-05	4.414	SS
OMC		COV	1	33.798	1.65E-05	4.414	SS
MDD	Gs	COV	1	33.067	1.89E-05	4.414	SS
OMC		COV	1	33.254	1.82E-05	4.414	SS

SS = statistically significant at 5%

Table 2 ANOVA of reliability index values for compaction characteristics
2. táblázat A megbízhatósági index varianciaanalízisének értékei a tömörítési jellemzőkre

Variable	Beta Value		Acceptable Range of COV (%)	
	MDD	**OMC**	**MDD**	**OMC**
MDD	-0436 to -0.16	-	Nil	Nil
OMC	-	-0.456 to -0.365	Nil	Nil
Li	-0.723 to-0.722	-0.693 to -0.634	Nil	Nil
IOT	-0.725 to -0.72	-0.763 to -0.587	Nil	Nil
Gr	-0.723 to -0.723	-0.661 to -0.661	Nil	Nil
Sa	-0.723 to -0.699	-0.661 to -0.643	Nil	Nil
F	-0.723 to -0.723	-0.661 to -0.661	Nil	Nil
Gs	-0.19 to -0.0194	-0.534 to -0.0881	Nil	Nil

Table 3 Model estimation of acceptable reliability indices
3. táblázat Az elfogadható megbízhatósági indexek modellbecslése

5. Conclusions

A predictive model was established from laboratory results derived from British standard light (BSL) compaction and other associated soil variables (IOT, lime, Gs, Gr, Sa, F). Estimates of compaction characteristics of compacted Li-IOT treated BCS as structural sub-base formation for road pavement was implemented by integrating a predictive model into a FORTRAN-based first-order reliability program so as to estimate RI values for all the compositional variables. Specific gravity (Gs) show the most significant influence among all the compositional parameters followed by sand content(Sa) and then Iron ore tailing (IOT) and Lime(Li) content on MDD. In the case of OMC, specific gravity (Gs), iron ore tailing content (IOT), lime content (Li) and Sand content (Sa) compositional variables show high significant influence consecutively, on OMC. Although the beta values for all compositional values show significant influence on MDD and OMC, however, the safety index produced fall short of 1.0 as stated by the NKP for serviceability limit state design. From the results of reliability analysis, it could be observed that IOT and lime content has effect on both the MDD and OMC which could be related to the reaction mechanism initiated by the molding water content of compaction. This possibly could describe the variation of compaction characteristics due to the amount of IOT and lime content in the soil. It is thus important that caution on control of these variables is relevant in the course of field compaction specification and regulation in order to achieve a long lasting pavement. Finally, higher compactive efforts is suggested to model compaction characteristics of Li-IOT treated black cotton soil to achieve robust safety index.

References

[1] Köhler J. (2007) Reliability of Timber Structures, Unpublished Ph.D Thesis. Institute of Structural Engineering, Swiss Federal Institute of Technology, Zurich Switzerland.

[2] Clarke AB, Coverman, S.H. (1987) Structural Steelwork, limit State Design. J.W. Arrowsmith Ltd, Bristol, pp.59-62.

[3] Abubakar I, Ahmad IU (2007) Reliability Analysis of Steel Column Base Plates, Journal of Applied Sciences Research, 3(3):189-194.

[4] Moghal, AAB, Chittoori BCS, Basha, BM (2016) Effect of fibre reinforcement on CBR behavior of lime-blended expansive soils; reliability approach. Road Material and Pavement Design, http://dx.doi.org/10.1080/14680629.2016.1272497

[5] Osinubi KJ, Eberemu AO, Yohama, P, Etim, RK (2016) Reliability estimate of compaction characteristics of iron ore tailings treated tropical black clay as road pavement sub-base material, American society of Civil Engineering, Geotechnical Special publication, 271, pp 855-864. http://dx.doi.org/10.1061/9780784480144.085

[6] Sani, JE, Yohanna P, Etim KR, Osinubi JK, Eberemu, OA (2017) Reliability Evaluation of Optimum Moisture Content of Tropical Black Clay Treated with Locust Bean Waste Ash as Road Pavement Sub-base Material, Geotechnical and Geological Engineering 35:2421–2431, 2017. http://link.springer.com/article/10.1007/sl0706-017-0256-2

[7] Etim, RK, Yohanna P, Attah IC, Eberemu AO (2018) Reliability-Based Evaluation of Compaction Characteristics of Periwinkle Shell Ash Treated Lateritic soil as Road Pavement Subbase Materials, Proceedings of 2018 NBBRI International Conference, Theme: Sustainable Development Goal (SDGs) and the Nigerian Construction Industry-Challenges and the way forward. NAF Conference Centre, Abuja, 12-14th June 2018, pp. 408-420.

[8] Yang, J, - DeWolf, J.T. (2002) Reliability Assessment of Highway Truss Sign Supports, Journal of Structural Engineering, 128(11): 1429. https://doi.org/10.1061/(ASCE)0733-9445(2002)128:11(1429)

[9] Afolayan, J.O, - Nwaiwu. C.M.O. (2005) Reliability-Based Assessment of Compacted Lateritic Soil Liners, Journal of Computers and Geotechnics, Elsevier publishers, 2(7): 505-519.

[10] Oriola, F, - Moses, G (2011) Compacted Black Cotton Soil Treated with Cement Kiln Dust as Hydraulic Barrier Material, AJSIR, 2(4):521-530.

[11] Chen FH (1988) Foundation on Expansive Soils. Elsevier Scientific Publication Company, Amsterdam.

[12] Warren KW, Kirby TM (2004) Expansive Clay soil: A Widespread and Costly Geohazard, Geostrata, Geo-Institute of the American Society Civil Engineers, Jan pp. 24-28.

[13] Ola SA (1983) The Geotechnical Properties of Black Cotton Soils of North Eastern Nigeria, In S. A. Ola (ed.) Tropical Soils of Nigeria in Engineering Practice. Balkama, Rotterdam, pp. 160-178.

[14] Etim RK, Attah IC, Ekpo DU, Usanga IN (2021) Evaluation on Stabilization Role of Lime and Cement in Expansive Black Clay-Oyster Shell Ash Composite. Transportation Infrastructure Geotechnology. https://doi.org/10.1007/s40515-021-00196-1

[15] JCSS (2001) Joint Committee for Structural Safety, Probabilistic Model Code", 2001 http://www.jcss.ethz.ch/

[16] Babu GLS, Basha BM (2008) Optimum design of cantilever retaining walls using target reliability approach, International Journal of Geomechanics, 8(4):240-252.

[17] Holický M (2013) Introduction to Probability and Statistics for Engineers, Springer, Heidelberg, New York, London.

[18] Holický M (2018) Target reliability of civil engineering structures, IOP Conf. Series: Materials Science and Engineering, 365, 052002 https://doi.org/10.1088/1757-899X/365/5/052002

[19] Chou YT (1990) Reliability design procedures for flexible pavements, Journal of Transportation Engineering, 116(5):602–614.

[20] Chua KH, Kiuredhian AD, Monismith CL (1992) Stochastic model for pavement design, Journal of Transportation Engineering, 118(6):769–786.

[21] Kenis W, Wang W (1998) Pavement variability and reliability, International symposium on heavy vehicle weights and dimensions, Maroochydore, Queensland, Australia, Part 3, 1998, pp. 213–231.

[22] Kim HB, Buch N (2003) Reliability-based pavement design model accounting for inherent variability of design parameters, Transportation Research Board, 82nd Annual Meeting, Washington DC.

[23] Halim IS, Tang, WH (1991) Reliability of Undrained Clay Slope Considering Geologic Anomaly, Proceedings of 6th International. Conference on Application of Statistics and Probability in Soil and Structural. Engineering, Mexico City Mexico, 776-783.

[24] Basha BM, Babu GLS (2009) Seismic reliability assessment of external stability of reinforced soil walls using pseudo-dynamic method, Geosynthetics International, 16(3): 197–215.

[25] Basha BM, Babu, GLS (2010) Optimum design for external seismic stability of geosynthetic reinforced soil walls: reliability based approach, Journal of Geotechnical and Geoenvironmental Engineering, 136(6):797-812.

[26] Kotegoda M, Rosso R (1997) Statistics, Probability, and Reliability for Civil and Environmental Engineers," New York, McGraw-Hill.

[27] Sani JE, Bello AO, Nwadiogbu CP (2014) Reliability estimate of strength characteristics of black cotton soil pavement sub-base stabilized with bagasse ash and cement kiln dust," Civil and Environmental Research, 6(11):115–135.

[28] Afolayan JO, Abubakar I (2003) Reliability Analysis of Reinforced Concrete One-Way Slabs. The Ultimate Conditions, Nigerian Journal of Engineering, 11(2):28–31.

[29] Divinsky M, Ishai I, Livneh M (1996) Simplified generalized California Bearing Ratio pavement design equation, Transportation Research Record 1539, Transportation Research Board, National Research Council, Washington, DC, 44–50.

[30] Duncan MJ (2000) Factors of Safety and Reliability in Geotechnical Engineering, Journal of Geotechnical Geoenenviromental Engineering, ASCE, 126:307-316.

[31] Buki, JM (2016) Lime – Iron Ore Tailing Modification of Black Cotton Soil. Unpublished M.Sc. Thesis, Dept. of Civil Engineering, Ahmadu Bello University, Zaria, Kaduna State, 2016.

[32] Osinubi KJ, Yohanna P, Eberemu AO (2015) Cement Modification of Tropical Black Clay Using Iron Ore Tailing as Admixture, Journal of Transportation Geotechnics, 5:35-49. 2015.
http://dx.doi.org/10.1016/j.trgeo.2015.10.001

[33] Etim RK, Eberemu AO, Osinubi KJ (2017) Stabilization of black cotton soil with lime and iron ore tailings admixture, Journal of Transportation Geotechnics Elsevier, 10:85-95.
http://dx.doi.org/10.1016/j.trgeo.2017.01.002

[34] Moses G, Etim RK, Sani JE, Nwude M (2018) Desiccation effect of compacted tropical black clay treated with concrete waste, Leonardo Electronic Journal of Practices and Technologies, 33:69-88.

[35] Moses G, Etim RK, Sani JE, Nwude M (2019) Desiccation-Induced Volumetric Shrinkage Characteristics of Highly Expansive Tropical Black Clay Treated with Groundnut Shell Ash for Barrier Consideration, Civil and Environmental Research, 11(8):58–74.

[36] Etim RK, Ekpo, DU, Attah, IC, Onyelowe KC. (2021) Effect of micro sized quarry dust particle on the compaction and strength properties of cement stabilized lateritic soil. Cleaner Materials.
https://doi.org/10.1016/j.clema.2021.100023

[37] Attah IC, Etim RK, Yohanna P, Usanga, IN. (2021) Understanding the effect of compaction energies on the strength indices and durability of oyster shell ash-lateritic soil mixtures for use in road works. *Engineering and Applied Science Research.* 48(2):151-160.
https://doi.org/10.14456/easr.2021.17

[38] Etim, RK, Ekpo DU, Ebong UB, Usanga IN. (2021) Influence of periwinkle shell ash on the strength properties of cement-stabilized lateritic soil. Intl J. of Pavement Research Technology,
https://doi.org/10.1007/s42947-021-00072-8

[39] NKB (1978) NKB- Report No. 36. Recommendation for loading and safety regulations for structural design. Nordic Committee on Building Regulation.

[40] JCSS (1996) Joint Committee on Structural Safety. Background Documentation Eurocode 1 ENV, Part 1: Basis of Design, ECCS, Report No 94.

3rd ADVANCED

MATERIALS SCIENCE WORLD CONGRESS

MARCH 21-22, 2022

LONDON, UK

Theme " Anticipating Future Trends, New Insights, and Cutting-Edge Technologies in Materials Science andEngineering "

http://advanced-materialsscience.peersalleyconferences.com/

2 DAYS WITH MORE THAN 45 SESSIONS, KEYNOTES & TALKS

12+ INNOVATIVE FEATURED SPEAKERS

20+ HOURS OF NETWORKING EVENTS

60+ INTERNATIONAL SPEAKERS

125+ EDUCATIONAL SESSIONS

Some engineering properties of sustainable self- compacting mortar made with ceramic and glass powders

Aboubakeur BOUKHELKHAL ▪ Research Laboratory of Civil Engineering, University of Laghouat, Algeria ▪ a.boukhelkhal@lagh-univ.dz

Abderramane HAMDAOUI ▪ Research Laboratory of Civil Engineering, University of Laghouat, Algeria

Belkacem SEBGUIG ▪ Research Laboratory of Civil Engineering, University of Laghouat, Algeria

Aboubakeur BOUKHELKHAL
PhD, Associate professor at the Department of Civil Engineering, University of Laghouat, Algeria. His research interests include: self-compacting concrete, ordinary concrete, rheology, mechanical behavior and durability of concrete and mortar with ordinary Portland cement and mineral additions, effects of hot climate and elevated temperatures.

Abderramane HAMDAOUI
MSc, Department of Civil Engineering, University of Laghouat, Algeria. His research interests include: self-compacting concrete, reuse of waste and local materials, concrete technology.

Belkacem SEBGUIG
MSc, Department of Civil Engineering, University of Laghouat, Algeria. His research interests include: self-compacting concrete, reuse of waste and local materials, concrete technology.

Abstract

This work aims to produce a sustainable self-compacting mortar (SCM), by replacing a part of cement with powders from waste materials such as glass and ceramic. Nine mixtures have been prepared, one as reference mixture and includes only ordinary portland cement, and eight containing different proportions of ceramic and glass powders (5, 15, 25 and 50%). In the fresh state, two tests were carried out: slump flow and flow time. In order to evaluate the physical and mechanical properties of SCM mixtures, compressive strength, flexural strength, ultrasonic pulse velocity (UPV) and water absorption were measured. The results showed that adding glass and ceramic powders until 25% improved the fresh properties of SCM. At hardened state, replacing cement by 5% of glass and ceramic powders (GP and CP) resulted in acceptable physical and mechanical properties.

Keywords: self-compacting mortar, sustainable, ceramic and glass powders, fluidity, compressive strength, water absorption

Kulcsszavak: öntömörödő habarcs, fenntarthatság, kerámia- és üvegporok, folyékonyság, nyomószilárdság, vízfelvétel
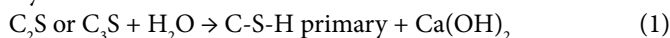
1. Introduction

Self-compacting mortar is a highly fluid mortar that can be flow and put in place without vibration or consolidation. It is generally used to formulate self-compacting concrete (SCC) when Okamura approach is used or to repair concrete structures since it can be full all formwork spaces even in narrow gaps [1]. Cement is the most expansive component in concrete and it has a negative environmental impact due to the emission of CO_2. Numerous researches were conducted around the world to produce new reduced carbon cement with low prize by using construction, industrial and agriculture wastes as fine additive materials [2-11]. Senthamarai and Manoharan [12] reported that daily production of ceramics generates about 30% of waste which their non employment poses a big environmental problem related to their deposit. Several research projects have been carried out to study the possibility of using ceramic waste as aggregates to replace natural aggregates or as filler to partially replace cement [12-14]. The use of ceramic powder (CP) in mortars and concretes results in acceptable compressive strengths with an optimal percentage of 50%. Eldieb and Kanaan [15] have shown that the addition of 10% of CP gave a concrete with good compressive strength, while a percentage ranging between 10% and 20% improved the workability retention. From durability point of view, a percentage of 40% decreased the penetration of chloride ions and permeability, and led to increase the electrical resistivity resulting in better protection against the risk of corrosion. The incorporation of CP as a filler material in the composition of SCC was found to enhance flowability and passing ability. However, the hardened properties such as strength and adhesion SCC-reinforcement

bars were negatively affected especially with the increase in the amount of CP [14]. High performance concretes have been successfully manufactured using CP with a substitution rate varying between 20% and 40% [16]. Lasseuguette et al. [17] conducted an experimental study in which two types of ceramic powder were used (white and red). They found that the white CP is more reactive, which was attributed to the difference observed in the chemical and mineralogical compositions.

A significant amount of glass waste is generates annually by production plants of glass elements (panels, mirrors, tubes and bottles), the workshops of glassworks and the population. This waste poses multiple problems, namely the hazardous effect related to their collection by cleaning agents, and the deterioration of the environment due to their deposit. The use of waste glass as fine additive material in cements and concretes is encouraging from multiple points of view. Rodier and Savastano [18] proved that the pozzolanic activity of glass powder (GP) increases with its grinding, and appears to have a better activity when is grinding to particles size less than 40 μm. Aliabdo et al. [19] have observed a linear decrease in the calcium hydroxide content with the addition of the glass powder. This is due to the reduction of the quantity of the cement is substituted by GP, and on the other hand to the pozzolanic reaction which consumes a part of C-H (*Eq. (2)*). Cement substitution with 10% and 20% GP improves the strength of concrete to fire and reduces the sorptivity [18]. In addition, concretes containing GP have developed superior resistance to freeze-thaw cycles compared to concrete without additions [20]. The combined use of GP and blast furnace slag was found to be very advantageous for both mechanical and transfer properties of concrete. The optimal binder composition

that have given the best performance in terms of compression and tensile strengths, water absorption and adhesion strength (concrete-reinforcement bars) is that containing 50% ordinary cement, 15% GP and 35% blast furnace slag [21].

Hydration reaction:

$$C_2S \text{ or } C_3S + H_2O \rightarrow \text{C-S-H primary} + Ca(OH)_2 \qquad (1)$$

Pozzolanic reaction:

$$Ca(OH)_2 + SiO_2 \text{ (glass powder)} + H_2O \rightarrow \text{C-S-H secondary} \qquad (2)$$
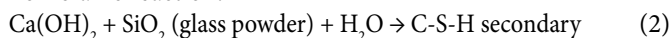
The aim of this paper is to formulate an eco-friendly self-compacting mortar by replacing ordinary cement with fine materials from glass and ceramic wastes. Fresh and hardened properties of SCM including four different ratios of glass and ceramic powders (5, 15, 25 and 50% by mass) substituted with cement have been investigated.

2. Materials

According to the European Standards EN 197-1 [22], ordinary Portland cement (CEM I 42.5) was used in all mixtures. The cementitious materials used in this study are ceramic and glass powders. Ceramic powder is obtained by cleaning and grinding the residues of ceramic elements that were collected from shops (broken or industrial fault pieces) and from waste building debris materials. Glass power is obtained from broken glass which was collected from shops in Laghouat region. *Table 1* shows the chemical composition and physical properties of the cement and mineral additives.

As fine aggregate, naturel river sand was used with a maximum size of 5 mm. The physical properties of sand are given in *Table 2*. The chemical admixture used to produce various mixtures, is a polycarboxylates based High-Range Water Reducers (HRWR). It has a specific gravity and pH of 1.07 g/cm^3 and 8, respectively.

Component	Cement	Ceramic powder	Glass powder
SiO$_2$ (%)	18.37	62.3	70.40
CaO (%)	64.04	5.94	11.20
MgO (%)	1.52	0.72	1.60
Al$_2$O$_3$ (%)	4.26	16.5	2.54
Fe$_2$O$_3$ (%)	3.89	2.37	0.37
SO$_3$ (%)	3.01	0.01	0.04
K$_2$O (%)	-	0.65	12.25
T$_i$O$_2$ (%)	-	6.78	0.36
Na$_2$O (%)	0.12	0.31	0.16
Loss ignition (%)	4.23	3.65	0.82
Specific gravity	3.1	2.6	2.7
Fineness (cm²/g)	3921	3734	2805

Table 1 Chemical composition and physicals properties of cement, CP and GP
1. táblázat Cement, CP és GP kémiai összetétele és fizikai tulajdonságai

Properties	Sand 0/5
Absorption coefficient (%)	0.59
Density	2.6
Property coefficient (%)	89

Table 2 Physical properties of fine aggregate
2. táblázat A használt homok fizikai tulajdonságai

3. Mix proportion design

Nine mortar mixtures were designed and prepared to study the effect of the ceramic and glass powders on the fresh and hardened properties of self-compacting concrete. Ceramic and glass powders were included by replacing a part of cement at substitution levels of 5, 15, 25 and 50%. In all SCM mixtures, the amount of binder, W/B ratio and dosage of SP were kept equal to 690.65 kg, 0.4 and 1.1%, respectively. The mix proportions of all SCM are given in *Table 3*.

Mixes	w/b	Cement (kg)	Ceramic powder (kg)	Glass powder (kg)	Sand (kg)	Water (kg)	Superplasticizer (%)	(kg)
100C		690.65	-	-	1300	285.98	1.1	7.6
5CP		656.12	34.53	-				
15CP		587.05	103.60	-				
25CP		517.99	172.66	-				
50CP	0.4	345.33	345.33					
5GP		656.12	-	34.53				
15GP		587.05	-	103.60				
25GP		517.99	-	172.66				
50GP		345.33		345.33				

Note: *100C → 100% of cement, 5CP → 5% of ceramic powder and 95% of cement, 5GP → 5% of glass powder and 95% of cement*

Table 3 Mix proportions of SCM mixtures
3. táblázat Az SCM keverékek összetétele

4. Test procedure

4.1 Fresh mortar

The mini slump flow and mini v-funnel tests were conducted to characterize the flowability, filling ability and stability of fresh mortar. In the mini slump flow (*Fig. 1.a*), a truncated cone mold was filled with mortar and lifted upwards. The final diameter of the mortar through two perpendicular directions was measured and the mean is calculated. Slump flow ranging between 27.5 and 33.5 cm are suggested to obtain a slump flow of 55-85 cm for SCC [23-24].

It can be noted that it is possible to evaluate the trend to segregation or bleeding of SCM through visual control. The mini v-funnel was filled completely with mortar and the bottom outlet is opened allowing to the mortar to flow out (*Fig. 1.b*). The v-funnel flow time Tv which is the elapsed time (s) between the opening of the bottom outlet and the time when the light becomes visible from the top was measured [25].
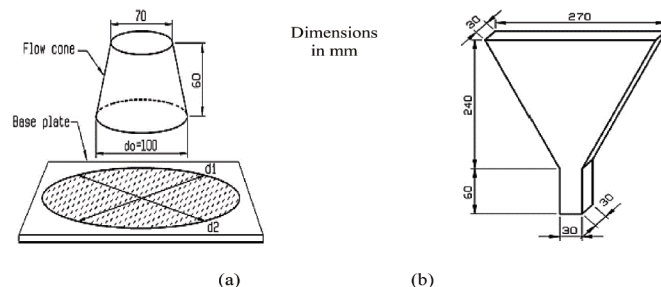

Fig. 1 Self-compacting mortar tests, (a) schematization of the mini-slump flow test, (b) mini V-funnel test
1. ábra Öntömörödő habarcsvizsgálatok sematikus ábrái: (a), mini roskadásvizsgálat (b) mini V-tölcséres vizsgálat

4.2 Hardened mortar

From each mortar mixture, prismatic specimens of 40×40×160 mm in size were cast. After casting, all specimens were covered with plastic sheets for 24 hours, before they unmolded and transferred to conservation in water saturated with lime at 20±2 °C and 95% relative humidity until the aging test. For each mix, three specimens were used to determine flexural strength, ultrasonic pulse velocity, water absorption, and six specimens to measure compressive strength at 3, 28 and 90 days. All these measures were carried out following European Standard EN 196-1 and EN 12504-4 [26-27].

5. Results and discussion

5.1 Fresh mortar

5.1.1 Slump flow

The evolution of slump flow as function of mineral addition percentages is presented in *Fig. 2*. The results indicated an increase in slump flow when a part of cement is replaced by glass and ceramic powders. The heights values of slump diameter were noted in mixtures containing 5 and 50% of CP and 50% of GP. All mixtures satisfied flowability requirements in term of slump flow values (27.5 - 33.5 cm) [23-24]. Subaci et al. [14] were observed an improvement on the flowability properties of self-compacting concrete with waste ceramic powder until substitution level of 15%. Through visual control, it was noted some bleeding in mixtures having 50% of GP and CP. From these results, it can be concluded that flowability and homogeneity of SCM in which cement was partially replaced by different proportions of ceramic and glass powders were relatively higher compared to reference SCM mixture, with exception for mixtures containing a large proportion of glass and ceramic powders (50%).
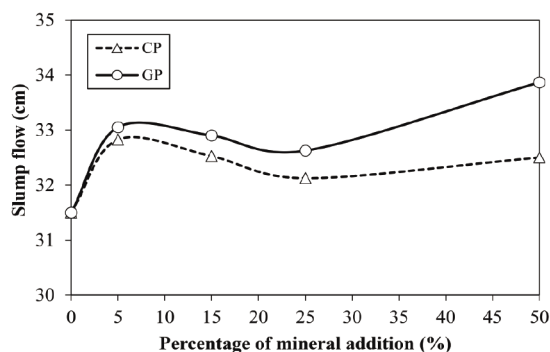

Fig. 2   Slump flow for mortar mixtures with plain and blended cements
2. ábra   Sima és kevert cementes habarcskeverékek roskadásvizsgálatának eredményei

5.1.2 Flow time

The values of flow time are plotted against the percentage of mineral additions in *Fig. 3*. The results showed that the flow time values of all mixtures were between 2.71 and 3.90 s, these values are acceptable since they are in the range proposed by EFNARC (2 to 10 s) [25]. It was noted that all mixtures had lower flow time values than the reference mixture. The obtained results from *Figs. 2* and *3* indicated that partial replacement of cement with both ceramic and glass powders with a percentage lower than 25% was found to be very positive in improving the fluidity and homogeneity of self-compacting mortar.

These results may be explained by improving the cohesion at the interface paste-fine aggregate in reason of the replacement of cement with a fine materials that having different size and shape. Another reason can explain these results which is the lower density of ceramic and glass powders compared to the cement which increases the paste volume, reduces the contacts between fine aggregate, and improves therefore the fluidity and facilities the movement of SCM [28]. It can be concluded that it is possible to reduce the amount of superplasticizer in order to produce homogeneous and economical SCM with similar fluidity to the control mixture by using waste local materials such as glass and ceramic as powders.
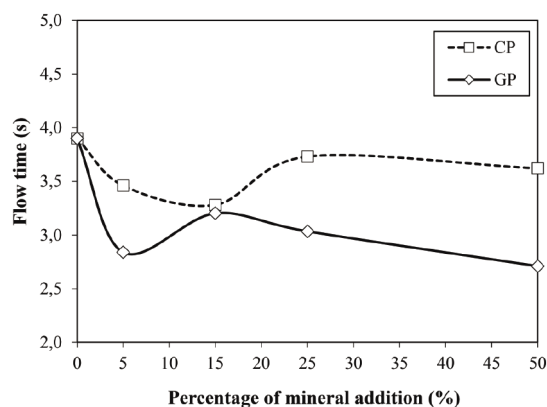

Fig. 3   Flow time for mortar mixtures with plain and blended cements
3. ábra   Folyási idő sima és kevert cementekkel készült habarcskeverékeknél

5.2 Hardened mortar

5.2.1 Compressive strength

The effect of ceramic and glass powders on compressive strength at 3, 28 and 56 days can be observed in *Figs 4, 5* and *6*, respectively. As it can be seen in *Fig. 4*, mixtures made with 5% of GP and CP were developed compressive strength higher (35.79 and 33.43 MPa, respectively) than that of reference mix (33.20 MPa). On the other hand, the results showed that the mixtures including 50% of ceramic and glass powders have the lowest compressive strength with 14.84 MPa and 12.84MPa, respectively, these values are 61 and 55% lower compared to mixture with plain cement. It was noted that increasing powders content led to lower compressive strength. In addition, mixtures containing GP have developed superior compressive strength compared to mixtures with corresponding CP content. The same results were observed at 28 days (*Fig. 5*). The decrease in compressive strength for mixtures including 5, 15, 25 and 50% of ceramic powder was 4, 15, 34 and 57%, respectively. In the case of glass powder, the compressive strength was reduced by 5, 24, 34 and 48% for mixtures with GP content of 5, 15, 25 and 50%, respectively. *Fig. 6* showed an improvement in compressive for mixtures made with GP. Adding 5 and 15% of GP resulted in similar compressive strength to control mix, whereas percentage of 25% led to compressive strength superior by 3% to that of mixture without additions. In their research, Aliabdo et al. [19] were noted an enhancement in compressive strength, tensile strength, absorption voids ratio and density as a result of using 10% glass powder cement replacement.
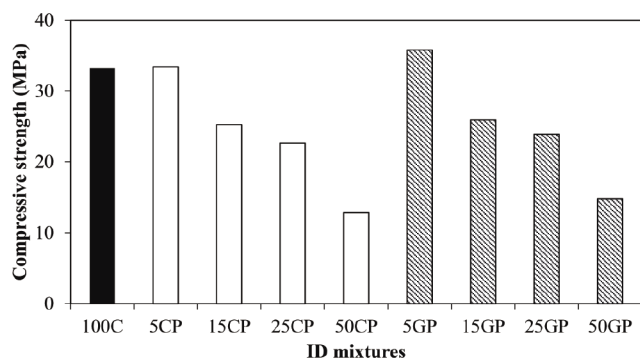
Fig. 4 Compressive strength for mortar mixtures with plain and blended cements at 3 days
4. ábra Nyomószilárdság habarcskeverékekhez sima és kevert cementekkel 3 napos korban

Fig. 5 Compressive strength for mortar mixtures with plain and blended cements at 28 days
5. ábra Nyomószilárdság habarcskeverékekhez sima és kevert cementekkel 28 napos korban

The increase of the compressive strength of mixtures including GP and CP at 56 days demonstrated the positive affect of partial replacement of cement with fine pozzolanic powders. This participate to filling the voids and pores which increases the density. The pozzolanic reaction between SiO_2 (from powders) and calcium hydroxide, which lead to the formation of new hydrated compounds (hydrated calcium silicate), this fills the micro spaces and results in higher compaction and strength.
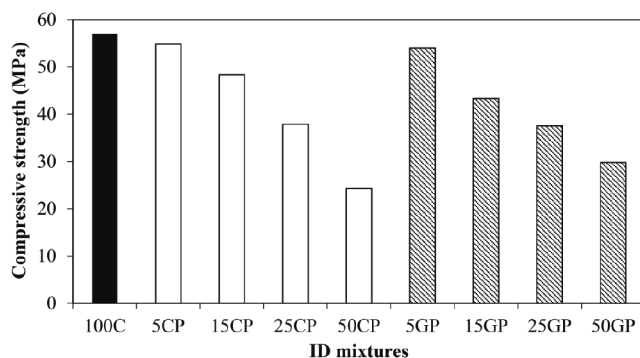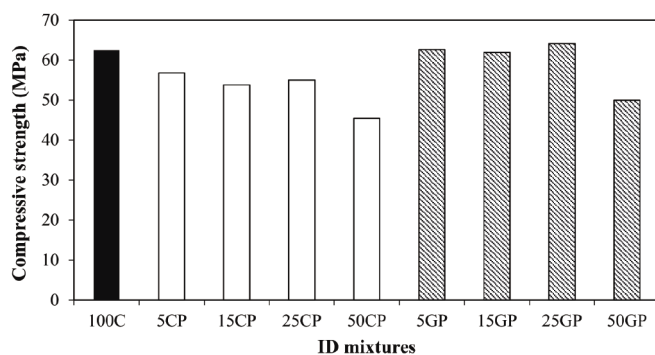

Fig. 6 Compressive strength for mortar mixtures with plain and blended cements at 56 days
6. ábra Nyomószilárdság habarcskeverékekhez sima és kevert cementekkel 56 napos korban

Torkittikul and Chaipanich [29] were studied the effect of ceramic waste as fine aggregate on some engineering properties of concretes. They reported an increase in the compressive strength by increasing the substitution level (0, 10, 20, 30, 40 et 50%) of natural sand by ceramic waste.

5.2.2 Flexural strength

Fig. 7 depicts the variation of flexural strength for different compositions. The results of *Fig. 7* indicated that the use of ceramic and glass powders at 5 and 15% resulted in flexural strength superior by 4 and 19% to that of plain cement mixture, while increasing the percentage of cement substituted by ceramic and glass powders to more than 15% led to a significant decrease in the flexural strength. This decrease achieved higher values in the mixtures made with 50% of glass and ceramic powders.

The effect of GP and CP replacement as fine powders at 5, 15, 25 and 50% on the flexural strength of SCM at 28 days is shown in *Fig. 8*. By analyzing the results of flexural strength after 28 days, it can note an improvement in flexural strength for mixture with 5% of glass powder, which reached flexural strength value of 7.44 MPa, whereas control mix had a flexural strength of 7.38 MPa. The addition of glass and ceramic powders by 15 and 25% led to lower flexural strength compared to the plain cement mixture. Increasing the percentage of fine additions resulted in poor flexural strength.

Fig. 7 Flexural strength for mortar mixtures with plain and blended cements at 3 days
7. ábra Hajlítószilárdság habarcskeverékekhez sima és kevert cementekkel 3 napos korban

Fig. 8 Flexural strength for mortar mixtures with plain and blended cements at 28 days
8. ábra Hajlítószilárdság habarcskeverékekhez sima és kevert cementekkel 28 napos korban

Fig. 9 illustrates the evolution of flexural strength at 56 days for all tested SCM mixtures. It can be remarked an increase in flexural strength in mixtures containing GP especially those

made with 5 and 25% of GP. Replacing cement by GP gave higher flexural strength compared to mixtures with corresponding content of CP. The higher values of flexural strength, especially in mixtures containing 5, 15 and 25% of ceramic and glass powders, are attributed to the irregular particles shape of these powders, this increases the cohesion between the particles of paste and contributes to better flexural strength.
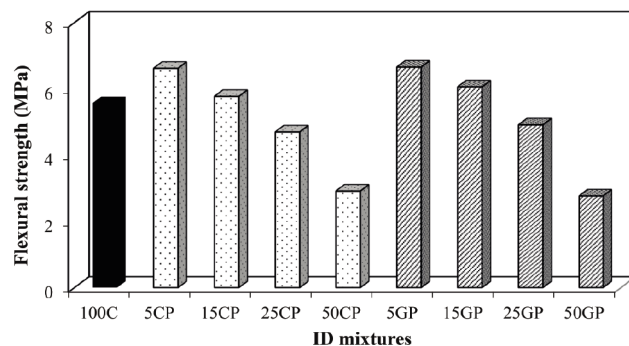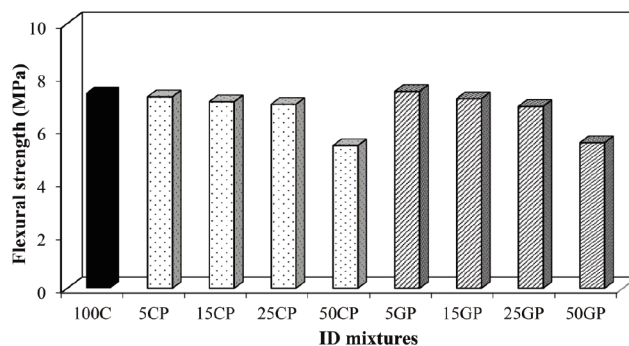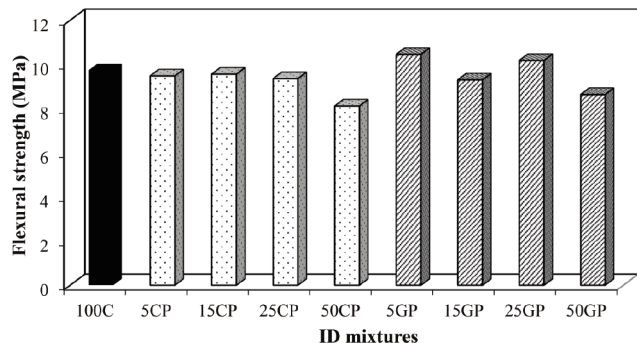

Fig. 9   Flexural strength for mortar mixtures with plain and blended cements at 56 days
9. ábra   Hajlítószilárdság habarcskeverékekhez sima és kevert cementekkel 56 napos korban

5.2.3 Ultrasonic Pulse Velocity

Fig. 10 presents the variation of ultrasonic pulse velocity at 28 and 56 days. It was observed a decrease in UPV at 28 days with the addition of ceramic and glass powder. At 56 days, UPV increased for all mixtures by 1 to 5%. Adding 5% of glass powder appeared to be the optimal percentage as it gave similar UPV to control mix.

The increase in UPV between 28 and 56 days is mainly due to the continuation of cement hydration which led to the formation of hydrated components. Glass and ceramic powders are considered as a pozzolanic materials, so they contribute to increase the density of SCM, by filling the voids and pores and by the formation of additionally hydrated calcium silicate (C-S-H), which in turn plays in important role in filling spaces and micro spaces.

Whitehurst [30] was classified the concretes according to their quality as following: excellent, good, moderate, bad and very bad for an UPV values above 4.5 km/s, 3.5-4.5 km/s, 3.0-3.5 km/s, 2.0-3.0 km/s and lower or equal to 2.0 km/s, respectively. This classification indicated that all the mixtures tested at 28 and 56 days have a good quality.
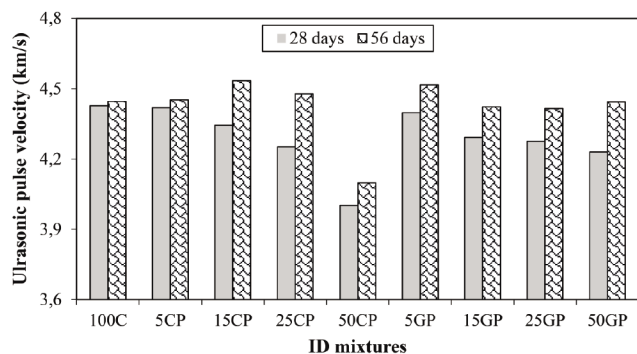

Fig. 10   Ultrasonic pulse velocity for mortar mixtures with plain and blended cements at 28 and 56 days
10. ábra   Ultrahangos impulzussebesség értékei sima és kevert cementet tartalmazó habarcskeverékeknél 28 és 56 napos korban

5.2.4. Water absorption

Fig. 11 shows the evolution of water absorption for all tested mixtures. It can be observed an increase in water absorption with adding glass and ceramic powders. Water absorption values of mixtures with blended cement are higher than mixture with plain cement, except for mixture made with 5% of GP which has the lowest value of water absorption. The replacement of cement with CP resulted in higher water absorption compared to mixtures including GP. It can conclude that the use of GP with 5% is optimal to reduce water absorption of SCM mixtures. According to Rodier and Savastano [18], the partial subsitution of cement by 10% of glass powder residue leads to a decrease in water absorption by about 15% in comparison to mortar without mineral addition.
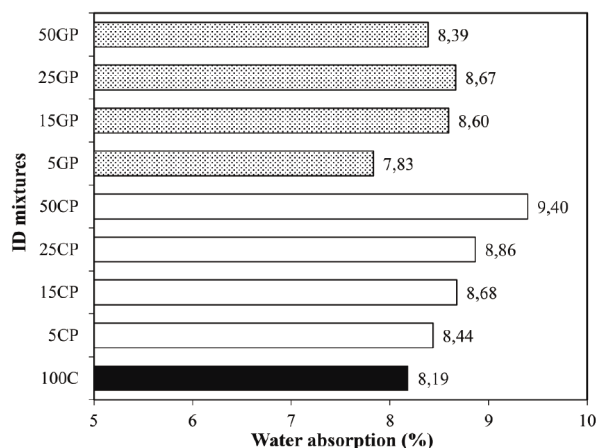
Fig. 11   Water absorption for mortar mixtures with plain and blended cements
11. ábra   Vízfelvétel sima és kevert cementes habarcskeverékekhez

6. Conclusions

Based on the experimental results and the analysis performed, the following conclusions can be drawn:

- The use of ceramic and glass powders by up to 25% contributes to the production of homogeneous self-compacting with acceptable fluidity and viscosity, while percentage of 50% led to heterogeneous mixtures with clear bleeding signs.

- Adding CP and GP makes possible to reduce the dosage of superplasticizer in order to produce an economical and homogeneous self-compacting mortar with similar flowability to control mix.

- The partial replacement of cement by 5% of ceramic and glass powders gave compressive and flexural strengths equal or greater than that of the plain cement mix, while exceeding this percentage, especially at 50%, had a negative effect on mechanical properties.

- Increasing ultrasonic pulse velocity led to compact mortar with longer life. Generally, UPV decreased with the increase in the percentage of glass and ceramic powders.

- The use of 5% glass powder is ideal for reducing water absorption.

Acknowledgments

References

[1] Benabed, B., Soualhi, H., Belaidi, A.S.E., Azzouz, L., Kadri, E.H., Kenai S. Effect of limestone powder as a partial replacement of crushed quarry sand on properties of self-compacting repair mortars. *Journal of Building Materials and Structures*, 2016. 3. Pp. 15-30. https://doi.org/10.5281/ZENODO.242480

[2] Saluja, S., Goyal, S., Bhattacharjee, B. Strength and abrasion resistance of roller compacted concrete incorporating GGBS and two types of coarse aggregates. *Advances in Concrete Construction*, 2019. 8. Pp. 127-137. https://doi.org/10.12989/acc.2019.8.2.127

[3] Boukhelkhal, A., Benabed, B. Fresh and hardened properties of self-compacting repair mortar made with a new reduced carbon blended cement. *Journal of Silicate Based and Composite Materials*, 2019. 71. Pp. 108-113. https://doi.org/10.14382/epitoanyag-jsbcm.2019.19

[4] Baghabra Al Amoudi, O.S., Shamsad, A., Khan, S.M.S., M. Maslehuddin. Durability performance of concrete containing Saudi natural pozzolans as supplementary cementitious material. *Advances in Concrete Construction*, 2019. 8. Pp. 119-126. https://doi.org/10.12989/acc.2019.8.2.119

[5] Boukhelkhal, A., Azzouz, L., Kenai, S., Kadri, E.H., Benabed, B. Combined effects of mineral additions and curing conditions on strength and durability of self-compacting mortars exposed to aggressive solutions in the natural hot-dry climate in North African desert region. *Construction and Building Materials*, 2019. 197. Pp. 307-318. https://doi.org/10.1016/j.conbuildmat.2018.11.233

[6] Ouldkhaou, Y., Benabed, B., Abousnina, R., Kadri, E.H. Experimental study on the reuse of cathode ray tubes funnel glass as fine aggregate for developing an ecological self-compacting mortar incorporating metakaolin, *Journal of Building Engineering*, 2020. 20. Pp. 1-11. https://doi.org/10.1016/j.jobe.2019.100951

[7] Boukhelkhal, A., Azzouz, L., Benabed, B., Belaïdi, A.S.E. Strength and durability of low-impact environmental self-compacting concrete incorporating waste marble powder, *Journal of Building Materials and Structures*, 2017. 4. Pp. 31-41. https://doi.org/10.5281/zenodo.1134146

[8] Laidani, Z.E.A., Benabed, B., Abousnina, R., Gueddouda, M.K., Kadri, E.H. Experimental investigation on effects of calcined bentonite on fresh, strength and durability properties of sustainable self-compacting concrete. *Construction and Building Materials*, 2020. 230. Pp. 1-11. https://doi.org/10.1016/j.conbuildmat.2019.117062

[9] Alipour, P., Namnevis, M., Tahmouresi, B., Mohseni, E., Tang, W. Assessment of flowing ability of self-compacting mortars containing recycled glass powder. *Advances in Concrete Construction* 2019. 8. Pp. 65-76. DOI: https://doi.org/10.12989/acc.2019.8.1.065

[10] Sasanipour, H., Aslani, F., Taherinezhad, J. Effect of silica fume on durability of self-compacting concrete made with waste recycled concrete aggregates. *Construction and Building Materials*, 2019. 227. Pp. 1-12. https://doi.org/10.1016/j.conbuildmat.2019.07.324

[11] Gritsada, S., Natt, M., Shanshan, C., Prakasit, S. Workability and compressive strength development of self-consolidating concrete incorporating rice husk ash and foundry sand waste – A preliminary experimental study. *Construction and Building Materials*, 2019. 228. Pp. 1-7. https://doi.org/10.1016/j.conbuildmat.2019.116813

[12] Senthamarai, R.M., Manoharan, P.D. Concrete with ceramic waste aggregate. *Cement and Concrete Composites*, 2005. 27. Pp. 910-913. https://doi.org/10.1016/j.cemconcomp.2005.04.003

[13] Gonzalez-Corominas, A., Etxeberria, M. Properties of high performance concrete made with recycled fine ceramic and coarse mixed aggregates. *Construction and Building Materials*, 2014. 68. Pp. 618-626. https://doi.org/10.1016/j.conbuildmat.2014.07.016

[14] Subaşı, S., Öztürk, H., Emiroğlu, M. Utilizing of waste ceramic powders as filler material in selfconsolidating concrete, *Construction and Building Materials*, 2017. 149. Pp. 567-574. https://doi.org/10.1016/j.conbuildmat.2017.05.180

[15] El-Dieb, A.S., Kanaan, D.M. Ceramic waste powder an alternative cement replacement–Characterization and evaluation. *Sustainable Materials Technologies*, 2018. 17. Pp. 1-11. https://doi.org/10.1016/j.susmat.2018.e00063

[16] Kannan, D.M., Aboubakr, A.H., EL-Dieb, A.S., Taha, M.M.R. High performance concrete incorporating ceramic waste powder as large partial replacement of Portland cement, *Construction and Building Materials*, 2017. 144. Pp. 35-41. https://doi.org/10.1016/j.conbuildmat.2017.03.115

[17] Lasseuguette, E., Burns, S., Simmons, D., Francis, E., Huang, Y. Chemical, microstructural and mechanical properties of ceramic waste blended cementitious systems. *Cleaner Production*, 2019. 211. Pp. 1228-1238. https://doi.org/10.1016/j.jclepro.2018.11.240

[18] Rodier, L., Savastano, H. Use of glass powder residue for the elaboration of eco-efficient cementitious materials. *Cleaner Production*, 2018. 184. Pp. 333-341. https://doi.org/10.1016/j.jclepro.2018.02.269

[19] Aliabdo, A., Abd Elmoaty, M.M., Aboshama, A.Y. Utilization of waste glass powder in the production of cement and concrete. *Construction and Building Materials*, 2016. 124. Pp. 866-877. https://doi.org/10.1016/j.conbuildmat.2016.08.016

[20] Lee, H., Hanif, A., Usman, M., Sim, J., Oh, H. Performance evaluation of concrete incorporating glass powder and glass sludge wastes as supplementary cementing material. *Cleaner Production*, 2018. 170. Pp. 683-693. https://doi.org/10.1016/j.jclepro.2017.09.133

[21] Ramakrishnan, K., Pugazhmani, G., Sripragadeesh, R., Muthu, D., Venkatasubramanian, C. Experimental study on the mechanical and durability properties of concrete with waste glass powder and ground granulated blast furnace slag as supplementary cementitious materials. *Construction and Building Materials*, 2017. 156. Pp. 739-749. https://doi.org/10.1016/j.conbuildmat.2017.08.183

[22] EN 197-1. Methods of testing cement-Part 1: Composition, specifications and conformity criteria for common cements. 2011.

[23] Skarendahl, A. The present-The future. *Proceedings of III International RILEM Symposium on Self-Compacting Concrete*. Bagneux, France, 2003. Pp. 6-14.

[24] Domone, P.L. Self-compacting concrete: An analysis of 11 years of case studies. *Cement and Concrete Composite*, 2006. 28. Pp. 197-208. https://doi.org/10.1016/j.cemconcomp.2005.10.003

[25] EFNARC. Specification and Guidelines for Selfcompacting Concrete. European Federation of Producers and Applicatorsof Specialist Products for Structures, EFNARC, Norfolk, 2002. 32 p.

[26] EN 196-1. Methods of testing cement-Part 1: Determination of strength. 2002.

[27] EN 12504-4. Essais pour béton dans les structures – Partie 4 : détermination de la vitesse de propagation du son. 2005.

[28] Boukhelkhal, A., Azzouz, L., Belaïdi, A.S.E., Benabed, B. Effects of marble powder as a partial replacement of cement on some engineering properties of self-compacting concrete. *Journal of Adhesion Science and Technologie*, 2016. 30. Pp. 2405-2419. https://doi.org/10.1080/01694243.2016.1184402

[29] Torkittikul, P., Chaipanich, A. Utilization of ceramic waste as fine aggregate within Portland cement and fly ash concretes. *Cement and Concrete Composite*, 2010. 32. Pp. 440-449. https://doi.org/10.1016/j.cemconcomp.2010.02.004

[30] Whitehurst, E.A. Soniscope tests concrete structures. *Journal of American Concrete Institute*, 1951. 47. Pp. 443-444.

Development a cement mortar based on dune sand used as an anti-carbonation coating of concrete

Youssef KORICHI ▪ Ammar Thélidji University of Laghouat, Algeria; Civil Engineering Research Laboratory ▪ koryou72@gmail.com

Ahmed MERAH ▪ Ammar Thélidji University of Laghouat,Algeria ; Civil Engineering Research Laboratory ▪ a.merah@yahoo.fr   a.merah@lagh-univ.dz

Med Mouldi KHENFER ▪ Ammar Thélidji University of Laghouat,Algeria; Civil Engineering Research Laboratory ▪ m.khenfer@lagh-univ.dz

Benharzallah KROBBA ▪ Ammar Thélidji University of Laghouat, Algeria; Structure Rehabilitation and Materials Laboratory (SREML) ▪ h.kroba@lagh-univ.dz

Abstract

Reinforced concrete structures are exposed throughout their life to the carbonation process due to the inevitable presence of CO_2 in the air, which causes corrosion of the reinforcements. In order to limit these harmful effects on reinforced concrete structures, anti-carbonation coatings are used. The purpose of these coatings is to limit the permeability of the embedding concrete to carbon dioxide. Each of these coatings has durability performance in terms of protection against this phenomenon. The main objective of this work is to study the effectiveness of a corrected mortar coating based on dune sand as an anti-carbonation coating of concrete using local materials, not presenting any danger, available in abundance in our countries. The obtained results clearly show that the formulated mortar has a very satisfactory compressive strength, a very low water porosity and the carbonation resistance is increases with the rate 60% compared to ordinary cement mortar based on alluvial sand.

Keywords: cement mortar, dune sand, coating, anti-carbonation, concrete

Kulcsszavak: cementhabarcs, dűnehomok, bevonat, karbonátosodás gátlás, beton

Youssef KORICHI
PhD Student, Civil engineering department. Researcher, Faculty of Civil Engineering and Architecture, Amar Telidji University of Laghouat, Algeria. His research interests include: concrete durability, concrete carbonation, anti-carbonation coatings.

Ahmed MERAH
Lecturer (MCA), Civil engineering department. Research Professor; Faculty of Civil Engineering and Architecture, Amar Telidji University of Laghouat, Algeria. His research interests include: concrete durability, concrete carbonation, anti-carbonation coatings.

Mohamed Mouldi KHENFER
Professor, Civil engineering department; Research Professor; Faculty of Civil Engineering and Architecture, Amar Telidji, University of Laghouat, Algeria. His research interests include: The use of local materials, light weight concrete

Benharzallah KROBBA
Lecturer (MCA), Department of Civil Engineering, Research professor, University of Laghouat, Algeria. His research interests include: formulation of cement reparation mortars, concrete durability, the use of local materials as the dune sand in concrete.

1. Introduction

Carbonation is widely recognized as a major cause of reinforcement corrosion in concrete [1]. The corrosion of reinforcements is shown to be the main cause of deterioration of reinforced concrete structures in the world [2]. With the aim of extending the life of reinforced concrete structures by protecting them against the carbonation phenomenon, several studies have been carried out in this direction using anti-carbonation coatings. Organic coatings, inorganic coatings and mortar coatings are the three main classes of anti-carbonation coatings. These coatings are used to form a barrier against chemical attack to protect concrete. They can consist of a single layer, two layers or more. Organic coatings depend mainly on their chemical inertness and their waterproofing. They are easy to apply on surfaces using brushes, sprays or rollers [3].

According to the experimental of José et al and Merah et al. [4,5] epoxy resin-based coatings give better protection against corrosion compared to acrylic coating and resinous cement-based coatings.

Furthermore, polyurethane and acrylic coatings provide better protection against diffusion and chloride permeability and water absorption compared to epoxy and chlorinated rubber coatings [6]. Other research has shown that acrylic coatings can provide a satisfactory level of protection against carbonation, and elastomeric coatings can protect steel bars from corrosion caused by chloride ions [7]. Benshausen et al. [8] concluded that acrylic coatings protect concrete against carbonation compared to cementitious coatings and increase the life of reinforced concrete structures. In this context, several researchers are interested in studying their effectiveness against the phenomenon of carbonation.

For anti-carbonation coatings in mortars, Huseyin et al. [9] and Miguel et al. [10] used mortar coatings composed of a mixture of (portland cement + very fine silica + active organic chemicals) which reduced permeability and minimized carbonation. According to Huang et al. [11]concrete coated with mortar (cement + sand and tile) whose thickness exceeds 50 mm have high resistance to carbonation. Researches also tested, a cement and sand mortar in two proportions, cement/sand equal to 0.33 and 0.5, the results obtained show that the mortar with the cement / sand rate equal to 0.5 can reduce the carbonation depth and that the latter is inversely proportional to the thickness of the surface coating [12]. This is, perhaps, explained by the large reserve of portlandite in the mortar made with this rate (cement/sand = 0.5) [3].

In addition, cement mortar with a thickness greater than 8 mm can protect reinforced concrete structures against carbonation for a period of 25 years[13,14]

This work is part of the valuation of local materials, which the effect of dune sand corrected based mortars on the durability of reinforced concrete structures against the carbonation phenomenon was studies.

2. Materials

2.1 Sands

The used alluvial sand comes from the quarry of Oued M'zi near the Laghouat region in Algeria, it is characterized by a regulatory particle size.

The used dune sand comes from the Laghouat region in Algeria, it is characterized by a regulatory particle size. The physical properties of used sands were presented in *Table 1*.

	Alluvial sand	Dune sand
Max Diameter (mm)	5	0.63
Apparent density (Kg / m³)	16.3	15.1
Absolute density (Kg / m³)	24	26
Sand equivalent (%)	60	97
Fineness modulus	2.70	0.84

Table   *Physical properties of the sands used*
1. táblázat   *Az alkalmazott homok fizikai tulajdonságai*

2.2 Cement

The used cement is a Portland cement (Algerian Cement) of the CEM I 42.5 CRS. The physical and chemical characteristics are given in *Table 2*.

Rate en %	C4AF clinker	C3A clinker	C2S clinker	C3S clinker	P.A.F	Cl	SO₃	Compressive strength in MPa	Specific surface cm²/g
	17	1.5	13	62	2.04	0.028	2.30	49.5	3420

Table 2   *Physical and chemical characteristics of the used cement CEMI 42.5 CRS*
2. táblázat   *CEM I 42.5 CRS cement fizikai és kémiai tulajdonságai*

2.3 Super plasticizer

The superplasticizer used is a MEDAPLAST SP 40 produced by the company Granitex (in Algeria). It is a better water reducer for ready-mixed concrete according to Standard EN 934-2 [15]. It is characterized by a density of 1.20 ± 0.01, with pH = 8, and a chloride ion content ≤ 1 g / l.

3. Preparation of mortars

To analyse the effect of adding dune sand to the cement mortar in order to choose the most effective mortar against the carbonation a prismatic sample ($4 \times 4 \times 16$ cm) for the six mixtures are made (*Fig. 1*) (*Table 3*) of different amounts of alluvial and dune sands with CEM I 42.5 cement and superplasticizer (*Table 4*)

Fig. 1   *Preparation of different mortars*
1. ábra   *A habarcs minták előkészítése*

N°	Compositions of mixtures	Designations of mixtures
01	Alluvial Sand + cement CEMI + water	MSA
02	80 % of alluvial sand + 20 % of dune sand + cement CEMI + water + superplasticizer (Sp).	8MSAD
03	60 % of alluvial sand + 40 % of dune sand + cement CEMI + water+ superplasticizer (Sp).	6MSAD
04	40 % of alluvial sand + 60 % of dune sand + cement CEMI + water+ superplasticizer (Sp).	4MSAD
05	20 % of alluvial Sand + 80 % of dune sand + cement CEMI + water + superplasticizer (Sp).	2MSAD
06	Dune sand + cement CEMI + water + superplasticizer (Sp).	MSD

Table 3   *Compositions of mortars mixtures*
3. táblázat   *A habarcs keverékek összetétele*

Designations of mixtures	MSA	8MSAD	6MSAD	4MSAD	2MSAD	MSD
Sp super-plasticizer	00	0.3%	0.7%	2 %	2.5 %	2.0 %
W/C	0.51	0.51	0.51	0.51	0.51	0.60

Table 4   *The W / C ratio and the amount of Sp in the mixtures*
4. táblázat   *A keverékek víz-cement tényezői valamint az alkalmazott folyósító adalékszer mennyiségei*

3.1 Preparation of samples test for different mixtures

According to AFREM recommendations, and before the start of the accelerated carbonation test, the samples which have undergone a cure in a humid environment (relative humidity greater than 95% or in water) for 28 days will be cut into cubes ($4 \times 4 \times 4$) cm³ (*Fig. 2*) and subjected to a preconditioning phase. This step consists of a phase where the samples (in cubes) are saturated with water for 24 h, followed by a second phase where they are placed in an oven set at a temperature of 40 ± 2 °C for 48 h. Two opposite sides of each cube are covered with adhesive aluminium foil to guide the diffusion of the CO_2. The samples are then weighed and placed in the carbonation chamber rich in CO_2 (50%), regulated at a temperature of 20 °C and a relative humidity of 65 ± 5% (*Fig. 3*).

Samples were removed from the carbonation chamber at different ages: 14, 28, 42 and 56 days. These are sawn in half (*Fig. 4*) and measurements of mass and depth of carbonation (by spraying the phenolphthalein solution at 0.1 g / 100 ml)) were carried out.

Fig. 2   *Cutting samples into cubes ($4 \times 4 \times 4$) cm³*
2. ábra   *Kocka próbatestek ($4 \times 4 \times 4$) cm³-sé vágása*

Fig. 3   The accelerated carbonation chamber
3. ábra   A karbonátosodás gyorsító kamra

Fig. 4   Samples sawn in half before spraying with phenolphthalein
4. ábra   A félbevágott minták a fenolftalein felhordása előtt

4. Results and discussions

4.1 Compressive strength of different mortars

The mechanical resistance tests were carried out on prismatic specimens $(4 \times 4 \times 16)$ cm³ according to standard NF EN 12390-3. The results are shown in *Fig. 5* and *Table 5*.

Mortars Mixtures	MSA	8MSAD	6MSAD	4MSAD	2MSAD	MSD
Compressive strengths at 28 days (MPa)	31.25	22	23	26	21.09	20

Table 5   Compressive strengths at 28 days of mortars mixtures (MPa)
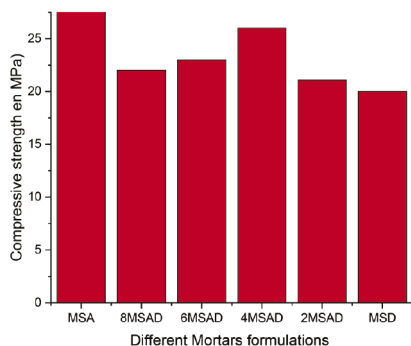*5. táblázat   A habarcsok 28 napos nyomószilárdsága (MPa)*

Fig. 5   Compressive strength at 28 days of mortars of different mixtures
5. ábra   A habarcsok 28 napos nyomószilárdsága (MPa)

From the *Fig. 5* it can be seen that alluvial sand mortars have a higher compressive strength than those of mixtures (alluvial-dune) mortars. For the other mortars, they have an acceptable compressive strength [35]. These values are sufficient for general use as an exterior and interior plaster. It should also be noted that

the E / C factor fixed at a value of 0.51 for all mixtures (except for MSD) has an influence on the value of the compressive strength.

4.2 Accelerated carbonation test

4.2.1 Carbonation depth

Fig. 6 shows the evolution of the carbonation depth as a function of the square root of the storage time of the mortars of different mixtures

4.2.1.1 Mortars MSD and MSA

From *Fig. 6* it is clearly seen that the mortar based on dune sand alone (MSD) is the most carbonated (*Fig. 6),* this constatation is due to the fineness of the dune sand, which possesses a very porosity high allowing the penetration of carbon dioxide. From *Fig. 7*, it is noted that after 56 days of accelerated carbonation, the MSD mortar reaches a carbonation depth more than 10 mm *(Figs. 7,8,9),* which implies that more than 50% of the MSD sample has been completely carbonated.
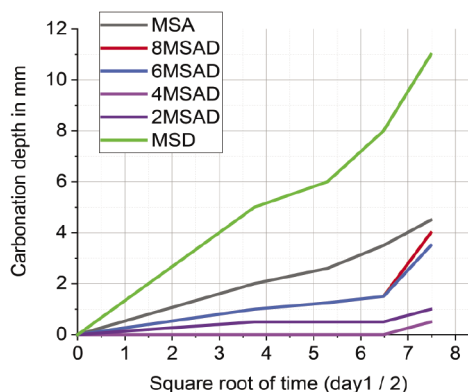
Fig. 6   Carbonation depth of the different mortars mixtures
6. ábra   A karbonátosodási mélység értékei a különböző minták esetén

Fig. 7   MSD mortar after 56th days in accelerated carbonation chamber
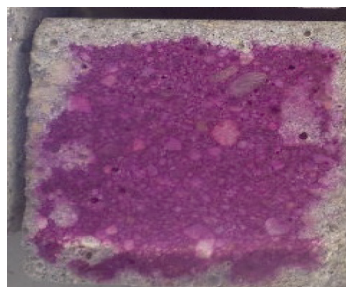*7. ábra   Az MSD habarcs 56 napnyi gyorsított karbonátosodási kamrában töltött idő után*

Fig. 8   MSA after 56th days in accelerated carbonation chamber
8. ábra   Az MSA habarcs 56 napnyi gyorsított karbonátosodási kamrában töltött idő után
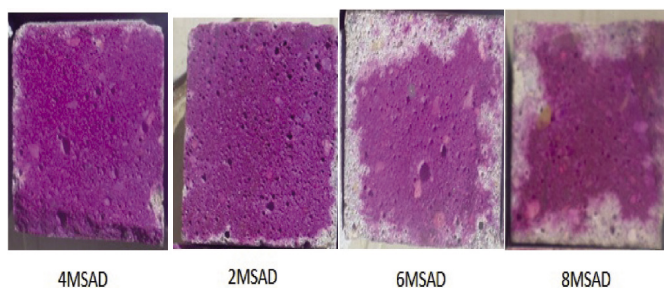
Fig. 9   Mortars of mixtures after 56th days of accelerated carbonation
9. ábra   Különböző habarcs minták 56 napnyi gyorsított karbonátosodási kamrában töltött idő után

In addition, it has been found that the mortar MSA is less porous than MSD, and therefore, it is less sensible for carbonation. This is due to the uniform granulometry of the alluvial sand, but and despite its good compressive strength, it is found that it carbonates at the first days of conservation in carbonation chamber, which makes it less durable.

4.2.1.2 Mortars 4MSAD, 2MSAD, 6MSAD, 8MSAD

The depth of carbonation after the 56th day for the four mixing mortars (alluvial sand - dune sand) is shown in *Fig. 9*.

Fig. 9 clearly illustrates the beneficial effect of adding dune sand in reducing the carbonation front. Therefore, these four mortars are more durable. In particular, 4MSAD mortar and 2MSAD mortar. The influence of adding sand to dune is very clear. The granulometry of the sands of the mixtures has been modified in order to give less porous and more compact mortars. These results are consistent with the absorption capacity values indicated above which confirms the close relationship between the porosity and the durability of reinforced concrete structures against the carbonation.

4.2.2 Evolution of the mass gain of the mortars during the accelerated carbonation test

Monitoring the evolution of mass gains is also a parameter indicating the evolution of carbonation. The results of mass gain for the different mortars are illustrated in *Fig. 10*:
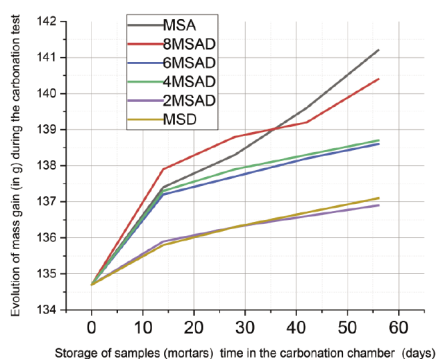

Fig. 10   Evolution of the mortars mass during the accelerated carbonation test
10. ábra   A habarcs tömegének alakulása a gyorsított karbonizációs vizsgálat során

Carbonation protects concrete by modifying its porous structure. The $CaCO_3$ formed closes certain pores, and

therefore the total porosity decreases, and the carbonation reaction of portlandite leads to an increase in the volume of the solid phase. It is clearly seen that the MSA and 8MSAD mortar require 4% mass gain. This is probably due to the greater pore volume than that of other mortars (6MSAD-4MSAD-2MSAD-MSD) which show a mass gain between 2% and 3%.

5. Conclusions

At the end of this study, the following conclusions can be drawn:

1. The mortars of mixtures (alluvial sand-dune sand) used as surface coatings of concretes against the carbonation phenomenon significantly reduce the carbonation depth by comparing them to the results obtained for MSD mortars (with dune sand alone) or with MSA mortars (with alluvial sand alone).

2. It has also been observed that the mortar composed of 40% alluvial sand and 60% dune sand with a CEMI Portland cement can reduce the carbonation front by more 50% compared to an ordinary mortar.

6. In addition, the mixture mortars studied through this work exhibit satisfactory compressive strengths suitable for general indoor and outdoor use.

8. With the use of dune sand which represents an abundant natural wealth, the repair of reinforced concrete structures will be less expensive, and it is hoped in the future to move away from use, industrial anti-carbonation coatings which sometimes present risks on the water, environment and on the structure at the same time.

References

[1] Arredondo Rea SP, Corral Higuera R, Gómez Soberón JMV, et al. Carbonation rate and reinforcing steel corrosion of concretes with recycled concrete aggregates and supplementary cementing materials. International journal of electrochemical science. 2012;7:1602–1610.

[2] Pollet V, Dooms B, Mosselmans G. Corrosion des armatures induite par la carbonatation du béton: comment s' en prémunir. Les dossiers du CSTC. 2007;2:1–7.

[3] Merah A. Concrete anti-carbonation coatings: a review. Journal of Adhesion Science and Technology. 2021;35:337–356. https://doi.org/10.1080/01694243.2020.1803594

[4] Merah A, Khenfer MM, Korichi Y. The effect of industrial coating type acrylic and epoxy resins on the durability of concrete subjected to accelerated carbonation. Journal of Adhesion Science and Technology. 2015;29:2446–2460. https://doi.org/10.1080/01694243.2015.1067004

[5] Aguiar JB, Júnior C. Carbonation of surface protected concrete. Construction and Building Materials. 2013;49:478–483. DOI: 10.1016/j.conbuildmat.2013.08.058[6] Almusallam AA, Khan FM, Dulaijan SU, et al. Effectiveness of surface coatings in improving concrete durability. Cement and Concrete Composites. 2003;25:473–481. https://doi.org/10.1016/S0958-9465(02)00087-2

[7] Zafeiropoulou T, Rakanta E, Batis G. Performance evaluation of organic coatings against corrosion in reinforced cement mortars. Progress in Organic Coatings. 2011;72:175–180. https://doi.org/10.1016/j.porgcoat.2011.04.005

[8] Beushausen H, Burmeister N. The use of surface coatings to increase the service life of reinforced concrete structures for durability class XC. Materials and Structures. 2015;48:1243–1252. DOI: https://doi.org/10.1617/s11527-013-0229-8

[9] Saricimen H, Maslehuddin M, Iob A, et al. Evaluation of a surface coating in retarding reinforcement corrosion. Construction and Building Materials. 1996;10:507–513. http://worldcat.org/issn/09500618

[10] Sanjuán MA, del Olmo C. Carbonation resistance of one industrial mortar used as a concrete coating. Building and Environment. 2001;36:949–953. https://doi.org/10.1016/S0360-1323(00)00045-7

[11] Huang NM, Chang JJ, Liang MT. Effect of plastering on the carbonation of a 35-year-old reinforced concrete building. Construction and Building Materials. 2012;29:206–214. https://doi.org/10.1016/j.conbuildmat.2011.08.049

[12] Papadakis VG, Fardis MN, Vayenas CG. Effect of composition, environmental factors and cement-lime mortar coating on concrete carbonation. Materials and Structures. 1992;25:293–304.

[13] Zhang G, Xie Q, Ma C, et al. Permeable epoxy coating with reactive solvent for anticorrosion of concrete. Progress in Organic Coatings. 2018;117:29–34. https://doi.org/10.1016/j.porgcoat.2017.12.018

[14] de Oliveira Andrade JJ, Possan E, Squiavon JZ, et al. Evaluation of mechanical properties and carbonation of mortars produced with construction and demolition waste. Construction and Building Materials. 2018;161:70–83. https://doi.org/10.1016/j.conbuildmat.2017.11.089

[15] EN B. 934-2: 2009+ A1: 2012, Admixtures for concrete, mortar and grout, Part 2, Concrete admixtures-Definitions, requirements, conformity, marking and labelling. Br Stand. 2012;

Invitation to Ceramics 2022

Dear Colleagues and fellow Ceramists,
As we all know only too well, the global pandemic has had some tragic consequences as well as disrupting our personal and professional lives very significantly. Whilst many valiant efforts have been made to continue with meeting and conferences on-line, our ability to talk face-to-face with each other and enjoy each other's company has in many cases simply not been possible. However, the good news is that, hopefully, things look as if we may be able to start planning again for a world where we can meet, learn and laugh together.

The undersigned below would very much like to invite all of you to a meeting that we hope will help to re-unify the worldwide ceramics community in one place and at one time. By agreement between the European Ceramics Society, the International Ceramic Federation and the International Committee of Electroceramics, and with excellent international co-operation, it has been decided to combine three major conferences into a single major conference. We realise just how busy 2022 is likely to be as many conferences that have had to be postponed are now jostling for timeslots – and attendees' budgets. Our move will see ECerS XVII, ICC9 and Electroceramics XVIII all held simultaneously in Krakow, Poland, 10-14 July 2022. A single registration fee will provide access to all three conferences, which are being hosted under the common title Ceramics in Europe 2022.

We truly hope that you will let this wonderful and ancient city with an old university and scientific tradition become the background for a tremendously fruitful meeting, which will give us all a much-needed boost for achieving progress again in our professional lives for the benefit of our world.

www.ceramicsineurope2022.org/

Inverse determination of material properties of timber beams reinforced with CFRP using the classical beam theory

K. SAAD ▪ Budapest University of Technology and Economics, Hungary
Budapest University of Technology and Economics, Hungary
A. LENGYEL ▪ Budapest University of Technology and Economics, Hungary
▪ lengyel.andras@emk.bme.hu

Khaled SAAD
Has a MSc degree in Civil Engineering at Budapest University of Technology and Economics. He is a PhD student at the Department of Structural Mechanics under the supervision of András Lengyel working on strengthening timber beams with fibre reinforced polymers.

András LENGYEL
Is an associate professor at the Department of Structural Mechanics, Budapest University of Technology and Economics. He has PhD degree in Engineering at the University of Oxford. He has co-authored 39 journal and conference papers.

Abstract

Fibre-reinforced polymers (FRP) are widely used to enhance the performance of structural elements of various materials, including timber. Measurements of reinforced beams mostly involve load-deflection relationships in order to experimentally verify mechanical improvements, while numerical simulations require material parameters for constitutive laws. In this study, a numerical method based on the classical beam theory is presented to inversely determine the elastic-plastic parameters of the timber material and the reinforcing FRP fabric using measurement data on full-scale composite beams. Data on bending tests of spruce beams obtained in a previous research stage are used to demonstrate the method. The method can provide material parameters for the full size composite structural element prepared under conditions relevant to actual design conditions, including the reinforcement preparation. It is found that the bilinear model is an adequate description for wood, and good agreement between simulated and measured data is obtained. Model material parameters are computed and presented for several specimens individually.

Keywords: spruce, beam, CFRP, modulus of elasticity, yield stress, bilinear model.

Kulcsszavak: lucfenyő, gerenda, CFRP, rugalmassági modulusz, folyási feszültség, bilineáris modell

1. Introduction

Wood is considered one of the widely used materials in construction, especially for lightweight structures, due to its easy processing, outstanding physical and mechanical properties compared to its low density and appearance. Wood has a more complex mechanical behaviour than steel or concrete, and the analytical methods to describe its behaviour are more cumbersome due to its orthotropic natural behaviour. The potential increase of loads such as dead loads during service life and the ageing of timber may lead to the decommissioning of pre-existing timber structures, though often structural elements can be efficiently repaired or strengthened as an alternative.

Fibre-reinforced polymers (FRP) are composites formed by embedding high-strength fibres (usually glass or carbon) in an adhesive matrix (usually epoxy). Carbon fibre reinforced polymers (CFRP), due to their high stiffness and strength-to-weight ratio, have become easily applicable ways of strengthening structural materials, including wood, to enhance structural performance in several ways. Studies on reinforcement of timber aim to examine the improvement of flexural capacity, stiffness, and ductility of the structural elements experimentally, analytically or numerically. Results on various wood species, reinforcement types, and applications can be found in the literature. With no intention to give here a detailed, comprehensive review, it is noted that the increase in load-bearing capacity is typically in the range of approximately 20% to 50% and sometimes higher, see, e.g. in [1-4], while the increase in stiffness does not mostly exceed 30% or often is insignificant, and sometimes higher, see, e.g. in [1, 4, 5, 6]. Also, the ductility of the reinforced beams is in most cases enhanced see, e.g. [3, 7]. Thus it has been proven that application of FRP to timber is a viable reinforcement way; hence, efforts in analytical and numerical modelling are due.

The reinforcing elements take various shapes and sizes. Usually, they are sheets, strips, or rods parallel to timber grains inserted in the tensile zone of the timber to boost tension capacity but can also be applied for compression or wrapped around the beam. The thinnest typical single plies are approx. 0.165 mm thick or sometimes thinner (used, e.g. in [8-9]) but lamellae of various thicknesses in the range of a few millimetres were investigated by several researchers (e.g. [5, 10-13]), including, e.g. more than 2 mm thick bidirectional fabrics used in [6]. Rods and pultruded elements can take even larger dimensions. Reinforcement in the nanoscale by, e.g. CNTs (carbon nanotube) is also a possible field to investigate, see, e.g. [14].

Anisotropy of wood is somewhat similar to the transversely isotropic fibre-matrix composite material because of its stress-strain characteristics, failure modes, and predominant fibre direction, though it is more complex. Fortunately, the linear orthotropic material model with nine material constants can always be applied to describe the behaviour of timber in the elastic range. A number of previous studies have addressed the

analysis of the complex behaviour of carbon-reinforced timber beams by developing linear and non-linear mechanical models relying on experimental works and the finite element method (FEM), which provides a powerful numerical approach [11, 13, 15-19].

Numerical analysis requires constitutive models populated with appropriate material parameters. Fibre-reinforced composites are usually regarded as linearly elastic with brittle rupture, whereas a more sophisticated description is necessary for timber. Unfortunately, the linear orthotropic model is applicable only in the linear range, and non-linear stress-strain relationships are needed beyond that, especially in the compression range where several different variations have been used, e.g. perfectly plastic (e.g. [2, 11-12]), bilinear (e.g. [1, 20-22]), higher-order (e.g. [23]), etc. A tri-linear stress-strain diagram was proposed by [24] to analyse the failure behaviour of wood in the compression parallel to the grain. Furthermore, the bilinear anisotropic stress-strain relationship proposed by Hill can be applied to predict the orthotropic linear elastic–quasi rigid behaviour in tension as well as the orthotropic linear elastic–perfectly plastic and sometimes bilinear behaviour in compression satisfying the consistency conditions [24-25]:

$$\frac{\partial f}{\partial \sigma_{ij}} d\sigma_{ij} = 0 \tag{1}$$

An orthotropic elastic and ideally plastic model was presented in [2] for the behaviour of timber beams strengthened with CFRP.

Material constants required for the numerical analysis are mostly obtained from the manufacturer, own experiments, or literature data. In the case of FRP, parameters of either the fibres or the prefabricated fibre–matrix composites are provided by the manufacturer. In the case of wood material, however, properties show a large variation depending on various factors, e.g. species, age, moisture content, density, location, etc. Properties may even differ from sample to sample and quite often are indicative only.

In an experimental study preceding the present work [4], four-point bending tests were performed on Norway spruce beams reinforced with CFRP fabric. Such experiments highlight various difficulties of acquiring adequate material data for the numerical analysis of these composite structures. Test specimens for measurement of material properties following standards may differ in quality from those under investigation, especially if old historical structures are to be reinforced. On the one hand, standardized testing of wood for compression parallel to grain has small scale specimens of prescribed length to width ratio producing a typical loading mechanism with splitting parallel with grains and partial lateral buckling. Also, the measured stress-strain curve may show significant variations with respect to the observed failure mode.

On the other hand, compression in full-scale timber beams under bending have different geometric conditions as the compression zone is not a stand-alone specimen. The elastic limit in compression and the non-linear behaviour of the material are important factors in the global behaviour in bending. The quality of FRP reinforcement is also a function of various factors. While factory produced lamellae are likely to follow the nominal specifications, manual in situ fabrication is prone to produce errors. As mentioned above, the stiffness increase due to reinforcing is generally moderate. It is often in good accordance with analytical predictions (see, e.g. [1, 10, 12, 13, 26-27]); however, several studies report experimental behaviour that differs from expectation to a lesser or larger degree and have to be considered as ill-performance (see, e.g. [5-6, 21, 28]). (Analytical derivation of stiffness is based on the fundamental elastic formulation stress resultants in inhomogeneous cross-sections as stiffness is interpreted in the elastic range.) As we experienced a similar phenomenon in our experimental study [4] as well, the present research aims to address this problem, utilizing the obtained measurement data.

Considering the above-mentioned challenges regarding material data, it may be prudent to apply inverse calculation of material properties of timber–CFRP composite structures. Very few studies have addressed that, for example, elastoplastic material model parameters in the generalized anisotropic Hill potential model were calculated for two wood species for the purpose of finite element modelling in [29]. The stress-strain behaviour of the Hill model was assumed to be linear elastic-quasi rigid in tension, bilinear ductile in compression. Validation was done by comparison of FE simulation with statistics of a sample of experimental data on small scale specimens.

This research was further inspired by an industrial project communicated to the authors where old timber beams extracted from a historical industrial building were offered for FRP reinforcement and testing. Measurements on composite beams of original timber material can provide the design of reinforcement of the remaining structural elements with realistic and actual material properties for both constituents.

This paper presents a numerical method for the indirect determination of material properties of timber–CFRP composite beams based on measured load-deflection curves. Measurement data obtained from own testing of full-size beams are used to illustrate the applicability of the method. It can address several difficulties in obtaining relevant material parameters as the composite is analysed in its entirety on a full scale as opposed to its constituents individually on a small scale, each specimen is investigated individually and not the whole sample statistically, various constitutive models can be implemented and recommendations given, and the FRP reinforcement is produced under the same conditions as expected in a real application. The outline of the paper is as follows: Section 2 briefly introduces the experiments, Section 3 elaborates the method, Section 4 presents the results through a selection of specimens, and the conclusions are summarized in Section 5.

2. Experiments

In a previous research project [4], a series of measurements were conducted on timber beams fitted with CFRP material to investigate the efficacy of reinforcing. The experimental program was designed to imitate the conditions corresponding to the manufacturer's intention. The aim was to test a technique that was not time-consuming and could be executed under

various conditions, including retrospective reinforcement on site. Accordingly, the fibre material provided by the manufacturer was a relatively thick fabric of pure carbon fibres (with no epoxy) in rolls. It was bidirectional with only 1 per cent in weft and 99 per cent in warp, the thickness is 1.4 mm when compact, and a volume ratio of ninety per cent was assumed. The epoxy resin was suitable for spreading with a roller.

A total of 44 beam specimens were prepared for four-point bending, see *Fig. 1*. The timber was sawn wood of Norway spruce (*Picea abies*). Eight specimens were left unaltered for reference, and the rest were reinforced with various amounts of fabric on the tension side. Twenty specimens were fitted with a single layer (1.4 mm thick), eight with a double layer (total 2.8 mm thick), and another eight with a narrow single layer (half-width of the beam). The four groups are also shown in *Fig. 1*.

The reinforcement was prepared in situ by spreading a thin layer of epoxy by a roller on the surface, then placing the fabric, and finishing with rolling a sufficient amount of epoxy to saturate the fabric and thus make the bond to the timber and form the composite simultaneously.

During the process, the magnitude of the load and mid-point displacement were measured and recorded digitally. These load-deflection curves provide the basis for the analysis introduced in the next section, though the method is not specific to these data.
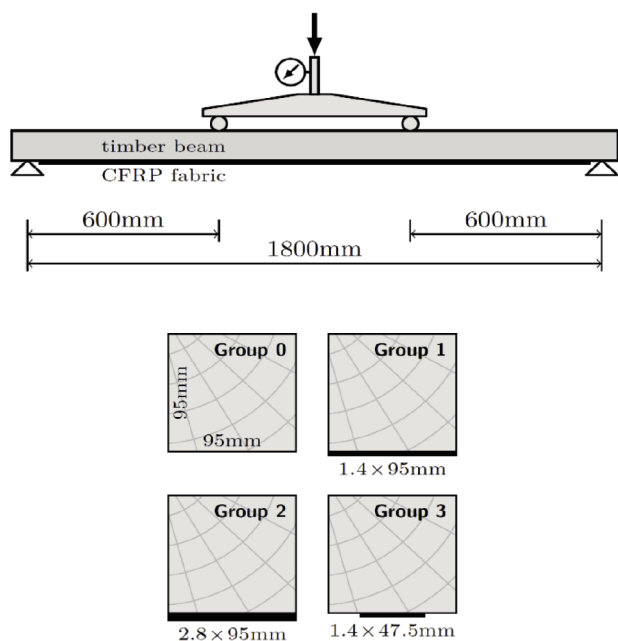
Fig. 1 Sketch of test arrangement and cross-sections with various reinforcement types.
1. ábra Kísérleti elrendezés vázlata és a keresztmetszet különböző megerősítésekkel.

3. Material constants

The reinforced beam is a three-dimensional continuum composed of an orthotropic wooden part and a transversely isotropic fibre-matrix composite such that the fibre/grain direction of both materials is aligned with the axis of the beam. Since significant stresses and strains are not expected

in the transverse direction, the classical Euler beam theory is applied here, assuming rigid cross-sections and no shearing deformations. Therefore, the constitutive equations need to be given in the axial direction only.

The CFRP composite is linearly elastic for tension with brittle rupture at the end of its strength. The fabric is attached to the tension side of the beam (lower chord), and thus compressive stresses do not occur. The reinforcement is then given by the modulus of elasticity E_r as the only material parameter.

The wood is linearly elastic in a limited initial phase of the loading, then some kind of nonlinearity is usually considered. In the compression zone, the wood is often modelled as linearly elastic and perfectly plastic, bilinear (with hardening or softening), or some kind of higher-order relationship between stresses and strains beyond the elastic limit. In the tension zone, it is customary to consider brittle rupture, though other models can also be defined (e.g. bilinear).

The constitutive equation is formulated for the reinforcement as $\sigma_r = p_0 \varepsilon_r$, where σ_r and ε_r are the stress and strain in the reinforcement, respectively, and parameter p_0 represents modulus of elasticity E_r. For the wood material, we have $\sigma_w = \sigma_w(\varepsilon_w; p_1, \ldots, p_n)$, where σ_w and ε_w are the stress and strain in the wood, respectively, and p_i ($i = 1, \ldots, n$) are the material parameters associated with the chosen model.

Deformations in the Euler beam theory are characterized by the curvature κ. In terms of the material parameters, strains and then stresses can be formulated for any given κ, see *Fig. 2*. The shape of the stress diagram depends on the stress-strain curve of the chosen model. In this study, it is assumed that reinforcement is applied in an unloaded state of the beam. If initial loading is considered, the pre-existing stress and strain states need to be incorporated in the models [30].

The stress resultant in the cross-section provides the bending moment M associated with curvature κ. This way, the M - κ diagram can be generated for a selected interval of the curvature. For any given load F, the bending moment diagram and, therefore, the curvature diagram of a beam with given dimensions and loading arrangement can be determined, e.g. for the beam shown in *Fig. 1*. Finally, the mid-span deflection is easily obtained using geometric relationships based on the principle of small displacements.
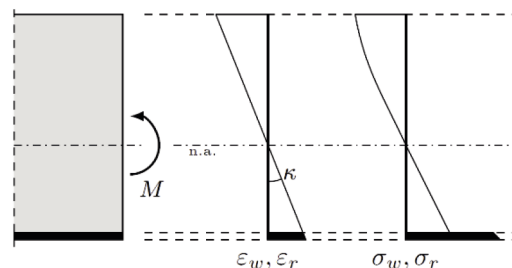
Fig. 2 Axial stresses and strains in the Euler beam.
2. ábra Normálfeszültségek és -alakváltozások az Euler-gerendában.

For a selected set of load values F_j ($j = 1, \ldots, m$) numerically simulated mid-span deflections $d^{sim}(p_i)$ can be generated. Naturally, the load values need to be chosen to match the range of the load data recorded during the measurement. Measured mid-span deflections (d_j) associated with the loads are to be

compared with the above mentioned simulated values. The basis for the comparison is an error function we define as

$$f_{err}(p_i) = \int_0^{F_{\max}} \left[d - d^{sim}(p_i) \right]^2 dF \qquad (2)$$

which is a non-negative quantity. For computational purposes, the integral is replaced with a discretized form of function (1) based on the trapezoidal rule as:

$$f_{err}(p_i) = \sum_{j=1}^{m-1} \frac{1}{2} \Delta F_j (g_j + g_{j+1}) \qquad (3)$$

Where $g_j = (d_j - d_j^{sim}(pi))^2$ and $\Delta F_j = F_{j+1} - F_j$. The sampling of load values ought to be dense enough to represent the measured data accurately while keeping the computational costs acceptable. The adequacy of any set of parameters p_i, ($i = 0, \ldots, n$) is then characterized by the magnitude of the error obtained by Eq. (2). The objective is to find the optimal set of parameters p_i, which minimizes $f_{err}(p_i)$ for a given load-deflection data set (F_j, d_j). The error function cannot be expressed explicitly as it requires lengthy numerical computations; therefore, a gradient approach is not convenient. Since it is known that an optimum of the objective function may not be found starting from an arbitrary configuration [31], and the measured data are irregular to some extent, it is assumed that several local minima may exist. Therefore, a robust grid search is applied in the parameter space to find a first approximation of the optimal parameters (grid search or parameter sweep is a numerical strategy for nonlinear inverse problems and can be competitive for a small number of parameters. It examines trial values in a regular grid in the parameter space and chooses the one with the smallest error. See, e.g. Menke, 2012., Sec. 9.4. [32]). Then the grid is refined in a few consecutive steps until the required precision is achieved, which is set to 1 N/mm² for moduli of elasticity and 10^{-3} N/mm² for stresses (e.g. compression yield stress).

4. Results

The method is demonstrated by the load-deflection curves obtained in the tests introduced in Section 2. The four specimen groups are shown separately in *Fig. 3*. The mean values of ultimate load and elastic stiffness in the initial linear range of the curves are summarized in *Table 1*. (Stiffness was determined by fitting a regression line for the range between 10% and 40% of the ultimate load for each specimen, obtaining coefficient of determination (R^2) of 99.2% and above.) For a detailed statistical analysis and evaluation of the measurements, see [4].

4.1 Wood models

Four material models are chosen for the wood, see *Fig. 4*. In the first case, nonlinearity is accounted for by plasticity in the compression zone. Wood is considered perfectly plastic for compression beyond the elastic limit, while unlimited tension capacity is assumed. This model is characterized by two parameters, modulus E_w and plastic yield stress σ_{cy}. The tensile strength of the wood corresponds to the endpoint of the load-deflection curves.

Spec. group	Number of specimens	Stiffness [kN/mm]	Ultimate load [kN]
0	8	0.6477	23.220
1	20	0.7463	30.527
2	8	0.7534	30.959
3	8	0.7068	27.448

Table 1   Mean values of elastic stiffness and ultimate load in specimen groups.
1. táblázat   A rugalmassági modulusz és a törőteher átlagértékei a tesztcsoportokban

In the second case, a brittle rupture in tension is considered, while plasticity in compression is omitted to investigate the effect of tensile failure only. It implies that no additional load-bearing capacity is available after the first rupture. This model is characterized by the modulus E_w and the ultimate tensile stress σ_{tu}. This approach can be used if rapid progressive collapse is assumed following the first rupture. In the presence of reinforcement (groups 1 to 3), however, further load-bearing is possible.

The third case combines the first and the second (three parameters: E_w, σ_{cy}, and σ_{tu}), i.e. nonlinearity in both tension and compression.

The last case assumes bilinear behaviour in the compression zone and unlimited tension capacity. The parameters are E_w, σ_{cy}, and E_t, the latter one referring to the tangent modulus in compression. This way, the compression behaviour is refined by allowing hardening or softening after the elastic limit. With the tangent modulus, the load-deflection curve can be followed more closely. Tension rupture is not considered in this case. In all cases, modulus E_r for the reinforcement is also added to the parameter set for groups 1 to 3 (but not for group 0). A few out of the 44 specimens had insignificant non-linear behaviour, where only the elastic moduli had to be determined. In the majority, however, some kind of nonlinearity is observed; therefore, Models 1 to 4 in *Fig. 4* are applied to the timber.

4.2 Examples

A detailed analysis is not possible to be presented here for all specimens, but the method can be well illustrated in detail through a selected few. First, load-deflection curves of a non-reinforced specimen are shown in *Fig. 5*. The measured data are plotted in dash-dotted lines while the rest are numerically simulated curves obtained by using models in *Fig. 4*, respectively. The first model considers linearly elastic and perfectly plastic behaviour in compression and unlimited tension capacity. The load-deflection curve obtained by the optimization method apparently follows the measured data quite closely both in the linear and the non-linear range. The second model considers tension rupture only. Since rupture involves immediate failure, no nonlinearity occurs, and the simulated line is inevitably straight and cannot approximate the measured data. The third model is the extension of the first with tension rupture. Since rupture can occur only at the final failure, the results are identical to those for the first model. However, the plots suggest that further improvement may be possible, so the fourth model is applied, which incorporates softening or hardening beyond the elastic limit in the compression range. With this model, a better approximation is achieved, as evident in *Fig. 5*. The

adequateness of each model is also represented by the error values (obtained using (2)) associated with the four models, i.e. 12866.20 Nmm², 432865.16 Nmm², 12866.20 Nmm², 747.10 Nmm², respectively. Optimal material parameters for the models are also shown in *Fig. 5*.
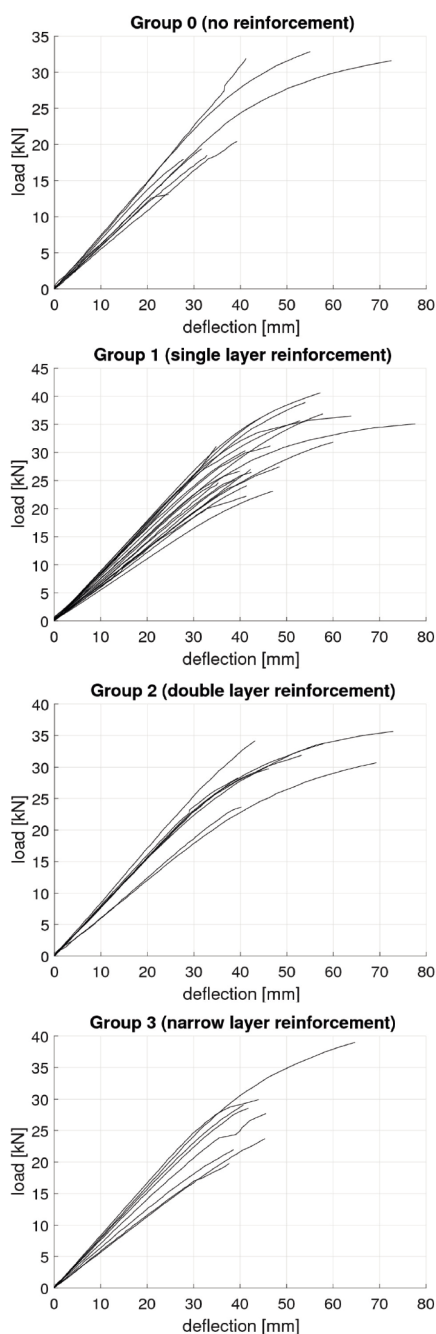

Fig. 3   Load-deflection curves for all specimen groups.
3. ábra   Erő-lehajlás-görbék minden tesztcsoportban.

The second example is a specimen with a single layer reinforcement, see *Fig. 6*. In this case, extensive plastic behaviour is observed with a definite curvature in the plot. The first model captures the general trend of the measured data curve but clearly not adequately enough. The third model again gives the same result. The fourth model is again expected to yield a better approximation by introducing possible hardening or softening behaviour beyond the

elastic limit in compression. It is found that with appropriate softening, the curvature of the non-linear part of the curve can be approximated more closely. The material properties are indicated in the figure. In the case of the second model, tension rupture does not involve the immediate failure of the structure since the fibre reinforcement can replace timber in tension. However, the sudden loss of load-bearing in timber results in a quick increase of displacement and hardening occurs only when the reinforcement develops sufficient stress. It results in a concave curve, which clearly does not follow the measured curve. Accordingly, the error values associated with the models are 27460.50 Nmm², 83269.50 Nmm², 27460.50 Nmm², 1373.87 Nmm², respectively. Comparison of models 1 and 4 clearly shows that the fourth model with bilinear behaviour can significantly improve the results, as seen in the figure.

The third example is a specimen with a double layer reinforcement, see *Fig. 7*. In this case, the findings are similar to those in the previous example. The error values associated with the models are 12404.40 Nmm², 78458.04 Nmm², 12404.40 Nmm², and 8882.93 Nmm², respectively. However, in this case, even the fourth model cannot approximate the measurements as well as before. The plot shows that the measured data curve is not smooth but has a breakpoint near the end (a localised change of slope), which suggests that a partial tensile failure might have taken place without causing total collapse. Model 2 with tension rupture can only give a highly exaggerated approximation with a sharp breakpoint. In order to capture the phenomenon of the delicate breakpoint in the curve, a more sophisticated material model is needed, which handles partial rupture within the cross-section. With appropriate parametrization, such a model can be formulated, though it is not the topic of this study.
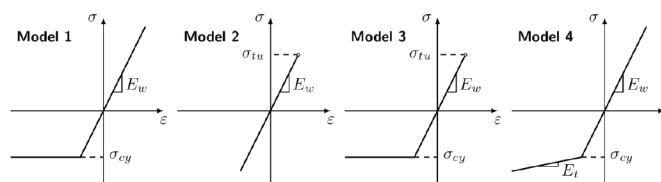

Fig. 4   Stress-strain curves for four different wood models.
4. ábra   Feszültség-alakváltozás-görbék négy különböző faanyagmodellre.
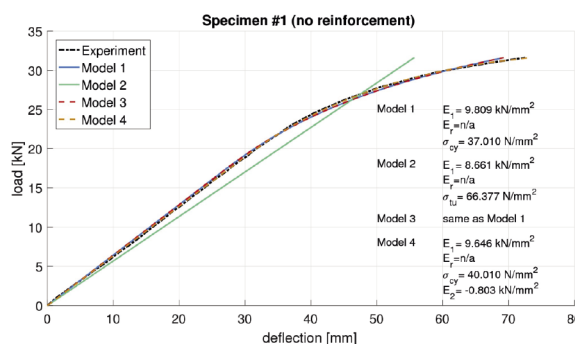

Fig. 5   Measured and simulated load-deflection curves for specimen 1.
5. ábra   Mért és számított erő-lehajlás-görbék az 1. Mintadarabra.

The last example is a specimen with a single layer reinforcement. The load-deflection curve shows a moderate

nonlinearity, and the maximum deflection is average, thus representing a typical case (*Fig. 8*). Though for this specimen, the difference between the individual models is visually not as accentuated as in the previous cases, the numeric computation can clearly evaluate and rank the models. The results are similar to those of the second example. The error values associated with the four models are 1093.10 Nmm², 3048.03 Nmm², 1093.10 Nmm², 641.97 Nmm², respectively. Here again, the fourth model provides the best approximation improving the outcome of the elastic-plastic model by introducing the bilinearity.
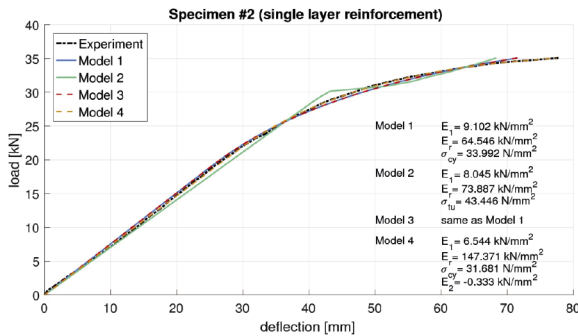

Fig. 6   Measured and simulated load-deflection curves for specimen 2.
6. ábra   Mért és számított erő-lehajlás-görbék az 2. Mintadarabra.

4.3 Comparison of models

The selected specimens shown in the previous subsection provide a good sample of the general behaviour. *Table 2* summarizes the statistics of the results for all models. Numbers in the table are the mean values of the parameters in each group, with corresponding standard deviations shown in parentheses. Reinforcement modulus is not applicable for group 0 (n/a).

The basic model with perfect plasticity in compression can generally capture the trend of the load-deflection curves in most cases, except when the specimen shows insignificant nonlinearity (brittle rupture before plasticity could take place) or when a localized change occurs, which breaks the smooth character of the curve (e.g. partial rupture at a particular point during the loading process, etc.). The average modulus of elasticity of the wood material is between 8.16 kN/mm² and 9.89 kN/mm² in the four specimen groups, with a relative standard deviation between 11.5% and 18.8%. These values are within the typical range for these species. Average compression yield stresses range between 32.228 N/mm² and 36.59 N/mm² with a relative standard deviation between 15.3% and 19.7%. Note that similar results were obtained in the four specimen groups, which indicates that the method can adequately extract wood material properties from the data regardless of the amount of reinforcement. Results on the reinforcement are somewhat unexpected. In groups 1 to 3, the average moduli range between cca. 45 kN/mm² and 85 kN/mm² with large relative standard deviations (20 kN/mm² to 50 kN/mm²).

The second model, which considers only tension rupture, gives incorrect results, as apparent through the examples shown in the previous subsection. It is found through the simulations that rupture in the tension zone at the full width of the cross-section results in such a large immediate loss of load-bearing capacity that the slope of the load-deflection curve drops significantly. None of the test specimens exhibited such extreme behaviour, except at the final failure just prior to collapse. Therefore, tensile rupture alone cannot be responsible for the nonlinearity of the structure, and the results of Model 2 are discarded. As seen through the example specimens in the previous section, Model 3, which combines plastic compression with tension rupture, gives results similar to Model 1 since

Mod	Gr	E_w(kN/mm²)	E_r(kN/mm²)	δ_{cy}(N/mm²)	δ_{tu}(N/mm²)	E_t(kN/mm²)
1	0	9.899 (1.142)	n/a (n/a)	32.228 (6.340)		
	1	8.578 (1.343)	77.139 (28.850)	36.594 (5.589)		
	2	8.168 (1.534)	45.813 (24.268)	34.067 (5.567)		
	3	9.129 (1.252)	85.395 (51.275)	34.717 (5.356)		
2	0	9.603 (1.120)	n/a (n/a)		48.748 (16.158)	
	1	7.780 (1.074)	100.903 (42.405)		35.374 (10.346)	
	2	7.562 (0.646)	52.646 (20.486)		31.940 (5.629)	
	3	8.896 (1.215)	77.860 (44.843)		49.032 (7.582)	
3	0	9.899 (1.142)	n/a (n/a)	32.228 (6.340)	53.883 (21.450)	
	1	8.561 (1.357)	77.445 (30.999)	36.723 (5.628)	54.784 (14.371)	
	2	8.168 (1.534)	45.813 (24.268)	34.067 (5.567)	46.352 (12.218)	
	3	9.129 (1.252)	85.395 (51.275)	34.717 (5.356)	50.697 (9.707)	
4	0	9.892 (1.127)	n/a (n/a)	31.307 (8.356)		0.266 (3.838)
	1	8.685 (1.757)	74.728 (41.563)	37.177 (7.106)		-0.557 (2.282)
	2	8.448 (1.466)	40.216 (19.546)	35.270 (3.248)		-0.844 (2.191)
	3	9.547 (1.438)	62.577 (31.414)	34.538 (7.693)		0.614 (2.284)

Table 2   Mean values and standard deviations of optimal material parameters (wood modulus E_t, reinforcement modulus E_r, wood compression yield stress σ_{cy}, wood tension ultimate stress σ_{tu}, wood tangent modulus E_t) in all specimen groups (Gr) for all models (Mod). Standard deviations are given in parentheses. Ultimate stresses shown in italics are computed at failure load.

2. táblázat   Optimális anyagi paraméterek átlaga és szórása (E_t: fa rugalmassági modulusza, E_r: megerősítés rugalmassági modulusza, σ_{cy}: fa folyási feszültsége nyomásra, σ_{tu}: fa húzószilárdsága, E_t: fa érintőmodulusza) minden tesztcsoportban (Gr) minden modellre (Mod). A szórások zárójelben vannak megadva. A dőlten szedett szilárdságértékek a töretteherre vonatkoznak.

the latter behaviour is not dominant. Nearly in all cases, the results are the same, i.e. for groups 0, 2, and 3, where the statistics give the same figures in terms of wood modulus and plastic yield stress. Ultimate tension stresses shown in the table are computed at the instant of failure and not obtained through the optimization algorithm; such figures are shown in italics. However, in the case of group 1 (with a single layer of reinforcement), some specimens differ, so the mean values for modulus and plastic yield stress are slightly different. Here the statistics refer to the results of the optimization, though the calculated failure stresses are similar, too.
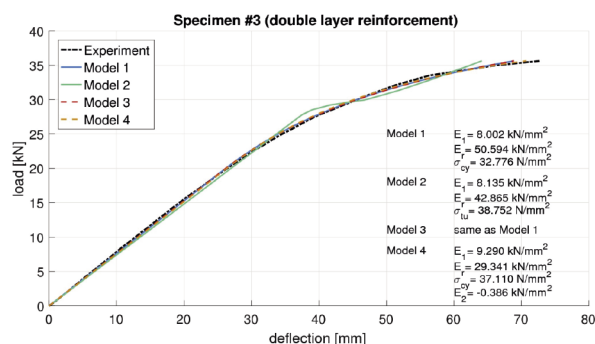

Fig. 7   Measured and simulated load-deflection curves for specimen 3
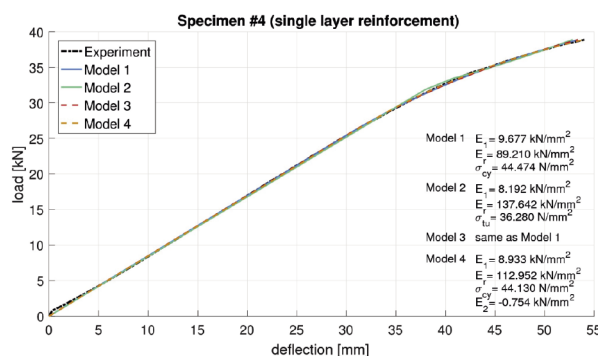*7. ábra   Mért és számított erő-lehajlás-görbék az 3. Mintadarabra*

Fig. 8   Measured and simulated load-deflection curves for specimen 4.
8. ábra   Mért és számított erő—lehajlás-görbék az 4. Mintadarabra.

Model 4 provides the best approximation of the load-deflection curves among the models applied in this study. The average modulus of elasticity of the wood material is between 8.44 kN/mm^2 and 9.89 kN/mm^2 in the four specimen groups with relative standard deviation between 11.3% and 20.2%, similar figures to those obtained for Model 3. Average compression yield stresses range between 31.30 N/mm^2 and 37.17 N/mm^2 with a relative standard deviation between 9.2% and 26.6%. Yield stresses again are similar to previous results. This model incorporates possible softening or hardening in the plastic range via the tangent modulus, the mean values of which ranging between -0.844 kN/mm^2 and +0.614 kN/mm^2 in the four groups. Note that the standard deviations are large, indicating that the non-linear behaviour of individual species might differ substantially. Results on the reinforcement are also similar to previous results, with mean values ranging between cca. 40 kN/mm^2 and 75 kN/mm^2 with large relative standard deviations.

4.4 Discussion

The wood material models applied to the four different specimen groups lead to important conclusions. Timber beams tested in the experiments were obtained from the same source and possessed similar properties, as well as the fibre reinforcement, were prepared with the same material using the same technique. Numerical calculations presented here have verified that values obtained for the elastic modulus of wood are in the range characteristic of this species with ordinary variation (i.e. standard deviation). No significant differences are observed between specimen groups with different amounts of reinforcement. Each of the four wood material models had practically identical results with the exception of Model 2, in which case the validity of the results is questionable, as discussed previously.

In terms of the compression yield stresses in Models 1, 3, and 4, the results show very good agreement both modelwise and groupwise. It indicates that the algorithm was able to capture the nonlinearity of wood material regardless of the amount of reinforcement. However, differences are observed with respect to the degree of nonlinearity. Models 1 and 3 could simulate the curvature of the load-deflection diagram by means of the perfectly plastic behaviour in the compression zone, though they could not provide further adjustment.

Model 4, on the contrary, was able to fine-tune the degree of nonlinearity of the curve by applying potential softening or hardening. A significantly better fit is achieved through this though it is found that the tangent moduli are somewhat scattered in a range covering both positive and negative values. It indicates that the individual specimens were different in their compression behaviour.

The apparent inadequacy of Model 2 suggests that tension rupture should be modelled in a more refined way. Some of the specimens showed that observable tension rupture occurred during the loading process without causing complete failure, indicating that grains in the wood naturally have different strengths. Therefore, rupture may occur locally and gradually. In order to capture this effect, wood models that attribute different properties to different parts of the cross-section should be applied. With appropriate parametrization, the algorithm can incorporate such models. However, most specimens failed due to rupture in the tension zone immediately followed by progressive failure of the entire beam, indicating the importance of weak points in the timber material on the behaviour. The reliability of the specimens is primarily affected by the amount of material weak points such as defects or knots, see, e.g. [33]. Since wood is a natural material, this variation is reflected in the measured ultimate capacity of the specimens. Early tensile failure prevents the full utilization of the compression capacity of timber; therefore, the ductility of the beams varies in a range depending on when the rupture took place. An important difference between unreinforced and reinforced beams is manifested in the increased ductility of the latter case because the presence of reinforcement reduces the tensile stresses in the wood at the same load level, consequently higher ultimate load can be achieved, which in turn implies that the plastic compression capacity of the wood is utilized to a higher degree before failure.

In all groups with reinforcement, it has been observed that the modulus of the reinforcement material is below the theoretical modulus of the carbon fibre (i.e. 234 kN/mm² provided by the manufacturer). The reasons lie in the preparation of the CFRP fabric. The lamellae were prepared in situ by laying the glue on the surface with a roller forming the embedding matrix and the bond to the timber simultaneously. The procedure is efficient, can be applied for reinforcement in an arbitrary position, and provides an effective bond between fibres and timber. However, despite all its advantages, it has negative side effects. The extremely thin carbon fibres are sensitive to any action (e.g. bending) other than axial tension, so in situ preparation of the reinforcement lamellae inevitably inflicts damage to some degree. It is also inevitable to introduce geometric imperfections to the fibres (e.g. waviness), which further reduce the elastic modulus. Since the thickness of the fabric is larger than usual and the consistency of the epoxy is high, a considerable force is required to make the epoxy penetrate the fabric; hence its influence is large. The simulations have also shown that the elastic modulus is smaller in the case of double reinforcement because the application of the epoxy requires larger pressure and hence may cause a larger disturbance.

However, counter-intuitive, low increase in stiffness is by no means exceptional and has been reported in other research. Some researchers measured negligible increase simultaneously with considerable improvement of capacity. There are even recommendations not to consider fibre reinforcement for the purpose of enhancing stiffness see, e.g. [34]. Regarding the low increase in stiffness, see also other papers, e.g. [5, 10, 28]. Values of modulus of elasticity for the reinforcement obtained in this study are, in fact, in good agreement with the increase of stiffness obtained from the measurements. If the nominal modulus of the fibres as issued by the manufacturer are assumed (i.e. without any damage or imperfection), an increase of over 65% in stiffness is obtained by performing simple computations using the Euler beam model. A 3D finite element analysis gives the same figures. It obviously contradicts the observed 15 or 16% increase from the measurements (*Table 1*), however, if the values obtained from the algorithm are used, a good agreement with the measurements is achieved, providing verification for the results. A continuation of this research aims to model the behaviour of fibre reinforcement in detail.

5. Conclusions

In this study, a method was shown for the inverse determination of material properties of composite beams based on load-deflection diagrams using the Euler beam model. The optimal set of model constants minimizes the difference between the simulated and the measured load-deflection curves.

- The effectiveness of the method has been illustrated through a series of data obtained from four-point bending tests conducted in previous research on timber beams reinforced with CFRP fabric [4].
- Four different wood material models and one reinforcement model were applied, and the optimal material properties were computed. It is found that

assuming linearly elastic behaviour in tension and bilinear stress-strain relationship in compression for the wood leads to a very accurate simulation of load-deflection curves.
- Material parameters of wood are realistic and in the typical range specific to the species in question. The effective modulus of the reinforcement falls short of the nominal value.

The advantages of the procedure presented here are that
- each specimen can be analysed individually;
- the obtained parameters may be considered more realistic with respect to the global behaviour of the beam if source data are obtained from tests on full-scale specimens (such as in this study) as opposed to data obtained from small scale ones;
- computation of parameters takes into consideration the real conditions and quality of the preparation of the reinforcement, enabling reinforcement design of existing structures with more reliable and appropriate data;
- computation of parameters also takes into consideration the actual conditions of timber that may not always be reproducible in a laboratory.

Note that constitutive models other than those presented here can also be implemented in the model, though the achieved accuracy does not demand that. The algorithm can also be used with other numerical solvers, e.g. with embedded user-created finite element analysis codes, or alternatively, coupled with commercially available finite element software. Test runs have already been performed.

As mentioned above, the computations have shown that the effective stiffness of the fibre material is reduced compared to the theoretical values. It is important to note that these results are in accordance with the measurements used in this study. The measured mean increase of stiffness due to reinforcement with respect to the unreinforced specimens is smaller than what one would theoretically obtain from the analysis of inhomogeneous elastic beams. It is by no means an exceptional case as a very low or moderate stiffness increase was reported in several works. As mentioned in the Introduction, in several cases, the results fall short of the expectations, though we have not found an appropriate discussion of the reasons behind. In the case of our study, we assume that the observed deficiency is due to geometrical imperfections and potential damage inflicted to the fibres by in situ preparation of reinforcement. Since the fabric was thicker than the typical ones, considerable pressure was required by rolling to make the epoxy saturate the fabric. The method presented here has also provided important data on the physical capabilities of the current preparation technique prompting to refine or adjust the treatment to exploit the full potential of fibre reinforcement. The future plans of the authors aim for detailed investigations along this line.

Acknowledgements

References

[1] A. Borri, M. Corradi, and A. Grazini. A method for flexural reinforcement of old wood beams with CFRP materials. *Composites Part B*, 36(2):143–153, 2005. doi = https://doi.org/10.1016/j.compositesb.2004.04.013

[2] T.P. Nowak, J. Jasieńko J, Czepiżak D. Experimental tests and numerical analysis of historic bent timber elements reinforced with CFRP strips. *Construction and Building Materials*, 40:197–206, 2013. doi = https://doi.org/10.1016/j.conbuildmat.2012.09.106

[3] Y.F. Li, Y.M. Xie, and M.J. Tsai. Enhancement of the flexural performance of retrofitted wood beams using CFRP composite sheets. *Construction and Building Materials*, 23(1):411–422, 2009. doi = https://doi.org/10.1016/j.conbuildmat.2007.11.005

[4] K. Andor, A. Lengyel, R. Polgár, T. Fodor, and Z. Karácsonyi. Experimental and statistical analysis of spruce timber beams reinforced with CFRP fabric. *Construction and Building Materials*, 99:200–207, 2015. doi = https://doi.org/10.1016/j.conbuildmat.2015.09.026

[5] A.M. de Jesus, J.M. Pinto, and J.J. Morais. Analysis of solid wood beams strengthened with CFRP laminates of distinct lengths. *Construction and Building Materials*, 35:817–828, 2012. doi = https://doi.org/10.1016/j.conbuildmat.2012.04.124

[6] T.W. Buell and H. Saadatmanesh. Strengthening timber bridge beams using carbon fiber. *Journal of Structural Engineering*, 131(1):173–187, 2005. doi = https://doi.org/10.1061/(asce)0733-9445(2005)131:1(173)

[7] Y.J. Kim, M. Hossain, and K.A. Harries. CFRP strengthening of timber beams recovered from a 32 year old quonset: Element and system level tests. *Engineering Structures*, 57:213–221, 2013. doi = https://doi.org/10.1016/j.engstruct.2013.09.028

[8] M. Corradi, A. Borri, L. Righetti, and E. Speranzini. Uncertainty analysis of FRP reinforced timber beams. *Composites: Part B*, 113:174–184, 2017. doi = https://doi.org/10.1016/j.compositesb.2017.01.030

[9] P. de la Rosa García, A.C. Escamilla, and M.N.G. García. Bending reinforcement of timber beams with composite carbon fiber and basalt fiber materials. *Composites Part B*, 55:528–536, 2013. doi = https://doi.org/10.1016/j.compositesb.2013.07.016

[10] J. Fiorelli and A.A. Dias. Analysis of the strength and stiffness of timber beams reinforced with carbon fiber and glass fiber. *Materials Research*, 6:193–202, 2003. doi = https://doi.org/10.1590/s1516-14392003000200014

[11] G.M. Raftery and A.M. Harte. Nonlinear numerical modelling of FRP reinforced glued laminated timber. *Composites Part B: Engineering*, 52:40–50, 2013. doi = https://doi.org/10.1016/j.compositesb.2013.03.038

[12] Y. Nadir, P. Nagarajan, M. Ameen, and M. Arif M. Flexural stiffness and strength enhancement of horizontally glued laminated wood beams with GFRP and CFRP composite sheets. *Construction and Building Materials*, 112:547–555, 2016. doi = https://doi.org/10.1016/j.conbuildmat.2016.02.133

[13] Y.J. Kim and K.A. Harries. Modeling of timber beams strengthened with various CFRP composites. *Engineering Structures*, 32(10):3225–3234, 2010. doi = https://doi.org/10.1016/j.engstruct.2010.06.011

[14] O⁻. Civalek, S. Dastjerdi, and B. Akgo̎z. Buckling and free vibrations of CNT-reinforced cross-ply laminated composite plates. *Mechanics Based Design of Structures and Machines*, 2020. Published online 21 May 2020. doi = https://doi.org/10.1080/15397734.2020.1766494

[15] D.A. Tingley. *The stress-strain relationships in wood and fiber-reinforced plastic laminae of reinforced glue laminated wood beams*. Ph.D. thesis, Oregon State University, Corvallis, OR, 1996.

[16] C.P. Kirlin. *Experimental and finite-element analysis of stress distributions near the end of reinforce- ment in partially reinforced glulam*. Ph.D. thesis, Oregon State University, 1996. url = http://hdl.handle.net/1957/12262

[17] E. Serrano. Glued-in rods for timber structures - a 3D model and finite element parameter studies. *International Journal of Adhesion and Adhesives*, 21(2):115–127, 2001. doi = https://doi.org/10.1016/S0143-7496(00)00043-9

[18] B. Kasal and A. Heiduschke. Radial reinforcement of curved glue laminated wood beams with com- posite materials. *Forest Products Journal*, 54(1):74–79, 2004.

[19] M. Khelifa, N. Vila Loperena, L. Bleron, and A. Khennane. Analysis of CFRP-strengthened timber beams. *Journal of Adhesion Science and Technology*, 28(1):1–14, 2014. doi = https://doi.org/10.1080/01694243.2013.815096

[20] J. Fiorelli and A.A. Dias. Glulam beams reinforced with FRP externally-bonded: theoretical and ex- perimental evaluation. *Materials and Structures*, 44:1431–1440, 2011. doi = https://doi.org/10.1617/s11527-011-9708-y

[21] H. Johnsson, T. Blanksvärd, and A Carolin. Glulam members strengthened by carbon fibre reinforce- ment. *Materials and Structures*, 40:47–56, 2006. doi = https://doi.org/10.1617/s11527-006-9119-7

[22] K.-U. Schober, A.M. Harte, R. Kliger, R. Jockwer, Q. Xu, and J.-F. Chen. FRP reinforcement of timber structures. *Construction and Building Materials*, 97:106–118, 2015. doi = https://doi.org/10.1016/j.conbuildmat.2015.06.020

[23] Y.F. Li, M.J. Tsai, T.F. Wei, and W.C. Wang. A study on wood beams strengthened by FRP composite materials. *Construction and Building Materials*, 62:118–125, 2014. doi = https://doi.org/10.1016/j.conbuildmat.2014.03.036

[24] D.M. Moses and H.G. Prion. Anisotropic plasticity and failure prediction in wood composites. Re- search report, University of British Columbia, Canada, 2002. url = https://www.semanticscholar.org/paper/ANISOTROPIC-PLASTICITY-AND-FAILURE-PREDICTION-IN-Moses/7d3354bf340e9af1ab19a16702c8cb28015143b3

[25] ANSYS Inc. *ANSYS advanced analysis techniques guide*, 2007.

[26] G.M. Raftery and A.M. Harte. Low-grade glued laminated timber reinforced with FRP plate. *Compos- ites: Part B*, 42:724–735, 2011. doi = https://doi.org/10.1016/j.compositesb.2011.01.029

[27] J.R. Gilfillan, S.G. Gilbert, and G.R.H. Patrick. The use of FRP composites in enhancing the structural behavior of timber beams. *Journal of Reinforced Plastics and Composites*, 22:1373–1388, 2003. doi = https://doi.org/10.1177/073168403035583

[28] P. Neubauerová. Timber beams strengthened by carbon fiber reinforced lamellas. *Procedia Engineering*, 40:292–297, 2012. doi = https://doi.org/10.1016/j.proeng.2012.07.097

[29] J. Milch, J. Tippner, V. Sebera, and M. Brabec. Determination of the elasto-plastic material charac- teristics of norway spruce and european beech wood by experimental and numerical analyses. *Holz- forschung*, 70(11):1081–1092, 2016. doi = https://doi.org/10.1515/hf-2015-0267

[30] A. Garsteckl. Optimal redesign of elastic structures in the state of initial loading. *Journal of Structural Mechanics*, 12:279–301, 1984. doi = https://doi.org/10.1080/03601218408907473

[31] W. Prager. Unexpected results in structural optimization. *Journal of Structural Mechanics*, 9:71–90, 1981. doi = https://doi.org/10.1080/03601218108907377

[32] Menke, W., 2012. Geophysical data analysis: discrete inverse theory: MATLAB edition (Vol. 45). Academic press. url= https://books.google.hu/books?id=sUDAqFV_oRAC

[33] O. Ditlevsen. Reliability against defect generated fracture. *Journal of Structural Mechanics*, 9:115– 137, 1981. doi = https://doi.org/10.1080/03601218108907379

[34] H. Alhayek and D. Svecova. Flexural stiffness and strength of GFRP-reinforced timber beams. *Journal of Composites for Construction*, 16:245–252, 2012. doi = https://doi.org/10.1061/(asce)cc.1943-5614.0000261

GUIDELINE FOR AUTHORS

The manuscript must contain the followings: title; author's name, workplace, e-mail address; abstract, keywords; main text; acknowledgement (optional)**; references; figures, photos with notes; tables with notes; short biography** (information on the scientific works of the authors).

The full manuscript should not be more than 6 pages including figures, photos and tables. Settings of the word document are: 3 cm margin up and down, 2,5 cm margin left and right. Paper size: A4. Letter size 10 pt, type: Times New Roman. Lines: simple, justified.

TITLE, AUTHOR
The title of the article should be short and objective.
Under the title the name of the author(s), workplace, e-mail address.
If the text originally was a presentation or poster at a conference, it should be marked.

ABSTRACT, KEYWORDS
The abstract is a short summary of the manuscript, about a half page size. The author should give keywords to the text, which are the most important elements of the article.

MAIN TEXT
Contains: materials and experimental procedure (or something similar), results and discussion (or something similar), conclusions.

REFERENCES
References are marked with numbers, e.g. [6], and a bibliography is made by the reference's order. References should be provided together with the DOI if available.
Examples:
Journals:
[6] Mohamed, K. R. – El-Rashidy, Z. M. – Salama, A. A.: In vitro properties of nano-hydroxyapatite/chitosan biocomposites. *Ceramics International.* 37(8), December 2011, pp. 3265–3271, http://doi.org/10.1016/j.ceramint.2011.05.121
Books:
[6] Mehta, P. K. – Monteiro, P. J. M.: Concrete. Microstructure, properties, and materials. *McGraw-Hill*, 2006, 659 p.

FIGURES, TABLES
All drawings, diagrams and photos are figures. The **text should contain references to all figures and tables**. This shows the place of the figure in the text. Please send all the figures in attached files, and not as a part of the text. **All figures and tables should have a title**.
Authors are asked to submit color figures by submission. Black and white figures are suggested to be avoided, however, acceptable.
The figures should be: tiff, jpg or eps files, 300 dpi at least, photos are 600 dpi at least.

BIOGRAPHY
Max. 500 character size professional biography of the author(s).

CHECKING
The editing board checks the articles and informs the authors about suggested modifications. Since the author is responsible for the content of the article, the author is not liable to accept them.

CONTACT
Please send the manuscript in electronic format to the following e-mail address: femgomze@uni-miskolc.hu and epitoanyag@szte.org.hu or by post: Scientific Society of the Silicate Industry, Budapest, Bécsi út 122–124., H-1034, HUNGARY

We kindly ask the authors to give their e-mail address and phone number on behalf of the quick conciliation.